Equipment for Distillation, Gas Absorption, Phase Dispersion, and Phase Separation

Henry Z. Kister, M.E., C.Eng., C.Sc. *Senior Fellow and Director of Fractionation Technology, Fluor Corporation; Fellow, American Institute of Chemical Engineers; Fellow, Institution of Chemical Engineers (UK); Member, Institute of Energy (Section Editor, Equipment for Distillation and Gas Absorption)*

Paul M. Mathias, Ph.D. *Technical Director, Fluor Corporation; Member, American Institute of Chemical Engineers (Design of Gas Absorption Systems)*

D. E. Steinmeyer, P.E., M.A., M.S. *Distinguished Fellow, Monsanto Company (retired); Fellow, American Institute of Chemical Engineers; Member, American Chemical Society (Phase Dispersion)*

W. R. Penney, Ph.D., P.E. *Professor of Chemical Engineering, University of Arkansas; Member, American Institute of Chemical Engineers (Gas-in-Liquid Dispersions)*

B. B. Crocker, P.E., S.M. *Consulting Chemical Engineer; Fellow, American Institute of Chemical Engineers; Member, Air Pollution Control Association (Phase Separation)*

James R. Fair, Ph.D., P.E. *Professor of Chemical Engineering, University of Texas; Fellow, American Institute of Chemical Engineers; Member, American Chemical Society, American Society for Engineering Education, National Society of Professional Engineers (Section Editor of the 7th edition and major contributor to the 5th, 6th, and 7th editions)*

EQUIPMENT FOR DISTILLATION AND GAS ABSORPTION: TRAY COLUMNS

EQUIPMENT FOR DISTILLATION AND GAS ABSORPTION: PACKED COLUMNS

OTHER TOPICS FOR DISTILLATION AND GAS ABSORPTION EQUIPMENT

PHASE DISPERSION

PHASE SEPARATION

Nomenclature

a, a_e	Effective interfacial area	m^2/m^3	ft^2/ft^3
a_p	Packing surface area per unit volume	m^2/m^3	ft^2/ft^3
A	Absorption factor $L_M/(mG_M)$	-/-	-/-
A	Cross-sectional area	m^2	ft^2
A_a	Active area, same as bubbling area	m^2	ft^2
A_B	Bubbling (active) area	m^2	ft^2
A_D	Downcomer area (straight vertical downcomer)	m^2	ft^2
A_{da}	Downcomer apron area	m^2	ft^2
A_{DB}	Area at bottom of downcomer	m^2	ft^2
A_{DT}	Area at top of downcomer	m^2	ft^2
A_e, A'	Effective absorption factor (Edmister)	-/-	-/-
A_f	Fractional hole area	-/-	-/-
A_h	Hole area	m^2	ft^2
A_N	Net (free) area	m^2	ft^2
A_S	Slot area	m^2	ft^2
A_{SO}	Open slot area	m^2	ft^2
A_T	Tower cross-section area	m^2	ft^2
c	Concentration	$kg{\cdot}mol/m^3$	$lb{\cdot}mol/ft^3$
c'	Stokes-Cunningham correction factor for terminal settling velocity	-/-	-/-
C	C-factor for gas loading, Eq. (14-77)	m/s	ft/s
C_1	Coefficient in regime transition correlation, Eq. (14-129)	-/-	-/-
C_1, C_2	Parameters in system limit equation	m/s	ft/s
C_3, C_4	Constants in Robbins' packing pressure drop correlation	-/-	-/-
CAF	Flood C-factor, Eq. (14-88)	m/s	ft/s
CAF_0	Uncorrected flood C-factor, Fig. 14-30	—	ft/s
C_d	Coefficient in clear liquid height correlation, Eq. (14-116)	-/-	-/-
C_G	Gas C-factor; same as C	m/s	ft/s
C_L	Liquid loading factor, Eq. (14-144)	m/s	ft/s
C_{LG}	A constant in packing pressure drop correlation, Eq. (14-143)	$(m/s)^{0.5}$	$(ft/s)^{0.5}$
CP	Capacity parameter (packed towers), Eq. (14-140)		
C_{SB}, C_{sb}	C-factor at entrainment flood, Eq. (14-80)	m/s	ft/s
C_{sbf}	Capacity parameter corrected for surface tension	m/s	ft/s
C_v, C_V	Discharge coefficient, Fig. 14-35	-/-	-/-
C_w	A constant in weep rate equation, Eq. (14-123)	-/-	-/-
C_{XY}	Coefficient in Eq. (14-159) reflecting angle of inclination	-/-	-/-
d	Diameter	m	ft
d_b	Bubble diameter	m	ft
d_h, d_H	Hole diameter	mm	in
d_o	Orifice diameter	m	ft
d_{pc}	Cut size of a particle collected in a device, 50% mass efficiency	μm	ft
d_{psd}	Mass median size particle in the pollutant gas	μm	ft
d_{pa50}	Aerodynamic diameter of a real median size particle	μm	ft
d_w	Weir diameter, circular weirs	mm	in
D	Diffusion coefficient	m^2/s	ft^2/s
D	Tube diameter (wetted-wall columns)	m	ft
D_{32}	Sauter mean diameter	m	ft
D_g	Diffusion coefficient	m^2/s	ft^2/h
D_p	Packing particle diameter	m	ft
D_T	Tower diameter	m	ft
D_{tube}	Tube inside diameter	m	ft
D_{vm}	Volume mean diameter	m	ft
e	Absolute entrainment of liquid	kg·mol/h	lb·mol/h
e	Entrainment, mass liquid/mass gas	kg/kg	lb/lb
E	Plate or stage efficiency, fractional	-/-	-/-
E	Power dissipation per mass	W	Btu/lb
E_a	Murphree tray efficiency, with entrainment, gas concentrations, fractional	-/-	-/-
E_g	Point efficiency, gas phase only, fractional	-/-	-/-
E_{oc}	Overall column efficiency, fractional	-/-	-/-
E_{OG}	Overall point efficiency, gas concentrations, fractional	-/-	-/-
E_{mv}, E_{MV}	Murphree tray efficiency, gas concentrations, fractional	-/-	-/-
E_s	Entrainment, kg entrained liquid per kg gas upflow	kg/kg	lb/lb
f	Fractional approach to flood	-/-	-/-
f	Liquid maldistribution fraction	-/-	-/-
f_{max}	Maximum value of f above which separation cannot be achieved	-/-	-/-
f_w	Weep fraction, Eq. (14–121)	-/-	-/-
F	Fraction of volume occupied by liquid phase, system limit correlation, Eq. (14-170)	-/-	-/-
F	F-factor for gas loading Eq. (14-76)	$m/s(kg/m^3)^{0.5}$	$ft/s(lb/ft^3)^{0.5}$
F_{LG}	Flow parameter, Eq. (14-89) and Eq. (14-141)	-/-	-/-
F_p	Packing factor	m^{-1}	ft^{-1}
F_{pd}	Dry packing factor	m^{-1}	ft^{-1}
FPL	Flow path length	m	ft
Fr	Froude number, clear liquid height correlation, Eq. (14-120)	-/-	-/-
Fr_h	Hole Froude number, Eq. (14-114)	-/-	-/-
F_w	Weir constriction correction factor, Fig. 14-38	-/-	-/-
g	Gravitational constant	m/s^2	ft/s^2
g_c	Conversion factor	1.0 kg·m/(N·s^2)	32.2 lb·ft/(lbf·s^2)
G	Gas phase mass velocity	$kg/(s.m^2)$	$lb/(hr{\cdot}ft^2)$
G_f	Gas loading factor in Robbins' packing pressure drop correlation	$kg/(s{\cdot}m^2)$	$lb/(h{\cdot}ft^2)$
G_M	Gas phase molar velocity	kg·mol/($s.m^2$)	lb·mol/($h.ft^2$)
GPM	Liquid flow rate	—	gpm
h	Pressure head	mm	in
h'_{dc}	Froth height in downcomer	mm	in
h'_L	Pressure drop through aerated mass on tray	mm	in
h_c	Clear liquid height on tray	mm	in
h_{cl}	Clearance under downcomer	mm	in
h_{ct}	Clear liquid height at spray to froth transition	mm	in
h_d	Dry pressure drop across tray	mm	in
h_{da}	Head loss due to liquid flow under downcomer apron	mm	in
h_{dc}	Clear liquid height in downcomer	mm	in
h_{ds}	Calculated clear liquid height, Eq. (14-108)	mm	in
h_f	Height of froth	mm	in
h_{fow}	Froth height over the weir, Eq. (14-117)	mm	in
h_{hg}	Hydraulic gradient	mm	in
h_{Lo}	Packing holdup in preloading regime, fractional	-/-	-/-
h_{Lt}	Clear liquid height at froth to spray transition, corrected for effect of weir height, Eq. (14-96)	mm	in
h_{ow}	Height of crest over weir	mm	in
h_T	Height of contacting	m	ft
h_t	Total pressure drop across tray	mm	in
h_w	Weir height	mm	in
H	Height of a transfer unit	m	ft
H	Henry's law constant	kPa/mol fraction	atm /mol fraction
H'	Henry's law constant	$kPa/(kmol{\cdot}m^3)$	$psi/(lb{\cdot}mol.ft^3)$
H_G	Height of a gas phase transfer unit	m	ft
H_L	Height of a liquid phase transfer unit	m	ft
H_{OG}	Height of an overall transfer unit, gas phase concentrations	m	ft
H_{OL}	Height of an overall transfer unit, liquid phase concentrations	m	ft

Nomenclature (*Continued*)

H'	Henry's law coefficient	kPa/mol frac	atm/mol frac
HETP	Height equivalent to a theoretical plate or stage	m	ft
J_G^*	Dimensionless gas velocity, weep correlation, Eq. (14-124)	-/-	-/-
J_L^*	Dimensionless liquid velocity, weep correlation, Eq. (14-125)	-/-	-/-
k	Individual phase mass transfer coefficient	kmol /(s·m²· mol frac)	lb·mol/(s·ft²· mol frac)
k_1	First order reaction velocity constant	1/s	1/s
k_2	Second order reaction velocity constant	m³/(s·kmol)	ft³/(h·lb·mol)
k_g	Gas mass-transfer coefficient, wetted-wall columns [see Eq. (14-171) for unique units]		
k_G	gas phase mass transfer coefficient	kmol /(s·m²· mol frac)	lb.mol/(s·ft²· mol frac)
k_L	liquid phase mass transfer coefficient	kmol /(s·m²· mol frac)	lb·mol/(s·ft²· mol frac)
K	Constant in trays dry pressure drop equation	mm·s²/m²	in·s²/ft²
K	Vapor-liquid equilibrium ratio	-/-	-/-
K_C	Dry pressure drop constant, all valves closed	mm·s²/m²	in·s²/ft²
K_D	Orifice discharge coefficient, liquid distributor	-/-	-/-
K_g	Overall mass-transfer coefficient	kg·mol/ (s·m²·atm)	lb·mol/ (h·ft²·atm)
K_O	Dry pressure drop constant, all valves open	mm·s²/m²	in·s²/ft²
K_{OG}, K_G	Overall mass transfer coefficient, gas concentrations	kmol / (s·m²·mol) frac)	lb·mol/ (s·ft²·mol frac)
K_{OL}	Overall mass transfer coefficient, liquid concentrations	kmol/ (s·m²·mol frac)	lb.mol/ (s·ft²·mol frac)
L	Liquid mass velocity	kg/(m²·s)	lb/ft²·h
L_f	Liquid loading factor in Robbins' packing pressure drop correlation	kg/(s·m²)	lb/(h·ft²)
L_m	Molar liquid downflow rate	kg·mol/h	lb·mol/h
L_M	Liquid molar mass velocity	kmol/(m²·s)	lb·mol/(ft²·h)
L_S	Liquid velocity, based on superficial tower area	m/s	ft/s
L_w	Weir length	m	in
m	An empirical constant based on Wallis' countercurrent flow limitation equation, Eqs. (14-123) and (14-143)	-/-	-/-
m	Slope of equilibrium curve = dy^*/dx	-/-	-/-
M	Molecular weight	kg/kmol	lb/(lb·mol)
n	Parameter in spray regime clear liquid height correlation, Eq. (14-84)	mm	in
n_A	Rate of solute transfer	kmol/s	lb·mol/s
n_D	Number of holes in orifice distributor	-/-	-/-
N_a	Number of actual trays	-/-	-/-
N_A, N_t	Number of theoretical stages	-/-	-/-
N_{OG}	Number of overall gas-transfer units	-/-	-/-
N_p	Number of tray passes	-/-	-/-
p	Hole pitch (center-to-center hole spacing)	mm	in
p	Partial pressure	kPa	atm
P_{BM}	Logarithmic mean partial pressure of inert gas	kPa	atm
P, p_T	Total pressure	kPa	atm
P^0	Vapor pressure	kpa	atm
Q, q	Volumetric flow rate of liquid	m³/s	ft³/s
Q'	Liquid flow per serration of serrated weir	m·³/s	ft³/s
Q_D	Downcomer liquid load, Eq. (14-79)	m/s	ft/s
Q_L	Weir load, Eq. (14-78)	m³/(h·m)	gpm/in
Q_{MW}	Minimum wetting rate	m³/(h·m²)	gpm/ft²
R	Reflux flow rate	kg·mol/h	lb·mol/h
R	Gas constant		
R_h	Hydraulic radius	m	ft
R_{vw}	Ratio of valve weight with legs to valve weight without legs, Table (14-11)	-/-	-/-
S	Length of corrugation side, structured packing	m	ft
S	Stripping factor mG_M/L_M	-/-	-/-
S	Tray spacing	mm	in
S_e, S'	Effective stripping factor (Edmister)	-/-	-/-
SF	Derating (system) factor, Table 14-9	-/-	-/-
t_t	Tray thickness	mm	in
t_v	Valve thickness	mm	in
T	Absolute temperature	K	°R
TS	Tray spacing; same as S	mm	in
U,u	Linear velocity of gas	m/s	ft/s
U_a	Velocity of gas through active area	m/s	ft/s
U_a^*	Gas velocity through active area at froth to spray transition	m/s	ft/s
U_{h,u_h}	Gas hole velocity	m/s	ft/s
U_L, u_L	Liquid superficial velocity based on tower cross-sectional area	m/s	ft/s
U_n	Velocity of gas through net area	m/s	ft/s
U_{nf}	Gas velocity through net area at flood	-/-	-/-
U_t	Superficial velocity of gas	m/s	ft/s
v_H	Horizontal velocity in trough	m/s	ft/s
V	Linear velocity	m/s	ft/s
V	Molar vapor flow rate	kg·mol/s	lb·mol/h
W	Weep rate	m³/s	gpm
x	Mole fraction, liquid phase (note 1)	-/-	-/-
x'	Mole fraction, liquid phase, column 1 (note 1)		
x''	Mole fraction, liquid phase, column 2 (note 1)		
x^*, x°	Liquid mole fraction at equilibrium (note 1)	-/-	-/-
y	Mole fraction, gas or vapor phase (note 1)	-/-	-/-
y'	Mole fraction, vapor phase, column 1 (note 1)		
y''	Mole fraction, vapor phase, column 2 (note 1)		
y^*, y°	Gas mole fraction at equilibrium (note 1)		
Z	Characteristic length in weep rate equation, Eq. (14-126)	m	ft
Z_p	Total packed height	m	ft

Greek Symbols

α	Relative volatility	-/-	-/-
β	Tray aeration factor, Fig. (14-37)	-/-	-/-
ε	Void fraction	-/-	-/-
ϕ	Contact angle	deg	deg
ϕ	Relative froth density	-/-	-/-
γ	Activity coefficient	-/-	-/-
Γ	Flow rate per length	kg/(s·m)	lb/(s·ft)
δ	Effective film thickness	m	ft
η	Collection eficiency, fractional	-/-	-/-
η	Factor used in froth density correlation, Eq. (14-118)	-/-	-/-
λ	Stripping factor = $m/(L_M/G_M)$	-/-	-/-
μ	Absolute viscosity	Pa·s	cP or lb/(ft·s)
μm	Micrometers	m	-/-
ν	Kinematic viscosity	m²/s	cS
π	3.1416. . . .	-/-	-/-
θ	Residence time	s	s
θ	Angle of serration in serrated weir	deg	deg
ρ	Density	kg/m³	lb/ft³
ρ_M	Valve metal density	kg/m³	lb/ft³
σ	Surface tension	mN/m	dyn/cm
χ	Parameter used in entrainment correlation, Eq. (14-95)	-/-	-/-
ψ	Fractional entrainment, moles liquid entrained per mole liquid downflow	k·mol/ k·mol	lb·mol/ lb·mol
Φ	Fractional approach to entrainment flood	-/-	-/-
ΔP	Pressure drop per length of packed bed	mmH_2O/m	inH_2O/ft
$\Delta\rho$	$\rho_L - \rho_G$	kg/m³	lb/ft³

Subscripts

A	Species A
AB	Species A diffusing through species B

Nomenclature (*Concluded*)

Subscripts	
B	Species B
B	Based on the bubbling area
d	Dry
da	Downcomer apron
dc	Downcomer
dry	Uncorrected for entrainment and weeping
e	Effective value
f	Froth
Fl	Flood
flood	At flood
G, *g*	Gas or vapor
h	Based on hole area (or slot area)
H_2O	Water
i	Interface value
L, *l*	Liquid
m	Mean
min	Minimum
MOC	At maximum operational capacity

Subscripts	
n, N	On stage *n*
N	At the inlet nozzle
NF, nf	Based on net area at flood
p	Particle
S	Superficial
t	Total
ult	At system limit (ultimate capacity)
V	Vapor
w	Water
1	Tower bottom
2	Tower top

Dimensionless Groups	
N_{Fr}	Froude number = $(U_L^2)/(Sg)$,
N_{Re}	Reynolds number = $(D_{tube}U_{ge}\rho_G)/(\mu_G)$
N_{Sc}	Schmidt number = $\mu/(\rho D)$
N_{We}	Weber number = $(U_L^2\rho_L S)/(\sigma g_e)$

NOTE: 1. Unless otherwise specified, refers to concentration of more volatile component (distillation) or solute (absorption).

General References: Astarita, G., *Mass Transfer with Chemical Reaction,* Elsevier, New York, 1967. Astarita, G., D. W. Savage and A. Bisio, *Gas Treating with Chemical Solvents,* Wiley, New York, 1983. Billet, R., *Distillation Engineering,* Chemical Publishing Co., New York, 1979. Billet, R., *Packed Column Analysis and Design,* Ruhr University, Bochum, Germany, 1989. Danckwerts, P. V., *Gas-Liquid Reactions,* McGraw-Hill, New York, 1970. *Distillation and Absorption 1987,* Rugby, U.K., Institution of Chemical Engineers. *Distillation and Absorption 1992,* Rugby, U.K., Institution of Chemical Engineers. *Distillation and Absorption 1997,* Rugby, U.K., Institution of Chemical Engineers. *Distillation and Absorption 2002,* Rugby, U.K., Institution of Chemical Engineers. *Distillation and Absorption 2006,* Rugby, U.K., Institution of Chemical Engineers. *Distillation Topical Conference Proceedings,* AIChE Spring Meetings (separate Proceedings Book for each Topical Conference): Houston, Texas, March 1999; Houston, Texas, April 22–26, 2001; New Orleans, La., March 10–14, 2002; New Orleans, La., March 30–April 3, 2003; Atlanta, Ga., April 10–13, 2005. Hines, A. L., and R. N. Maddox, *Mass Transfer—Fundamentals and Applications,* Prentice Hall, Englewood Cliffs, New Jersey, 1985. Hobler, T., *Mass Transfer and Absorbers,* Pergamon Press, Oxford, 1966. Kister, H. Z., *Distillation Operation,* McGraw-Hill, New York, 1990. Kister, H. Z., *Distillation Design,* McGraw-Hill, New York, 1992. Kister, H. Z., and G. Nalven (eds.), *Distillation and Other Industrial Separations,* Reprints from CEP, AIChE, 1998. Kister, H. Z., *Distillation Troubleshooting,* Wiley, 2006. Kohl, A. L., and R. B. Nielsen, *Gas Purification,* 5th ed., Gulf, Houston, 1997. Lockett, M.J., *Distillation Tray Fundamentals,* Cambridge, U.K., Cambridge University Press, 1986. Maćkowiak, J., "Fluiddynamik von Kolonnen mit Modernen Füllkorpern und Packungen für Gas/Flussigkeitssysteme," Otto Salle Verlag, Frankfurt am Main und Verlag Sauerländer Aarau, Frankfurt am Main, 1991. Schweitzer, P. A. (ed.), *Handbook of Separation Techniques for Chemical Engineers,* 3d. ed., McGraw-Hill, New York, 1997. Sherwood, T. K., R. L. Pigford, C. R. Wilke, *Mass Transfer,* McGraw-Hill, New York, 1975. Stichlmair, J., and J. R. Fair, *Distillation Principles and Practices,* Wiley, New York, 1998. Strigle, R. F., Jr., *Packed Tower Design and Applications,* 2d ed., Gulf Publishing, Houston, 1994. Treybal, R. E., *Mass Transfer Operations,* McGraw-Hill, New York, 1980.

INTRODUCTION

Definitions Gas absorption is a unit operation in which soluble components of a gas mixture are dissolved in a liquid. The inverse operation, called stripping or desorption, is employed when it is desired to transfer volatile components from a liquid mixture into a gas. Both absorption and stripping, in common with distillation (Sec. 13), make use of special equipment for bringing gas and liquid phases into intimate contact. This section is concerned with the design of gas-liquid contacting equipment, as well as with the design of absorption and stripping processes.

Equipment Absorption, stripping, and distillation operations are usually carried out in vertical, cylindrical columns or towers in which devices such as plates or packing elements are placed. The gas and liquid normally flow countercurrently, and the devices serve to provide the contacting and development of interfacial surface through which mass transfer takes place. Background material on this mass transfer process is given in Sec. 5.

Design Procedures The procedures to be followed in specifying the principal dimensions of gas absorption and distillation equipment are described in this section and are supported by several worked-out examples. The experimental data required for executing the designs are keyed to appropriate references or to other sections of the handbook.

For absorption, stripping, and distillation, there are three main steps involved in design:

1. *Data on the gas-liquid or vapor-liquid equilibrium for the system at hand.* If absorption, stripping, and distillation operations are considered equilibrium-limited processes, which is the usual approach, these data are critical for determining the maximum possible separation. In some cases, the operations are considered rate-based (see Sec. 13) but require knowledge of equilibrium at the phase interface. Other data required include physical properties such as viscosity and density and thermodynamic properties such as enthalpy. Section 2 deals with sources of such data.

2. *Information on the liquid- and gas-handling capacity of the contacting device chosen for the particular separation problem.* Such information includes pressure drop characteristics of the device, in order that an optimum balance between capital cost (column cross section) and energy requirements might be achieved. Capacity and pressure drop characteristics of the available devices are covered later in this Sec. 14.

3. *Determination of the required height of contacting zone for the separation to be made as a function of properties of the fluid mixtures and mass-transfer efficiency of the contacting device.* This determination involves the calculation of mass-transfer parameters such as heights of transfer units and plate efficiencies as well as equilibrium or rate parameters such as theoretical stages or numbers of transfer units. An additional consideration for systems in which chemical reaction occurs is the provision of adequate residence time for desired reactions to occur, or minimal residence time to prevent undesired reactions from occurring. For equilibrium-based operations, the parameters for required height are covered in the present section.

Data Sources in the Handbook Sources of data for the analysis or design of absorbers, strippers, and distillation columns are manifold, and a detailed listing of them is outside the scope of the presentation in this section. Some key sources within the handbook are shown in Table 14-1.

Equilibrium Data Finding reliable gas-liquid and vapor-liquid equilibrium data may be the most time-consuming task associated with the design of absorbers and other gas-liquid contactors, and yet it may be the most important task at hand. For gas solubility, an important data source is the set of volumes edited by Kertes et al., *Solubility Data Series,* published by Pergamon Press (1979 ff.). In the introduction to each volume, there is an excellent discussion and definition of the various methods by which gas solubility data have been reported, such as the Bunsen coefficient, the Kuenen coefficient, the Ostwalt coefficient, the absorption coefficient, and the Henry's law coefficient. The fifth edition of *The Properties of Gases and Liquids* by Poling, Prausnitz, and O'Connell (McGraw-Hill, New York, 2000) provides data and recommended estimation methods for gas solubility as well as the broader area of vapor-liquid equilibrium. Finally, the Chemistry Data Series by Gmehling et al., especially the title *Vapor-Liquid Equilibrium Collection* (DECHEMA, Frankfurt, Germany, 1979 ff.), is a rich source of data evaluated against the various models used for interpolation and extrapolation. Section 13 of this handbook presents a good discussion of equilibrium *K* values.

TABLE 14-1 Directory to Key Data for Absorption and Gas-Liquid Contactor Design

Type of data	Section
Phase equilibrium data	
Gas solubilities	2
Pure component vapor pressures	2
Equilibrium *K* values	13
Thermal data	
Heats of solution	2
Specific heats	2
Latent heats of vaporization	2
Transport property data	
Diffusion coefficients	
Liquids	2
Gases	2
Viscosities	
Liquids	2
Gases	2
Densities	
Liquids	2
Gases	2
Surface tensions	2
Packed tower data	
Pressure drop and flooding	14
Mass transfer coefficients	5
HTU, physical absorption	5
HTU with chemical reaction	14
Height equivalent to a theoretical plate (HETP)	
Plate tower data	
Pressure drop and flooding	14
Plate efficiencies	14
Costs of gas-liquid contacting equipment	14

DESIGN OF GAS ABSORPTION SYSTEMS

General Design Procedure The design engineer usually is required to determine (1) the best solvent; (2) the best gas velocity through the absorber, or, equivalently, the vessel diameter; (3) the height of the vessel and its internal members, which is the height and type of packing or the number of contacting trays; (4) the optimum solvent circulation rate through the absorber and stripper; (5) temperatures of streams entering and leaving the absorber and stripper, and the quantity of heat to be removed to account for the heat of solution and other thermal effects; (6) pressures at which the absorber and stripper will operate; and (7) mechanical design of the absorber and stripper vessels (predominantly columns or towers), including flow distributors and packing supports. This section covers these aspects.

The problem presented to the designer of a gas absorption system usually specifies the following quantities: (1) gas flow rate; (2) gas composition of the component or components to be absorbed; (3) operating pressure and allowable pressure drop across the absorber; (4) minimum recovery of one or more of the solutes; and, possibly, (5) the solvent to be employed. Items 3, 4, and 5 may be subject to economic considerations and therefore are left to the designer. For determination of the number of variables that must be specified to fix a unique solution for the absorber design, one may use the same phase-rule approach described in Sec. 13 for distillation systems.

Recovery of the solvent, occasionally by chemical means but more often by distillation, is almost always required and is considered an integral part of the absorption system process design. A more complete solvent-stripping operation normally will result in a less costly absorber because of a lower concentration of residual solute in the regenerated (lean) solvent, but this may increase the overall cost of the entire absorption system. A more detailed discussion of these and other economical considerations is presented later in this section.

The design calculations presented in this section are relatively simple and usually can be done by using a calculator or spreadsheet. In many cases, the calculations are explained through design diagrams. It is recognized that most engineers today will perform rigorous, detailed calculations using process simulators. The design procedures presented in this section are intended to be complementary to the rigorous computerized calculations by presenting approximate estimates and insight into the essential elements of absorption and stripping operations.

Selection of Solvent and Nature of Solvents When a choice is possible, preference is given to solvents with high solubilities for the target solute and high selectivity for the target solute over the other species in the gas mixture. A high solubility reduces the amount of liquid to be circulated. The solvent should have the advantages of low volatility, low cost, low corrosive tendencies, high stability, low viscosity, low tendency to foam, and low flammability. Since the exit gas normally leaves saturated with solvent, solvent loss can be costly and can cause environmental problems. The choice of the solvent is a key part of the process economic analysis and compliance with environmental regulations.

Typically, a solvent that is chemically similar to the target solute or that reacts with it will provide high solubility. Water is often used for polar and acidic solutes (e.g., HCl), oils for light hydrocarbons, and special chemical solvents for acid gases such as CO_2, SO_2, and H_2S. Solvents are classified as physical and chemical. A chemical solvent forms complexes or chemical compounds with the solute, while physical solvents have only weaker interactions with the solute. Physical and chemical solvents are compared and contrasted by examining the solubility of CO_2 in propylene carbonate (representative physical solvent) and aqueous monoethanolamine (MEA; representative chemical solvent).

Figures 14-1 and 14-2 present data for the solubility of CO_2 in the two representative solvents, each at two temperatures: 40 and 100°C.

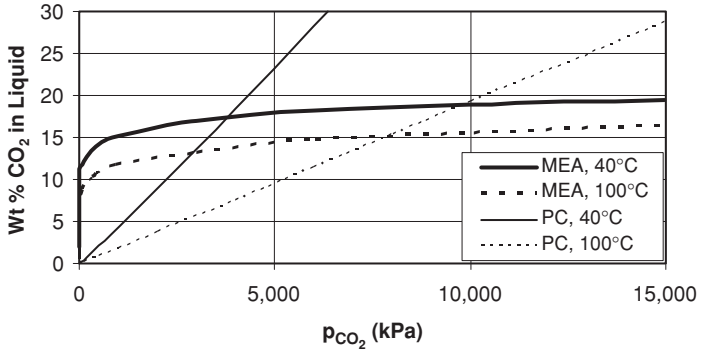

FIG. 14-1 Solubility of CO_2 in 30 wt% MEA and propylene carbonate. Linear scale.

The propylene carbonate data are from Zubchenko et al. [*Zhur. Priklad. Khim.*, **44**, 2044–2047 (1971)], and the MEA data are from Jou, Mather, and Otto [*Can. J. Chem. Eng.*, **73**, 140–147 (1995)]. The two figures have the same content, but Fig. 14-2 focuses on the low-pressure region by converting both composition and pressure to the logarithm scale. Examination of the two sets of data reveals the following characteristics and differences of physical and chemical solvents, which are summarized in the following table:

Characteristic	Physical solvent	Chemical solvent
Solubility variation with pressure	Relatively linear	Highly nonlinear
Low-pressure solubility	Low	High
High-pressure solubility	Continues to increase	Levels off
Heat of solution—related to variation of solubility with temperature at fixed pressure	Relatively low and approximately constant with loading	Relatively high and decreases somewhat with increased solute loading

Chemical solvents are usually preferred when the solute must be reduced to very low levels, when high selectivity is needed, and when the solute partial pressure is low. However, the strong absorption at low solute partial pressures and the high heat of solution are disadvantages for stripping. For chemical solvents, the strong nonlinearity of the absorption makes it necessary that accurate absorption data for the conditions of interest be available.

Selection of Solubility Data Solubility values are necessary for design because they determine the liquid rate necessary for complete or economic solute recovery. Equilibrium data generally will be found in one of three forms: (1) solubility data expressed either as weight or mole percent or as Henry's law coefficients; (2) pure-component vapor pressures; or (3) equilibrium distribution coefficients (K values). Data for specific systems may be found in Sec. 2; additional references to sources of data are presented in this section.

To define completely the solubility of gas in a liquid, it is generally necessary to state the temperature, equilibrium partial pressure of the solute gas in the gas phase, and the concentration of the solute gas in the liquid phase. Strictly speaking, the total pressure of the system should also be identified, but for low pressures (less than about 507 kPa or 5 atm), the solubility for a particular partial pressure of the solute will be relatively independent of the total pressure.

For many physical systems, the equilibrium relationship between solute partial pressure and liquid-phase concentration is given by Henry's law:

$$p_A = Hx_A \tag{14-1}$$

or

$$p_A = H'c_A \tag{14-2}$$

where H is Henry's law coefficient expressed in kPa per mole fraction solute in liquid and H' is Henry's law coefficient expressed in kPa·m^3/kmol.

Figure 14-1 indicates that Henry's law is valid to a good approximation for the solubility CO_2 in propylene carbonate. In general, Henry's law is a reasonable approximation for physical solvents. If Henry's law holds, the solubility is defined by knowing (or estimating) the value of the constant H (or H').

Note that the assumption of Henry's law will lead to incorrect results for solubility of chemical systems such as CO_2-MEA (Figs. 14-1 and 14-2) and HCl-H_2O. Solubility modeling for chemical systems requires the use of a *speciation model,* as described later in this section.

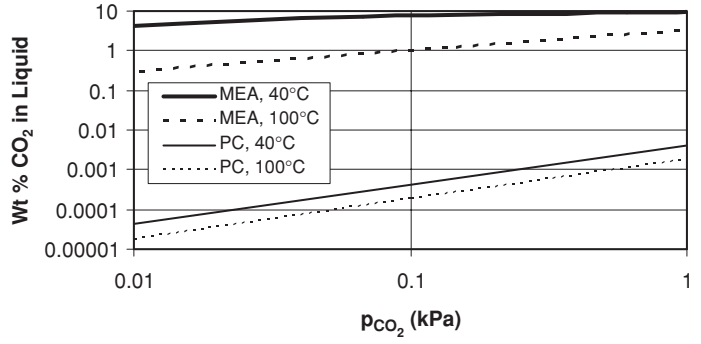

FIG. 14-2 Solubility of CO_2 in 30 wt% MEA and propylene carbonate. Logarithm scale and focus on low-pressure region.

For quite a number of physically absorbed gases, Henry's law holds very well when the partial pressure of the solute is less than about 101 kPa (1 atm). For partial pressures above 101 kPa, H may be independent of the partial pressure (Fig. 14-1), but this needs to be verified for the particular system of interest. The variation of H with temperature is a strongly nonlinear function of temperature as discussed by Poling, Prausnitz, and O'Connell (*The Properties of Gases and Liquids*, 5th ed., McGraw-Hill, New York, 2000). Consultation of this reference is recommended when temperature and pressure extrapolations of Henry's law data are needed.

The use of Henry's law constants is illustrated by the following example.

Example 1: Gas Solubility It is desired to find out how much hydrogen can be dissolved in 100 weights of water from a gas mixture when the total pressure is 101.3 kPa (760 torr; 1 atm), the partial pressure of the H_2 is 26.7 kPa (200 torr), and the temperature is 20°C. For partial pressures up to about 100 kPa the value of H is given in Sec. 3 as 6.92×10^6 kPa (6.83×10^4 atm) at 20°C. According to Henry's law,

$$x_{H_2} = p_{H_2}/H_{H_2} = 26.7/6.92 \times 10^6 = 3.86 \times 10^{-6}$$

The mole fraction x is the ratio of the number of moles of H_2 in solution to the total moles of all constituents contained. To calculate the weights of H_2 per 100 weights of H_2O, one can use the following formula, where the subscripts A and w correspond to the solute (hydrogen) and solvent (water):

$$\left(\frac{x_A}{1 - x_A}\right)\frac{M_A}{M_W}100 = \left(\frac{3.86 \times 10^{-6}}{1 - 3.86 \times 10^{-6}}\right)\frac{2.02}{18.02}100$$

$$= 4.33 \times 10^{-5} \text{ weights } H_2/100 \text{ weights } H_2O$$

$$= 0.43 \text{ parts per million weight}$$

Pure-component vapor pressure can be used for predicting solubilities for systems in which **Raoult's law** is valid. For such systems $p_A = p^0_A x_A$, where p^0_A is the pure-component vapor pressure of the solute and p_A is its partial pressure. Extreme care should be exercised when using pure-component vapor pressures to predict gas absorption behavior. Both vapor-phase and liquid-phase nonidealities can cause significant deviations from Raoult's law, and this is often the reason particular solvents are used, i.e., because they have special affinity for particular solutes. The book by Poling, Prausnitz, and O'Connell (op. cit.) provides an excellent discussion of the conditions where Raoult's law is valid. Vapor-pressure data are available in Sec. 3 for a variety of materials.

Whenever data are available for a given system under similar conditions of temperature, pressure, and composition, **equilibrium distribution coefficients** ($K = y/x$) provide a much more reliable tool for predicting vapor-liquid distributions. A detailed discussion of equilibrium K values is presented in Sec. 13.

Calculation of Liquid-to-Gas Ratio The minimum possible liquid rate is readily calculated from the composition of the entering gas and the solubility of the solute in the exit liquor, with equilibrium being assumed. It may be necessary to estimate the temperature of the exit liquid based upon the heat of solution of the solute gas. Values of latent heat and specific heat and values of heats of solution (at infinite dilution) are given in Sec. 2.

The actual liquid-to-gas ratio (solvent circulation rate) normally will be greater than the minimum by as much as 25 to 100 percent, and the estimated factor may be arrived at by economic considerations as well as judgment and experience. For example, in some packed-tower applications involving very soluble gases or vacuum operation, the minimum quantity of solvent needed to dissolve the solute may be insufficient to keep the packing surface thoroughly wet, leading to poor distribution of the liquid stream.

When the solvent concentration in the inlet gas is low and when a significant fraction of the solute is absorbed (this often the case), the approximation

$$y_1 G_M = x_1 L_M = (y_1^\circ/m)L_M \tag{14-3}$$

leads to the conclusion that the ratio mG_M/L_M represents the fractional approach of the exit liquid to saturation with the inlet gas, i.e.,

$$mG_M/L_M = y_1^\circ/y_1 \tag{14-4}$$

Optimization of the liquid-to-gas ratio in terms of total annual costs often suggests that the molar liquid-to-gas ratio L_M/G_M should be about 1.2 to 1.5 times the theoretical minimum corresponding to equilibrium at the rich end of the tower (infinite height or number of trays), provided flooding is not a problem. This, for example, would be an alternative to assuming that $L_M/G_M \approx m/0.7$.

When the exit-liquor temperature rises because of the heat of absorption of the solute, the value of m changes through the tower, and the liquid-to-gas ratio must be chosen to give reasonable values of m_1G_M/L_M and m_2G_M/L_M, where the subscripts 1 and 2 refer to the bottom and top of the absorber, respectively. For this case, the value of m_2G_M/L_M will be taken to be somewhat less than 0.7, so that the value of m_1G_M/L_M will not approach unity too closely. This rule-of-thumb approach is useful only when the solute concentration is low and heat effects are negligible.

When the solute has a large heat of solution or when the feed gas contains high concentrations of the solute, one should consider the use of internal cooling coils or intermediate liquid withdrawal and cooling to remove the heat of absorption.

Selection of Equipment Trays and random packings have been extensively used for gas absorption; structured packings are less common. Compared to trays, random packings have the advantages of availability in low-cost, corrosion-resistant materials (such as plastics and ceramics), low pressure drop (which can be an advantage when the tower is in the suction of a fan or compressor), easy and economic adaptability to small-diameter (less than 0.6-m or 2-ft) columns, and excellent handling of foams. Trays are much better for handling solids and fouling applications, offer greater residence time for slow absorption reactions, can better handle high L/G ratios and intermediate cooling, give better liquid turndown, and are more robust and less prone to reliability issues such as those resulting from poor distribution. Details on the operating characteristics of tray and packed towers are given later in this section.

Column Diameter and Pressure Drop Flooding determines the minimum possible diameter of the absorber column, and the usual design is for 60 to 80 percent of the flooding velocity. In near-atmospheric applications, pressure drop usually needs to be minimized to reduce the cost of energy for compression of the feed gas. For systems having a significant tendency to foam, the maximum allowable velocity will be lower than the estimated flooding velocity. Methods for predicting flooding velocities and pressure drops are given later in this section.

Computation of Tower Height The required height of a gas absorption or stripping tower for physical solvents depends on (1) the phase equilibria involved; (2) the specified degree of removal of the solute from the gas; and (3) the mass-transfer efficiency of the device. These three considerations apply to both tray and packed towers. Items 1 and 2 dictate the required number of theoretical stages (tray tower) or transfer units (packed tower). Item 3 is derived from the tray efficiency and spacing (tray tower) or from the height of one transfer unit (packed tower). Solute removal specifications are usually derived from economic considerations.

For tray towers, the approximate design methods described below may be used in estimating the number of theoretical stages, and the tray efficiencies and spacings for the tower can be specified on the basis of the information given later. Considerations involved in the rigorous design of theoretical stages for tray towers are treated in Sec. 13.

For packed towers, the continuous differential nature of the contact between gas and liquid leads to a design procedure involving the solution of differential equations, as described in the next subsection. Note that the design procedures discussed in this section are not applicable to reboiled absorbers, which should be designed according to the procedures described in Sec. 13.

Caution is advised in distinguishing between systems involving pure physical absorption and those in which chemical reactions can significantly affect design procedures. Chemical systems require additional procedures, as described later in this section.

Selection of Stripper Operating Conditions Stripping involves the removal of one or more components from the solvent through the application of heat or contacting it with a gas such as steam, nitrogen,

or air. The operating conditions chosen for stripping normally result in a low solubility of solute (i.e., high value of m), so that the ratio mG_M/L_M will be larger than unity. A value of 1.4 may be used for rule-of-thumb calculations involving pure physical absorption. For tray-tower calculations, the stripping factor $S = KG_M/L_M$, where $K = y^0/x$ usually is specified for each tray.

When the solvent from an absorption operation must be regenerated for recycling to the absorber, one may employ a "pressure-swing" or "temperature-swing" concept, or a combination of the two, in specifying the stripping operation. In pressure-swing operation, the temperature of the stripper is about the same as that of the absorber, but the stripping pressure is much lower. In temperature-swing operation, the pressures are about equal, but the stripping temperature is much higher than the absorption temperature.

In pressure-swing operation, a portion of the gas may be "sprung" from the liquid by the use of a flash drum upstream of the stripper feed point. This type of operation has been discussed by Burrows and Preece [*Trans. Inst. Chem. Eng.*, **32,** 99 (1954)] and by Langley and Haselden [*Inst. Chem. Eng. Symp. Ser. (London)*, no. 28 (1968)]. If the flashing of the liquid takes place inside the stripping tower, this effect must be accounted for in the design of the upper section in order to avoid overloading and flooding near the top of the tower.

Often the rate at which residual absorbed gas can be driven from the liquid in a stripping tower is limited by the rate of a chemical reaction, in which case the liquid-phase residence time (and hence the tower liquid holdup) becomes the most important design factor. Thus, many stripper regenerators are designed on the basis of liquid holdup rather than on the basis of mass-transfer rate.

Approximate design equations applicable only to the case of pure physical desorption are developed later in this section for both packed and tray stripping towers. A more rigorous approach using distillation concepts may be found in Sec. 13. A brief discussion of desorption with chemical reaction is given in the subsection "Absorption with Chemical Reaction."

Design of Absorber-Stripper Systems The solute-rich liquor leaving a gas absorber normally is distilled or stripped to regenerate the solvent for recirculation back to the absorber, as depicted in Fig. 14-3. It is apparent that the conditions selected for the absorption step (e.g., temperature, pressure, L_M/G_M) will affect the design of the stripping tower, and conversely, a selection of stripping conditions will affect the absorber design. The choice of optimum operating conditions for an absorber-stripper system therefore involves a combination of economic factors and practical judgments as to the operability of the system within the context of the overall process flow sheet. In Fig. 14-3, the stripping vapor is provided by a reboiler; alternately, an extraneous stripping gas may be used.

An appropriate procedure for executing the design of an absorber-stripper system is to set up a carefully selected series of design cases and then evaluate the investment costs, the operating costs, and the operability of each case. Some of the economic factors that need to be considered in selecting the optimum absorber-stripper design are discussed later in the subsection "Economic Design of Absorption Systems."

Importance of Design Diagrams One of the first things a designer should do is to lay out a carefully constructed equilibrium curve $y^0 = F(x)$ on an xy diagram, as shown in Fig. 14-4. A horizontal line corresponding to the inlet-gas composition y_1 is then the locus of feasible outlet-liquor compositions, and a vertical line corresponding to the inlet-solvent-liquor composition x_2 is the locus of outlet-gas compositions. These lines are indicated as $y = y_1$ and $x = x_2$, respectively on Fig. 14-4.

For gas absorption, the region of feasible operating lines lies above the equilibrium curve; for stripping, the feasible region for operating lines lies below the equilibrium curve. These feasible regions are bounded by the equilibrium curve and by the lines $x = x_2$ and $y = y_1$. By inspection, one should be able to visualize those operating lines that are feasible and those that would lead to "pinch points" within the tower. Also, it is possible to determine if a particular proposed design for solute recovery falls within the feasible envelope.

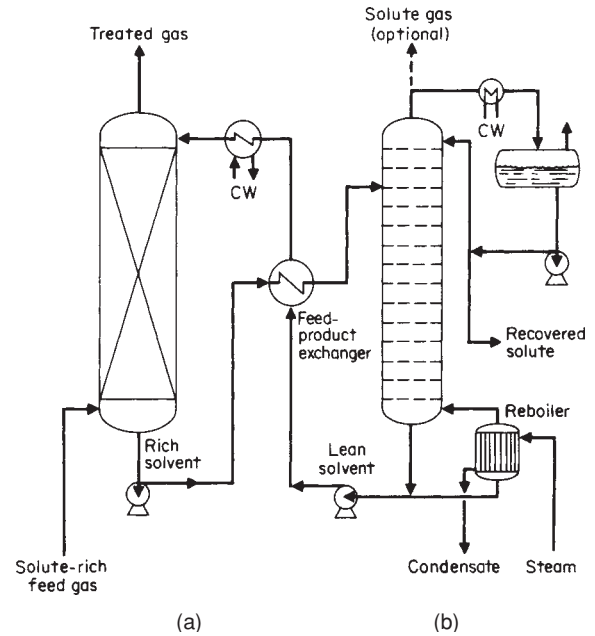

FIG. 14-3 Gas absorber using a solvent regenerated by stripping. (*a*) Absorber. (*b*) Stripper.

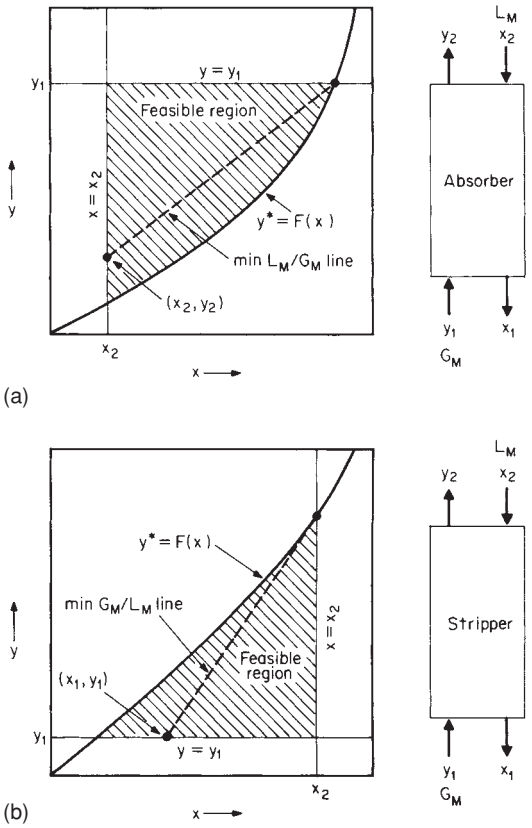

FIG. 14-4 Design diagrams for (*a*) absorption and (*b*) stripping.

Once the design recovery for an absorber has been established, the operating line can be constructed by first locating the point x_2, y_2 on the diagram. The intersection of the horizontal line corresponding to the inlet gas composition y_1 with the equilibrium curve $y^0 = F(x)$ defines the theoretical minimum liquid-to-gas ratio for systems in which there are no intermediate pinch points. This operating line which connects this point with the point x_2, y_2 corresponds to the minimum value of L_M/G_M. The actual design value of L_M/G_M should normally be around 1.2 to 1.5 times this minimum value. Thus, the actual design operating line for a gas absorber will pass through the point x_2, y_2 and will intersect the line $y = y_1$ to the left of the equilibrium curve.

For stripping one begins by using the design specification to locate the point x_1, y_1; then the intersection of the vertical line $x = x_2$ with the equilibrium curve $y^0 = F(x)$ defines the theoretical minimum gas-to-liquid ratio. The actual value of G_M/L_M is chosen to be about 20 to 50 percent higher than this minimum, so the actual design operating line will intersect the line $x = x_2$ at a point somewhat below the equilibrium curve.

PACKED-TOWER DESIGN

Methods for estimating the height of the active section of counterflow differential contactors such as packed towers, spray towers, and falling-film absorbers are based on rate expressions representing mass transfer at a point on the gas-liquid interface and on material balances representing the changes in bulk composition in the two phases that flow past each other. The rate expressions are based on the interphase mass-transfer principles described in Sec. 5. Combination of such expressions leads to an integral expression for the number of transfer units or to equations related closely to the number of theoretical stages. The paragraphs which follow set forth convenient methods for using such equations, first in a general case and then for cases in which simplifying assumptions are valid.

Use of Mass-Transfer-Rate Expression Figure 14-5 shows a section of a packed absorption tower together with the nomenclature that will be used in developing the equations that follow. In a differential section dh, we can equate the rate at which solute is lost from the gas phase to the rate at which it is transferred through the gas phase to the interface as follows:

$$-d(G_M y) = -G_M\,dy - y\,dG_M = N_A a\,dh \tag{14-5}$$

In Eq. (14-5), G_M is the gas-phase molar velocity [kmol/(s·m^2)], N_A is the mass-transfer flux [kmol/(s·m^2)], and a is the effective interfacial area (m^2/m^3).

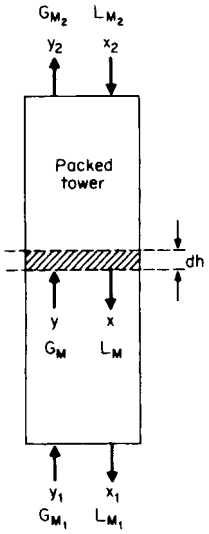

FIG. 14-5 Nomenclature for material balances in a packed-tower absorber or stripper.

When only one component is transferred,

$$dG_M = -N_A a\,dh \tag{14-6}$$

Substitution of this relation into Eq. (14-5) and rearranging yield

$$dh = -\frac{G_M\,dy}{N_A a\,(1-y)} \tag{14-7}$$

For this derivation we use the gas-phase rate expression $N_A = k_G(y - y_i)$ and integrate over the tower to obtain

$$h_T = \int_{y_2}^{y_1} \frac{G_M\,dy}{k_G a(1-y)(y-y_i)} \tag{14-8}$$

Multiplying and dividing by y_{BM} place Eq. (14-8) into the $H_G N_G$ format

$$h_T = \int_{y_2}^{y_1} \left(\frac{G_M}{k_G\,a y_{BM}}\right) \frac{y_{BM}\,dy}{(1-y)(y-y_i)}$$

$$= H_{G,\text{av}} \int_{y_2}^{y_1} \frac{y_{BM}\,dy}{(1-y)(y-y_i)} = H_{G,\text{av}} N_G \tag{14-9}$$

The general expression given by Eq. (14-8) is more complex than normally is required, but it must be used when the mass-transfer coefficient varies from point to point, as may be the case when the gas is not dilute or when the gas velocity varies as the gas dissolves. The values of y_i to be used in Eq. (14-8) depend on the local liquid composition x_i and on the temperature. This dependency is best represented by using the operating and equilibrium lines as discussed later.

Example 2 illustrates the use of Eq. (14-8) for scrubbing chlorine from air with aqueous caustic solution. For this case one can make the simplifying assumption that y_i, the interfacial partial pressure of chlorine over the caustic solution, is zero due to the rapid and complete reaction of the chlorine after it dissolves. We note that the feed gas is not dilute.

Example 2: Packed Height Requirement Let us compute the height of packing needed to reduce the chlorine concentration of 0.537 kg/(s·m^2), or 396 lb/(h·ft^2), of a chlorine-air mixture containing 0.503 mole-fraction chlorine to 0.0403 mole fraction. On the basis of test data described by Sherwood and Pigford (*Absorption and Extraction,* McGraw-Hill, 1952, p. 121) the value of $k_G a y_{BM}$ at a gas velocity equal to that at the bottom of the packing is equal to 0.1175 kmol/(s·m^3), or 26.4 lb·mol/(h·ft^3). The equilibrium back pressure y_i can be assumed to be negligible.

Solution. By assuming that the mass-transfer coefficient varies as the 0.8 power of the local gas mass velocity, we can derive the following relation:

$$\hat{K}_G a = k_G a y_{BM} = 0.1175 \left[\frac{71y + 29(1-y)}{71y_1 + 29(1-y_1)}\left(\frac{1-y_1}{1-y}\right)\right]^{0.8}$$

where 71 and 29 are the molecular weights of chlorine and air respectively. Noting that the inert-gas (air) mass velocity is given by $G'_M = G_M(1-y) = 5.34 \times 10^{-3}$ kmol/(s·m^2), or 3.94 lb·mol/(h·ft^2), and introducing these expressions into the integral gives

$$h_T = 1.82 \int_{0.0403}^{0.503} \left[\frac{1-y}{29+42y}\right]^{0.8} \frac{dy}{(1-y)^2 \ln\,[1/(1-y)]}$$

This definite integral can be evaluated numerically by the use of Simpson's rule to obtain $h_T = 0.305$ m (1 ft).

Use of Operating Curve Frequently, it is not possible to assume that $y_i = 0$ as in Example 2, due to diffusional resistance in the liquid phase or to the accumulation of solute in the liquid stream. When the backpressure cannot be neglected, it is necessary to supplement the equations with a material balance representing the operating line or curve. In view of the countercurrent flows into and from the differential section of packing shown in Fig. 14-5, a steady-state material balance leads to the following equivalent relations:

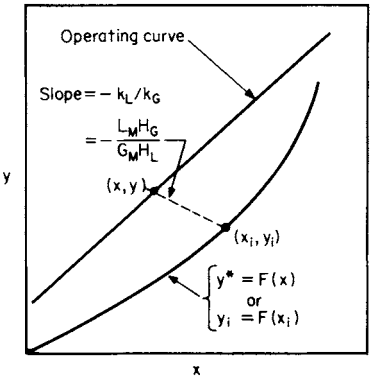

FIG. 14-6 Relationship between equilibrium curve and operating curve in a packed absorber; computation of interfacial compositions.

$$d(G_M y) = d(L_M x) \tag{14-10}$$

$$G'_M \frac{dy}{(1-y)^2} = L'_M \frac{dx}{(1-x)^2} \tag{14-11}$$

where L'_M = molar mass velocity of the inert-liquid component and G'_M = molar mass velocity of the inert gas; L_M, L'_M, G_M, and G'_M are superficial velocities based upon the total tower cross section.

Equation (14-11) is the differential equation of the operating curve, and its integral around the upper portion of the packing is the equation for the operating curve.

$$G'_M\left[\frac{y}{1-y} - \frac{y_2}{1-y_2}\right] = L'_M\left[\frac{x}{1-x} - \frac{x_2}{1-x_2}\right] \tag{14-12}$$

For dilute solutions in which the mole fractions of x and y are small, the total molar flows G_M and L_M will be nearly constant, and the operating-curve equation is

$$G_M(y - y_2) = L_M(x - x_2) \tag{14-13}$$

This equation gives the relation between the bulk compositions of the gas and liquid streams at each height in the tower for conditions in which the operating curve can be approximated as a straight line.

Figure 14-6 shows the relationship between the operating curve and the equilibrium curve $y_i = F(x_i)$ for a typical example involving solvent recovery, where y_i and x_i are the interfacial compositions (assumed to be in equilibrium). Once y is known as a function of x along the operating curve, y_i can be found at corresponding points on the equilibrium curve by

$$(y - y_i)/(x_i - x) = k_L/k_G = L_M H_G/G_M H_L \tag{14-14}$$

where L_M = molar liquid mass velocity, G_M = molar gas mass velocity, H_L = height of one transfer unit based upon liquid-phase resistance, and H_G = height of one transfer unit based upon gas-phase resistance. Using this equation, the integral in Eq. (14-8) can be evaluated.

Calculation of Transfer Units In the general case, the equations described above must be employed in calculating the height of packing required for a given separation. However, if the local mass-transfer coefficient $k_G a y_{BM}$ is approximately proportional to the first power of the local gas velocity G_M, then the height of one gas-phase transfer unit, defined as $H_G = G_M/k_G a y_{BM}$, will be constant in Eq. (14-9). Similar considerations lead to an assumption that the height of one overall gas-phase transfer unit H_{OG} may be taken as constant. The height of packing required is then calculated according to the relation

$$h_T = H_G N_G = H_{OG} N_{OG} \tag{14-15}$$

where N_G = number of gas-phase transfer units and N_{OG} = number of overall gas-phase transfer units. When H_G and H_{OG} are not constant, it may be valid to employ averaged values between the top and bottom of the tower and the relation

$$h_T = H_{G,av} N_G = H_{OG,av} N_{OG} \tag{14-16}$$

In these equations, the terms N_G and N_{OG} are defined by Eqs. (14-17) and (14-18).

$$N_G = \int_{y_2}^{y_1} \frac{y_{BM}\,dy}{(1-y)(y-y_i)} \tag{14-17}$$

$$N_{OG} = \int_{y_2}^{y_1} \frac{y^o_{BM}\,dy}{(1-y)(y-y^o)} \tag{14-18}$$

Equation (14-18) is the more useful one in practice. It requires either actual experimental H_{OG} data or values estimated by combining individual measurements of H_G and H_L by Eq. (14-19). Correlations for H_G, H_L, and H_{OG} in nonreacting systems are presented in Sec. 5.

$$H_{OG} = \frac{y_{BM}}{y^o_{BM}} H_G + \frac{mG_M}{L_M}\frac{x_{BM}}{y^o_{BM}} H_L \tag{14-19a}$$

$$H_{OL} = \frac{x_{BM}}{x^o_{BM}} H_L + \frac{L_M}{mG_M}\frac{y_{BM}}{x^o_{BM}} H_G \tag{14-19b}$$

On occasion, the changes in gas flow and in the mole fraction of inert gas can be neglected so that inclusion of terms such as $1 - y$ and y^0_{BM} can be approximated, as is shown below.

One such simplification was suggested by Wiegand [*Trans. Am. Inst. Chem. Eng.*, **36,** 679 (1940)], who pointed out that the logarithmic-mean mole fraction of inert gas y^0_{BM} (or y_{BM}) is often very nearly equal to the arithmetic mean. Thus, substitution of the relation

$$\frac{y^o_{BM}}{(1-y)} = \frac{(1-y^o)+(1-y)}{2(1-y)} = \frac{y-y^o}{2(1-y)} + 1 \tag{14-20}$$

into the equations presented above leads to the simplified forms

$$N_G = \frac{1}{2}\ln\frac{1-y_2}{1-y_1} + \int_{y2}^{y1}\frac{dy}{y-y_i} \tag{14-21}$$

$$N_{OG} = \frac{1}{2}\ln\frac{1-y_2}{1-y_1} + \int_{y2}^{y1}\frac{dy}{y-y^o} \tag{14-22}$$

The second (integral) terms represent the numbers of transfer units for an infinitely dilute gas. The first terms, usually only a small correction, give the effect of a finite level of gas concentration.

The procedure for applying Eqs. (14-21) and (14-22) involves two steps: (1) evaluation of the integrals and (2) addition of the correction corresponding to the first (logarithmic) term. The discussion that follows deals only with the evaluation of the integral term (first step).

The simplest possible case occurs when (1) both the operating and equilibrium lines are straight (i.e., the solutions are dilute); (2) Henry's law is valid ($y^0/x = y_i/x_i = m$); and (3) absorption heat effects are negligible. Under these conditions, the integral term in Eq. (14-21) may be computed by Colburn's equation [*Trans. Am. Inst. Chem. Eng.*, **35,** 211 (1939)]:

$$N_{OG} = \frac{1}{1 - mG_M/L_M}\ln\left[\left(1 - \frac{mG_M}{L_M}\right)\left(\frac{y_1 - mx_2}{y_2 - mx_2}\right) + \frac{mG_M}{L_M}\right] \tag{14-23}$$

Figure 14-7 is a plot of Eq. (14-23) from which the value of N_{OG} can be read directly as a function of mG_M/L_M and the ratio of concentrations. This plot and Eq. (14-23) are equivalent to the use of a logarithmic mean of terminal driving forces, but they are more convenient because one does not need to compute the exit-liquor concentration x_1.

In many practical situations involving nearly complete cleanup of the gas, an approximate result can be obtained from the equations just presented even when the simplifications are not valid, i.e., solutions are concentrated and heat effects occur. In such cases the driving forces in the upper part of the tower are very much smaller than those at the bottom, and the value of mG_M/L_M used in the equations should be the ratio of the operating line L_M/G_M in the low-concentration region near the top of the tower.

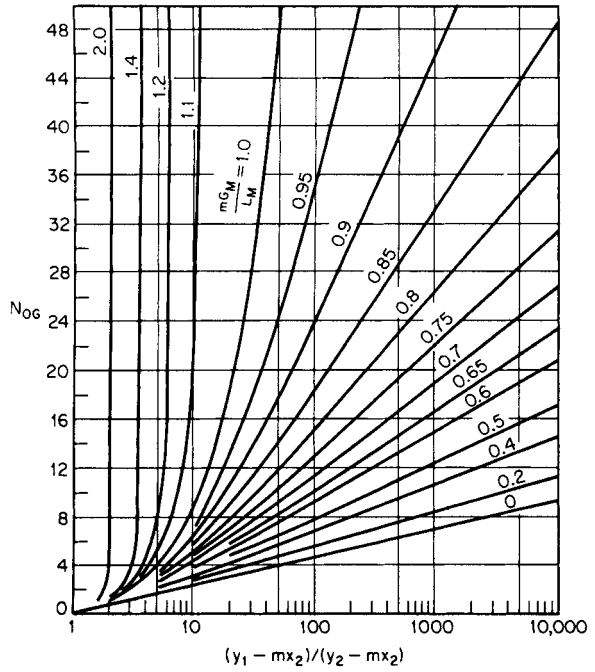

FIG. 14-7 Number of overall gas-phase mass-transfer units in a packed absorption tower for constant mG_M/L_M; solution of Eq. (14-23). (*From Sherwood and Pigford,* Absorption and Extraction, *McGraw-Hill, New York, 1952.*)

Another approach is to divide the tower arbitrarily into a lean section (near the top) where approximate methods are valid, and to deal with the rich section separately. If the heat effects in the rich section are appreciable, consideration should be given to installing cooling units near the bottom of the tower. In any event, a design diagram showing the operating and equilibrium curves should be prepared to check the applicability of any simplified procedure. Figure 14-10, presented in Example 6, is one such diagram for an adiabatic absorption tower.

Stripping Equations Stripping or desorption involves the removal of a volatile component from the liquid stream by contact with an inert gas such as nitrogen or steam or the application of heat. Here the change in concentration of the liquid stream is of prime importance, and it is more convenient to formulate the rate equation analogous to Eq. (14-6) in terms of the liquid composition x. This leads to the following equations defining the number of transfer units and height of transfer units based on liquid-phase resistance:

$$h_T = H_L \int_{x_2}^{x_1} \frac{x_{BM}\,dx}{(1-x)(x_i - x)} = H_L N_L \tag{14-24}$$

$$h_T H_{OL} \int_{x_2}^{x_1} \frac{x^0_{BM}\,dx}{(1-x)(x^o - x)} = H_{OL} N_{OL} \tag{14-25}$$

where, as before, subscripts 1 and 2 refer to the bottom and top of the tower, respectively (see Fig. 14-5).

In situations where one cannot assume that H_L and H_{OL} are constant, these terms need to be incorporated inside the integrals in Eqs. (14-24) and (14-25), and the integrals must be evaluated numerically (using Simpson's rule, for example). In the normal case involving stripping without chemical reactions, the liquid-phase resistance will dominate, making it preferable to use Eq. (14-25) together with the approximation $H_L \approx H_{OL}$.

The Weigand approximations of the above integrals, in which arithmetic means are substituted for the logarithmic means (x_{BM} and x^0_{BM}), are

$$N_L = \frac{1}{2} \ln \frac{1-x_1}{1-x_2} + \int_{x_1}^{x_2} \frac{dx}{x - x_i} \tag{14-26}$$

$$N_{OL} = \frac{1}{2} \ln \frac{1-x_1}{1-x_2} + \int_{x_1}^{x_2} \frac{dx}{x - x^o} \tag{14-27}$$

In these equations, the first term is a correction for finite liquid-phase concentrations, and the integral term represents the numbers of transfer units required for dilute solutions. In most practical stripper applications, the first (logarithmic) term is relatively small.

For dilute solutions in which both the operating and the equilibrium lines are straight and in which heat effects can be neglected, the integral term in Eq. (14-27) is

$$N_{OL} = \frac{1}{1 - L_M/mG_M} \ln \left[\left(1 - \frac{L_M}{mG_M}\right) \left(\frac{x_2 - y_1/m}{x_1 - y_1/m} \right) + \frac{L_M}{mG_M} \right] \tag{14-28}$$

This equation is analogous to Eq. (14-23). Thus, Fig. 14-7 is applicable if the concentration ratio $(x_2 - y_1/m)/(x_1 - y_1/m)$ is substituted for the abscissa and the parameter on the curves is identified as L_M/mG_M.

Example 3: Air Stripping of VOCs from Water A 0.45-m diameter packed column was used by Dvorack et al. [*Environ. Sci. Tech.* **20,** 945 (1996)] for removing trichloroethylene (TCE) from wastewater by stripping with atmospheric air. The column was packed with 25-mm Pall rings, fabricated from polypropylene, to a height of 3.0 m. The TCE concentration in the entering water was 38 parts per million by weight (ppmw). A molar ratio of entering water to entering air was kept at 23.7. What degree of removal was to be expected? The temperatures of water and air were 20°C. Pressure was atmospheric.

Solution. For TCE in water, the Henry's law coefficient may be taken as 417 atm/mf at 20°C. In this low-concentration region, the coefficient is constant and equal to the slope of the equilibrium line m. The solubility of TCE in water, based on $H = 417$ atm, is 2390 ppm. Because of this low solubility, the entire resistance to mass transfer resides in the liquid phase. Thus, Eq. (14-25) may be used to obtain N_{OL}, the number of overall liquid phase transfer units.

In the equation, the ratio $x_{BM}/(1-x)$ is unity because of the very dilute solution. It is necessary to have a value of H_L for the packing used, at given flow rates of liquid and gas. Methods for estimating H_L may be found in Sec. 5. Dvorack et al. found $H_{OL} = 0.8$ m. Then, for $h_T = 3.0$ m, $N_L = N_{OL} = 3.0/0.8 = 3.75$ transfer units.

Transfer units may be calculated from Eq. 14-25, replacing mole fractions with ppm concentrations, and since the operating and equilibrium lines are straight,

$$N_{OL} = \frac{38 - (\text{ppm})_{\text{exit}}}{\ln 38/(\text{ppm})_{\text{exit}}} = 3.75$$

Solving, $(\text{ppm})_{\text{exit}} = 0.00151$. Thus, the stripped water would contain 1.51 parts per billion of TCE.

Use of HTU and $K_G a$ Data In estimating the size of a commercial gas absorber or liquid stripper it is desirable to have data on the overall mass-transfer coefficients (or heights of transfer units) for the system of interest, and at the desired conditions of temperature, pressure, solute concentration, and fluid velocities. Such data should best be obtained in an apparatus of pilot-plant or semiworks size to avoid the abnormalities of scale-up. Within the packing category, there are both random and ordered (structured) packing elements. Physical characteristics of these devices will be described later.

When no $K_G a$ or HTU data are available, their values may be estimated by means of a generalized model. A summary of useful models is given in Sec. 5. The values obtained may then be combined by use of Eq. (14-19) to obtain values of H_{OG} and H_{OL}. This simple procedure is not valid when the rate of absorption is limited by chemical reaction.

Use of HETP Data for Absorber Design Distillation design methods (see Sec. 13) normally involve determination of the number of theoretical equilibrium stages N. Thus, when packed towers are employed in distillation applications, it is common practice to rate the efficiency of tower packings in terms of the height of packing equivalent to one theoretical stage (HETP).

The HETP of a packed-tower section, valid for either distillation or dilute-gas absorption and stripping systems in which constant molal overflow can be assumed and in which no chemical reactions occur, is related to the height of one overall gas-phase mass-transfer unit H_{OG} by the equation

$$\text{HETP} = H_{OG} \frac{\ln (mG_M/L_M)}{(mG_M/L_M - 1)} \tag{14-29}$$

For gas absorption systems in which the inlet gas is concentrated, the corrected equation is

$$\text{HETP} = \left(\frac{y^o_{BM}}{1-y} \right)_{\text{av}} H_{OG} \frac{\ln (mG_M/L_M)}{mG_M/L_M - 1} \tag{14-30}$$

where the correction term $y^0_{BM}/(1-y)$ is averaged over each individual theoretical stage. The equilibrium compositions corresponding to each theoretical stage may be estimated by the methods described in the next subsection, "Tray-Tower Design." These compositions are used in conjunction with the local values of the gas and liquid flow rates and the equilibrium slope m to obtain values for H_G, H_L, and H_{OG} corresponding to the conditions on each theoretical stage, and the local values of the HETP are then computed by Eq. (14-30). The total height of packing required for the separation is the summation of the individual HETPs computed for each theoretical stage.

TRAY-TOWER DESIGN

The design of a tray tower for gas absorption and gas-stripping operations involves many of the same principles employed in distillation calculations, such as the determination of the number of theoretical trays needed to achieve a specified composition change (see Sec. 13). Distillation differs from absorption because it involves the separation of components based upon the distribution of the various substances between a vapor phase and a liquid phase when all components are present in both phases. In distillation, the new phase is generated from the original phase by the vaporization or condensation of the volatile components, and the separation is achieved by introducing reflux to the top of the tower.

In gas absorption, the new phase consists of a relatively nonvolatile solvent (absorption) or a relatively insoluble gas (stripping), and normally no reflux is involved. This section discusses some of the considerations peculiar to gas absorption calculations for tray towers and some of the approximate design methods that can be applied (when simplifying assumptions are valid).

Graphical Design Procedure Construction of design diagrams (xy curves showing the equilibrium and operating curves) should be an integral part of any design involving the distribution of a single solute between an inert solvent and an inert gas. The number of theoretical trays can be stepped off rigorously, provided the curvatures of the operating and equilibrium lines are correctly represented in the diagram. The procedure is valid even though an inert solvent is present in the liquid phase and an inert gas is present in the vapor phase.

Figure 14-8 illustrates the graphical method for a three theoretical stage system. Note that in gas absorption the operating line is above the equilibrium curve, whereas in distillation this does not happen. In gas stripping, the operating line will be below the equilibrium curve.

On Fig. 14-8, note that the stepping-off procedure begins on the operating line. The starting point x_f, y_3 represents the compositions of the entering lean wash liquor and of the gas exiting from the top of the tower, as defined by the design specifications. After three steps one reaches the point x_1, y_f representing the compositions of the solute-rich feed gas y_f and of the solute-rich liquor leaving the bottom of the tower x_1.

Algebraic Method for Dilute Gases By assuming that the operating and equilibrium curves are straight lines and that heat effects are negligible, Souders and Brown [*Ind. Eng. Chem.*, **24,** 519 (1932)] developed the following equation:

$$(y_1 - y_2)/(y_1 - y_2^o) = (A^{N+1} - A)/(A^{N+1} - 1) \tag{14-31}$$

where N = number of theoretical trays, y_1 = mole fraction of solute in the entering gas, y_2 = mole fraction of solute in the leaving gas, $y_2^0 = mx_2$ = mole fraction of solute in equilibrium with the incoming solvent

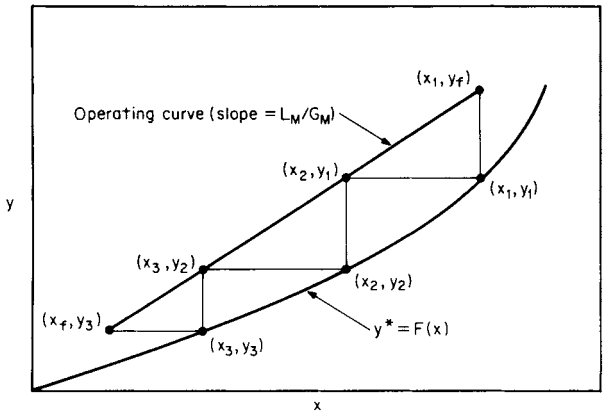

FIG. 14-8 Graphical method for a three-theoretical-plate gas-absorption tower with inlet-liquor composition x_f and inlet-gas composition y_f.

(zero for a pure solvent), and A = absorption factor = L_M/mG_M. Note that the absorption factor is the reciprocal of the expression given in Eq. (14-4) for packed columns.

Note that for the limiting case of $A = 1$, the solution is given by

$$(y_1 - y_2)/(y_1 - y_2^o) = N/(N+1) \tag{14-32}$$

Although Eq. (14-31) is convenient for computing the composition of the exit gas as a function of the number of theoretical stages, an alternative equation derived by Colburn [*Trans. Am. Inst. Chem. Eng.*, **35,** 211 (1939)] is more useful when the number of theoretical plates is the unknown:

$$N = \frac{\ln [(1 - A^{-1})(y_1 - y_2^o)/(y_2 - y_2^o) + A^{-1}]}{\ln (A)} \tag{14-33}$$

The numerical results obtained by using either Eq. (14-31) or Eq. (14-33) are identical. Thus, the two equations may be used interchangeably as the need arises.

Comparison of Eqs. (14-33) and (14-23) shows that

$$N_{OG}/N = \ln (A)/(1 - A^{-1}) \tag{14-34}$$

thus revealing the close relationship between theoretical stages in a plate tower and mass-transfer units in a packed tower. Equations (14-23) and (14-33) are related to each other by virtue of the relation

$$h_T = H_{OG} N_{OG} = (\text{HETP}) N \tag{14-35}$$

Algebraic Method for Concentrated Gases When the feed gas is concentrated, the absorption factor, which is defined in general as $A = L_M/KG_M$ and where $K = y^0/x$, can vary throughout the tower due to changes in temperature and composition. An approximate solution to this problem can be obtained by substituting the "effective" adsorption factors A_e and A' derived by Edmister [*Ind. Eng. Chem.* **35,** 837 (1943)] into the equation

$$\frac{y_1 - y_2}{y_1} = \left[1 - \frac{1}{A'} \frac{(L_M x)_2}{(G_M y)_1} \right] \frac{A_e^{N+1} - A_e}{A_e^{N+1} - 1} \tag{14-36}$$

where subscripts 1 and 2 refer to the bottom and top of the tower, respectively, and the absorption factors are defined by the equations

$$A_e = \sqrt{A_1(A_2 + 1) + 0.25} - 0.5 \tag{14-37}$$

$$A' = A_1(A_2 + 1)/(A_1 + 1) \tag{14-38}$$

This procedure has been applied to the absorption of C_5 and lighter hydrocarbon vapors into a lean oil, for example.

Stripping Equations When the liquid feed is dilute and the operating and equilibrium curves are straight lines, the stripping equations analogous to Eqs. (14-31) and (14-33) are

$$(x_2 - x_1)/(x_2 - x_1^0) = (S^{N+1} - S)/(S^{N+1} - 1) \tag{14-39}$$

where $x_1^0 = y_1/m$; $S = mG_M/L_M = A^{-1}$; and

$$N = \frac{\ln [(1 - A)(x_2 - x_1^0)/(x_1 - x_1^0) + A]}{\ln (S)} \tag{14-40}$$

For systems in which the concentrations are large and the stripping factor S may vary along the tower, the following Edmister equations [*Ind. Eng. Chem.*, **35,** 837 (1943)] are applicable:

$$\frac{x_2 - x_1}{x_2} = \left[1 - \frac{1}{S'} \frac{(G_M y)_1}{(L_M x)_2}\right] \frac{S_e^{N+1} - S_e}{S_e^{N+1} - 1} \tag{14-41}$$

where

$$S_e = \sqrt{S_2(S_1 + 1) + 0.25} - 0.5 \tag{14-42}$$

$$S' = S_2(S_1 + 1)/(S_2 + 1) \tag{14-43}$$

and the subscripts 1 and 2 refer to the bottom and top of the tower respectively.

Equations (14-37) and (14-42) represent two different ways of obtaining an effective factor, and a value of A_e obtained by taking the reciprocal of S_e from Eq. (14-42) will not check exactly with a value of A_e derived by substituting $A_1 = 1/S_1$ and $A_2 = 1/S_2$ into Eq. (14-37). Regardless of this fact, the equations generally give reasonable results for approximate design calculations.

It should be noted that throughout this section the subscripts 1 and 2 refer to the bottom and to the top of the apparatus respectively regardless of whether it is an absorber or a stripper. This has been done to maintain internal consistency among all the equations and to prevent the confusion created in some derivations in which the numbering system for an absorber is different from the numbering system for a stripper.

Tray Efficiencies in Tray Absorbers and Strippers Computations of the theoretical trays N assume that the liquid on each tray is completely mixed and that the vapor leaving the tray is in equilibrium with the liquid. In practice, complete equilibrium cannot exist since interphase mass transfer requires a finite driving force. This leads to the definition of an overall tray efficiency

$$E = N_{\text{theoretical}}/N_{\text{actual}} \tag{14-44}$$

which can be correlated with the system design variables.

Mass-transfer theory indicates that for trays of a given design, the factors that have the biggest influence on E in absorption and stripping towers are the physical properties of the fluids and the dimensionless ratio mG_M/L_M. Systems in which mass transfer is gas-film-controlled may be expected to have efficiencies as high as 50 to 100 percent, whereas tray efficiencies as low as 1 percent have been reported for the absorption of low-solubility (large-m) gases into solvents of high viscosity.

The fluid properties of interest are represented by the Schmidt numbers of the gas and liquid phases. For gases, the Schmidt numbers are normally close to unity and independent of temperature and pressure. Thus, gas-phase mass-transfer coefficients are relatively independent of the system.

By contrast, the liquid-phase Schmidt numbers range from about 10^2 to 10^4 and depend strongly on temperature. The temperature dependence of the liquid-phase Schmidt number derives primarily from the strong dependence of the liquid viscosity on temperature.

Consideration of the preceding discussion in connection with the relationship between mass-transfer coefficients (see Sec. 5)

$$1/K_G = 1/k_G + m/k_L \tag{14-45}$$

indicates that the variations in the overall resistance to mass transfer in absorbers and strippers are related primarily to variations in the liquid-phase viscosity μ and the slope m. O'Connell [*Trans. Am. Inst. Chem. Eng.*, **42,** 741 (1946)] used the above findings and correlated the tray efficiency in terms of the liquid viscosity and the gas solubility. The O'Connell correlation for absorbers (Fig. 14-9) has Henry's law constant in lb·mol/(atm·ft^3), the pressure in atmospheres, and the liquid viscosity in centipoise.

The best procedure for making tray efficiency corrections (which can be quite significant, as seen in Fig. 14-9) is to use experimental data from a prototype system that is large enough to be representative of the actual commercial tower.

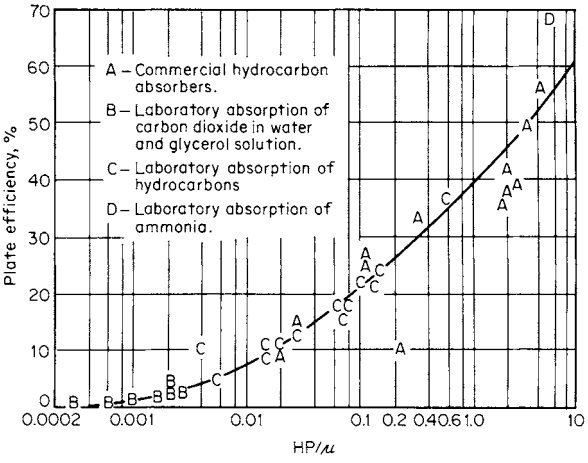

FIG. 14-9 O'Connell correlation for overall column efficiency E_{oc} for absorption. H is in lb·mol/(atm·ft^3), P is in atm, and μ is in cP. To convert HP/μ in pound-moles per cubic foot-centipoise to kilogram-moles per cubic meter-pascal-second, multiply by 1.60×10^4. [*O'Connell*, Trans. Am. Inst. Chem. Eng., ***42,*** 741 (*1946*).]

Example 4: Actual Trays for Steam Stripping The number of actual trays required for steam-stripping an acetone-rich liquor containing 0.573 mole percent acetone in water is to be estimated. The design overhead recovery of acetone is 99.9 percent, leaving 18.5 ppm weight of acetone in the stripper bottoms. The design operating temperature and pressure are 101.3 kPa and 94°C respectively, the average liquid-phase viscosity is 0.30 cP, and the average value of $K = y°/x$ for these conditions is 33.

By choosing a value of $mG_M/L_M = S = A^{-1} = 1.4$ and noting that the stripping medium is pure steam (i.e., $x_1° = 0$), the number of theoretical trays according to Eq. (14-40) is

$$N = \frac{\ln [(1 - 0.714)(1000) + 0.714]}{\ln (1.4)} = 16.8$$

The O'Connell parameter for gas absorbers is $\rho_L/KM\mu_L$, where ρ_L is the liquid density, lb/ft^3; μ_L is the liquid viscosity, cP; M is the molecular weight of the liquid; and $K = y°/x$. For the present design

$$\rho_L/KM\mu_L = 60.1/(33 \times 18 \times 0.30) = 0.337$$

and according to the O'Connell graph for absorbers (Fig. 14-7) the overall tray efficiency for this case is estimated to be 30 percent. Thus, the required number of actual trays is 16.8/0.3 = 56 trays.

HEAT EFFECTS IN GAS ABSORPTION

Overview One of the most important considerations involved in designing gas absorption towers is to determine whether temperatures will vary along the height of the tower due to heat effects; note that the solute solubility usually depends strongly on temperature. The simplified design procedures described earlier in this section become more complicated when heat effects cannot be neglected. The role of this section is to enable understanding and design of gas absorption towers where heat effects are important and cannot be ignored.

Heat effects that cause temperatures to vary from point to point in a gas absorber are (1) the heat of solution (including heat of condensation, heat of mixing, and heat of reaction); (2) the heat of vaporization or condensation of the solvent; (3) the exchange of sensible heat between the gas and liquid phases; and (4) the loss of sensible heat from the fluids to internal or external coils.

There are a number of systems where heat effects definitely cannot be ignored. Examples include the absorption of ammonia in

water, dehumidification of air using concentrated H_2SO_4, absorption of HCl in water, absorption of SO_3 in H_2SO_4, and absorption of CO_2 in alkanolamines. Even for systems where the heat effects are mild, they may not be negligible; an example is the absorption of acetone in water.

Thorough and knowledgeable discussions of the problems involved in gas absorption with significant heat effects have been presented by Coggan and Bourne [*Trans. Inst. Chem. Eng.*, **47,** T96, T160 (1969)]; Bourn, von Stockar, and Coggan [*Ind. Eng. Chem. Proc. Des. Dev.*, **13,** 115, 124 (1974)]; and von Stockar and Wilke [*Ind. Eng. Chem. Fundam.*, **16,** 89 (1977)]. The first two of these references discuss tray-tower absorbers and include experimental studies of the absorption of ammonia in water. The third reference discusses the design of packed-tower absorbers and includes a shortcut design method based on a semitheoretical correlation of rigorous design calculations. All these authors demonstrate that when the solvent is volatile, the temperature inside an absorber can go through a maximum. They note that the least expensive and most common of solvents—water—is capable of exhibiting this "hot-spot" behavior.

Several approaches may be used in modeling absorption with heat effects, depending on the job at hand: (1) treat the process as isothermal by assuming a particular temperature, then add a safety factor; (2) employ the classical adiabatic method, which assumes that the heat of solution manifests itself only as sensible heat in the liquid phase and that the solvent vaporization is negligible; (3) use semitheoretical shortcut methods derived from rigorous calculations; and (4) employ rigorous methods available from a process simulator.

While simpler methods are useful for understanding the key effects involved, rigorous methods are recommended for final designs. This subsection also discusses the range of safety factors that are required if simpler methods are used.

Effects of Operating Variables Conditions that give rise to significant heat effects are (1) an appreciable heat of solution and/or (2) absorption of large amounts of solute in the liquid phase. The second condition is favored when the solute concentration in the inlet gas is large, when the liquid flow rate is relatively low (small L_M/G_M), when the solubility of the solute in the liquid is high, and/or when the operating pressure is high.

If the solute-rich gas entering the bottom of an absorber tower is cold, the liquid phase may be cooled somewhat by transfer of sensible heat to the gas. A much stronger cooling effect can occur when the solute is volatile and the entering gas is not saturated with respect to the solvent. It is possible to experience a condition in which solvent is being evaporated near the bottom of the tower and condensed near the top. Under these conditions a pinch point may develop in which the operating and equilibrium curves approach each other at a point inside the tower.

In the references previously cited, the authors discuss the influence of operating variables upon the performance of towers when large heat effects are involved. Some key observations are as follows:

Operating Pressure Raising the pressure may increase the separation effectiveness considerably. Calculations for the absorption of methanol in water from water-saturated air showed that doubling the pressure doubles the allowable concentration of methanol in the feed gas while still achieving the required concentration specification in the off gas.

Temperature of Lean Solvent The temperature of the entering (lean) solvent has surprisingly little influence upon the temperature profile in an absorber since any temperature changes are usually caused by the heat of solution or the solvent vaporization. In these cases, the temperature profile in the liquid phase is usually dictated solely by the internal-heat effects.

Temperature and Humidity of the Rich Gas Cooling and consequent dehumidification of the feed gas to an absorption tower can be very beneficial. A high humidity (or relative saturation with the solvent) limits the capacity of the gas to take up latent heat and hence is unfavorable to absorption. Thus dehumidification of the inlet gas is worth considering in the design of absorbers with large heat effects.

Liquid-to-Gas Ratio The *L/G* ratio can have a significant influence on the development of temperature profiles in gas absorbers. High *L/G* ratios tend to result in less strongly developed temperature profiles due to the increased heat capacity of the liquid phase. As the *L/G* ratio is increased, the operating line moves away from the equilibrium line and more solute is absorbed per stage or packing segment. However, there is a compensating effect; since more heat is liberated in each stage or packing segment, the temperatures will rise, which causes the equilibrium line to shift up. As the *L/G* ratio is decreased, the concentration of solute tends to build up in the upper part of the absorber, and the point of highest temperature tends to move upward in the tower until finally the maximum temperature occurs at the top of the tower. Of course, the capacity of the liquid to absorb solute falls progressively as *L/G* is reduced.

Number of Stages or Packing Height When the heat effects combine to produce an extended zone in the tower where little absorption takes place (i.e., a pinch zone), the addition of trays or packing height will have no useful effect on separation efficiency. In this case, increases in absorption may be obtained by increasing solvent flow, introducing strategically placed coolers, cooling and dehumidifying the inlet gas, and/or raising the tower pressure.

Equipment Considerations When the solute has a large heat of solution and the feed gas contains a high concentration of solute, as in absorption of HCl in water, the effects of heat release during absorption may be so pronounced that the installation of heat-transfer surface to remove the heat of absorption may be as important as providing sufficient interfacial area for the mass-transfer process itself. The added heat-transfer area may consist of internal cooling coils on the trays, or the liquid may be withdrawn from the tower, cooled in an external heat exchanger, and then returned to the tower.

In many cases the rate of heat liberation is largest near the bottom of the tower, where the solute absorption is more rapid, so that cooling surfaces or intercoolers are required only at the lower part of the column. Coggan and Bourne [*Trans. Inst. Chem. Eng.*, **47,** T96, T160 (1969)] found, however, that the optimal position for a single interstage cooler does not necessarily coincide with the position of the maximum temperature of the center of the pinch. They found that in a 12-tray tower, two strategically placed interstage coolers tripled the allowable ammonia feed concentration for a given off-gas specification. For a case involving methanol absorption, it was found that greater separation was possible in a 12-stage column with two intercoolers than in a simple column with 100 stages and no intercoolers.

In the case of HCl absorption, a shell-and-tub heat exchanger often is employed as a cooled wetted-wall vertical-column absorber so that the exothermic heat of reaction can be removed continuously as it is released into a liquid film.

Installation of heat-exchange equipment to precool and dehumidify the feed gas to an absorber also deserves consideration, in order to take advantage of the cooling effects created by vaporization of solvent in the lower sections of the tower.

Classical Isothermal Design Method When the feed gas is sufficiently dilute, the exact design solution may be approximated by the isothermal one over the broad range of *L/G* ratios, since heat effects are generally less important when washing dilute-gas mixtures. The problem, however, is one of defining the term *sufficiently dilute* for each specific case. For a new absorption duty, the assumption of isothermal operation must be subjected to verification by the use of a rigorous design procedure.

When heat-exchange surface is being provided in the design of an absorber, the isothermal design procedure can be rendered valid by virtue of the exchanger design specification. With ample surface area and a close approach, isothermal operation can be guaranteed.

For preliminary screening and feasibility studies or for rough estimates, one may wish to employ a version of the isothermal design method which assumes that the liquid temperatures in the tower are everywhere equal to the inlet-liquid temperature. In their analysis of packed-tower designs, von Stockar and Wilke [*Ind. Eng. Chem. Fundam.*, **16,** 89 (1977)] showed that the isothermal method tended to underestimate the required height of packing by a factor of as much as

1.5 to 2. Thus, for rough estimates one may wish to employ the assumption that the absorber temperature is equal to the inlet-liquid temperature and then apply a design factor to the result.

Another instance in which the constant-temperature method is used involved the direct application of experimental K_Oa values obtained at the desired conditions of inlet temperatures, operating pressures, flow rates, and feed-stream compositions. The assumption here is that, regardless of any temperature profiles that may exist within the actual tower, the procedure of "working the problem in reverse" will yield a correct result. One should, however, be cautious about extrapolating such data from the original basis and be careful to use compatible equilibrium data.

Classical Adiabatic Design Method The classical adiabatic design method assumes that the heat of solution serves only to heat up the liquid stream and there is no vaporization of the solvent. This assumption makes it feasible to relate increases in the liquid-phase temperature to the solute concentration x by a simple enthalpy balance. The equilibrium curve can then be adjusted to account for the corresponding temperature rise on an xy diagram. The adjusted equilibrium curve will be concave upward as the concentration increases, tending to decrease the driving forces near the bottom of the tower, as illustrated in Fig. 14-10 in Example 6.

Colburn [*Trans. Am. Inst. Chem. Eng.*, **35,** 211 (1939)] has shown that when the equilibrium line is straight near the origin but curved slightly at its upper end, N_{OG} can be computed approximately by assuming that the equilibrium curve is a parabolic arc of slope m_2 near the origin and passing through the point x_1, K_1x_1 at the upper end. The Colburn equation for this case is

$$N_{OG} = \frac{1}{1 - m_2G_M/L_M} \times \ln\left[\frac{(1 - m_2G_M/L_M)^2}{1 - K_1G_M/L_M}\left(\frac{y_1 - m_2x_2}{y_2 - m_2x_2}\right) + \frac{m_2G_M}{L_M}\right] \quad (14\text{-}46)$$

Comparison by von Stockar and Wilke [*Ind. Eng. Chem. Fundam.*, **16,** 89 (1977)] between the rigorous and the classical adiabatic design methods for packed towers indicates that the simple adiabatic design methods underestimate packing heights by as much as a factor of 1.25 to 1.5. Thus, when using the classical adiabatic method, one should probably apply a design safety factor.

A slight variation of the above method accounts for increases in the solvent content of the gas stream between the inlet and the outlet of the tower and assumes that the evaporation of solvent tends to cool the liquid. This procedure offsets a part of the temperature rise that would have been predicted with no solvent evaporation and leads to the prediction of a shorter tower.

Rigorous Design Methods A detailed discussion of rigorous methods for the design of packed and tray absorbers when large heat effects are involved is beyond the scope of this subsection. In principle, material and energy balances may be executed under the same constraints as for rigorous distillation calculations (see Sec. 13). Further discussion on this subject is given in the subsection "Absorption with Chemical Reaction."

Direct Comparison of Design Methods The following problem, originally presented by Sherwood, Pigford, and Wilke (*Mass Transfer*, McGraw-Hill, New York, 1975, p. 616) was employed by von Stockar and Wilke (op. cit.) as the basis for a direct comparison between the isothermal, adiabatic, semitheoretical shortcut, and rigorous design methods for estimating the height of packed towers.

Example 5: Packed Absorber, Acetone into Water Inlet gas to an absorber consists of a mixture of 6 mole percent acetone in air saturated with water vapor at 15°C and 101.3 kPa (1 atm). The scrubbing liquor is pure water at 15°C, and the inlet gas and liquid rates are given as 0.080 and 0.190 kmol/s respectively. The liquid rate corresponds to 20 percent over the theoretical minimum as calculated by assuming a value of x_1 corresponding to complete equilibrium between the exit liquor and the incoming gas. H_G and H_L are given as 0.42 and 0.30 m respectively, and the acetone equilibrium data at 15°C are $p_A^0 =$ 19.7 kPa (147.4 torr), $\gamma_A = 6.46$, and $m_A = 6.46 \times 19.7/101.3 = 1.26$. The heat of solution of acetone is 7656 cal/gmol (32.05 kJ/gmol), and the heat of vaporization of solvent (water) is 10,755 cal/gmol (45.03 kJ/gmol). The problem calls for determining the height of packing required to achieve a 90 percent recovery of the acetone.

The following table compares the results obtained by von Stockar and Wilke (op. cit.) for the various design methods:

Design method used	N_{OG}	Packed height, m	Design safety factor
Rigorous	5.56	3.63	1.00
Shortcut rigorous	5.56	3.73	0.97
Classical adiabatic	4.01	2.38	1.53
Classical isothermal	3.30	1.96	1.85

It should be clear from this example that there is considerable room for error when approximate design methods are employed in situations involving large heat effects, even for a case in which the solute concentration in the inlet gas is only 6 mole percent.

Example 6: Solvent Rate for Absorption Let us consider the absorption of acetone from air at atmospheric pressure into a stream of pure water fed to the top of a packed absorber at 25°C. The inlet gas at 35°C contains 2 percent by volume of acetone and is 70 percent saturated with water vapor (4 percent H_2O by volume). The mole-fraction acetone in the exit gas is to be reduced to 1/400 of the inlet value, or 50 ppmv. For 100 kmol of feed-gas mixture, how many kilomoles of fresh water should be fed to provide a positive-driving force throughout the packing? How many transfer units will be needed according to the classical adiabatic method? What is the estimated height of packing required if $H_{OG} = 0.70$ m?

The latent heats at 25°C are 7656 kcal/kmol for acetone and 10,490 kcal/kmol for water, and the differential heat of solution of acetone vapor in pure water is given as 2500 kcal/kmol. The specific heat of air is 7.0 kcal/(kmol·K).

Acetone solubilities are defined by the equation

$$K = y^\circ/x = \gamma_a p_a/p_T \quad (14\text{-}47)$$

where the vapor pressure of pure acetone in mmHg (torr) is given by (Sherwood et al., *Mass Transfer,* McGraw-Hill, New York, 1975, p. 537):

$$p_A^0 = \exp(18.1594 - 3794.06/T) \quad (14\text{-}48)$$

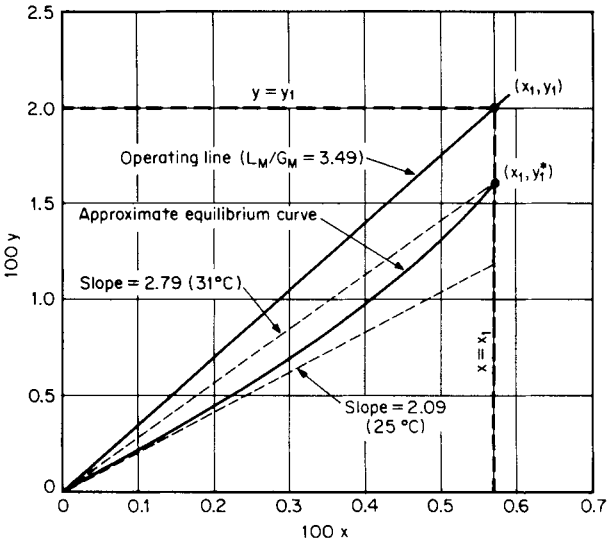

FIG. 14-10 Design diagram for adiabatic absorption of acetone in water, Example 6.

and the liquid-phase-activity coefficient may be approximated for low concentrations ($x \leq 0.01$) by the equation

$$\gamma_a = 6.5 \exp (2.0803 - 601.2/T) \tag{14-49}$$

Typical values of acetone solubility as a function of temperature at a total pressure of 760 mmHg are shown in the following table:

t, °C	25	30	35	40
γ_a	6.92	7.16	7.40	7.63
p_a, mmHg	229	283	346	422
$K = \gamma_a p_a^0/760$	2.09	2.66	3.37	4.23

For dry gas and liquid water at 25°C, the following enthalpies are computed for the inlet- and exit-gas streams (basis, 100 kmol of gas entering):

Entering gas:

Acetone	$2(2500 + 7656) = 20{,}312$ kcal
Water vapor	$4(10{,}490) = 41{,}960$
Sensible heat	$(100)(7.0)(35 - 25) = 7{,}000$
	69,272 kcal

Exit gas (assumed saturated with water at 25°C):

Acetone	$(2/400)(94/100)(2500) =$	12 kcal
Water vapor	$94\left(\frac{23.7}{760 - 23.7}\right)(10{,}490) =$	31,600
		31,612 kcal

Enthalpy change of liquid = 69,272 − 31,612 = 37,660 kcal/100 kmol gas. Thus, $\Delta t = t_1 - t_2 = 37{,}660/18L_M$, and the relation between L_M/G_M and the liquid-phase temperature rise is

$$L_M/G_M = (37{,}660)/(18)(100)\,\Delta t = 20.92/\Delta t$$

The following table summarizes the critical values for various assumed temperature rises:

Δt, °C	L_M/G_M	K_1	K_1G_M/L_M	m_2G_M/L_M
0		2.09	0.	0.
2	10.46	2.31	0.221	0.200
3	6.97	2.42	0.347	0.300
4	5.23	2.54	0.486	0.400
5	4.18	2.66	0.636	0.500
6	3.49	2.79	0.799	0.599
7	2.99	2.93	0.980	0.699

Evidently a temperature rise of 7°C would not be a safe design because the equilibrium line nearly touches the operating line near the bottom of the tower, creating a pinch. A temperature rise of 6°C appears to give an operable design, and for this case $L_M = 349$ kmol per 100 kmol of feed gas.

The design diagram for this case is shown in Fig. 14-10, in which the equilibrium curve is drawn so that the slope at the origin m_2 is equal to 2.09 and passes through the point $x_1 = 0.02/3.49 = 0.00573$ at $y_1^0 = 0.00573 \times 2.79 = 0.0160$.

The number of transfer units can be calculated from the adiabatic design equation, Eq. (14-46):

$$N_{OG} = \frac{1}{1 - 0.599} \ln \left[\frac{(1 - 0.599)^2}{(1 - 0.799)} (400) + 0.599 \right] = 14.4$$

The estimated height of tower packing by assuming $H_{OG} = 0.70$ m and a design safety factor of 1.5 is

$$h_T = (14.4)(0.7)(1.5) = 15.1 \text{ m } (49.6 \text{ ft})$$

For this tower, one should consider the use of two or more shorter packed sections instead of one long section.

Another point to be noted is that this calculation would be done more easily today by using a process simulator. However, the details are presented here to help the reader gain familiarity with the key assumptions and results.

MULTICOMPONENT SYSTEMS

When no chemical reactions are involved in the absorption of more than one soluble component from an insoluble gas, the design conditions (temperature, pressure, liquid-to-gas ratio) are normally determined by the volatility or physical solubility of the least soluble component for which the recovery is specified.

The more volatile (i.e., less soluble) components will only be partially absorbed even for an infinite number of trays or transfer units. This can be seen in Fig. 14-9, in which the asymptotes become vertical for values of mG_M/L_M greater than unity. If the amount of volatile component in the fresh solvent is negligible, then the limiting value of y_1/y_2 for each of the highly volatile components is

$$y_1/y_2 = S/(S - 1) \tag{14-50}$$

where $S = mG_M/L_M$ and the subscripts 1 and 2 refer to the bottom and top of the tower, respectively.

When the gas stream is dilute, absorption of each constituent can be considered separately as if the other components were absent. The following example illustrates the use of this principle.

Example 7: Multicomponent Absorption, Dilute Case Air entering a tower contains 1 percent acetaldehyde and 2 percent acetone. The liquid-to-gas ratio for optimum acetone recovery is $L_M/G_M = 3.1$ mol/mol when the fresh-solvent temperature is 31.5°C. The value of y^0/x for acetaldehyde has been measured as 50 at the boiling point of a dilute solution, 93.5°C. What will the percentage recovery of acetaldehyde be under conditions of optimal acetone recovery?

Solution. If the heat of solution is neglected, y^0/x at 31.5°C is equal to 50(1200/7300) = 8.2, where the factor in parentheses is the ratio of pure-acetaldehyde vapor pressures at 31.5 and 93.5°C respectively. Since L_M/G_M is equal to 3.1, the value of S for the aldehyde is $S = mG_M/L_M = 8.2/3.1 = 2.64$, and $y_1/y_2 = S/(S - 1) = 2.64/1.64 = 1.61$. The acetaldehyde recovery is therefore equal to $100 \times 0.61/1.61 = 38$ percent recovery.

In concentrated systems the change in gas and liquid flow rates within the tower and the heat effects accompanying the absorption of all the components must be considered. A trial-and-error calculation from one theoretical stage to the next usually is required if accurate results are to be obtained, and in such cases calculation procedures similar to those described in Sec. 13 normally are employed. A computer procedure for multicomponent adiabatic absorber design has been described by Feintuch and Treybal [*Ind. Eng. Chem. Process Des. Dev.*, **17,** 505 (1978)]. Also see Holland, *Fundamentals and Modeling of Separation Processes*, Prentice Hall, Englewood Cliffs, N.J., 1975.

In concentrated systems, the changes in the gas and liquid flow rates within the tower and the heat effects accompanying the absorption of all components must be considered. A trial-and-error calculation from one theoretical stage to the next is usually required if accurate and reliable results are to be obtained, and in such cases calculation procedures similar to those described in Sec. 13 need to be employed.

When two or more gases are absorbed in systems involving chemical reactions, the system is much more complex. This topic is discussed later in the subsection "Absorption with Chemical Reaction."

Graphical Design Method for Dilute Systems The following notation for multicomponent absorption systems has been adapted from Sherwood, Pigford, and Wilke (*Mass Transfer*, McGraw-Hill, New York, 1975, p. 415):

L_M^s = moles of solvent per unit time

G_M^0 = moles of rich feed gas to be treated per unit time

X = moles of one solute per mole of solute-free solvent fed to top of tower

Y = moles of one solute in gas phase per mole of rich feed gas

Subscripts 1 and 2 refer to the bottom and the top of the tower, respectively, and the material balance for any one component may be written as

$$L_M^s(X - X_2) = G_M^0(Y - Y_2) \tag{14-51}$$

or else as

$$L_M^s(X_1 - X) = G_M^0(Y_1 - Y) \tag{14-52}$$

For the special case of absorption from lean gases with relatively large amounts of solvent, the equilibrium lines are defined for each component by the relation

$$Y^0 = K'X \tag{14-53}$$

Thus, the equilibrium line for each component passes through the origin with slope K', where

$$K' = K(G_M/G_M^0)/(L_M/L_M^S) \tag{14-54}$$

and $K = y^0/x$. When the system is sufficiently dilute, $K' = K$.

The liquid-to-gas ratio is chosen on the basis of the least soluble component in the feed gas that must be absorbed completely. Each component will then have its own operating line with slope equal to L_M^S/G_M^0 (i.e., the operating lines for the various components will be parallel).

A typical diagram for the complete absorption of pentane and heavier components is shown in Fig. 14-11. The oil used as solvent is assumed to be solute-free (i.e., $X_2 = 0$), and the "key component," butane, was identified as that component absorbed in appreciable amounts whose equilibrium line is most nearly parallel to the operating lines (i.e., the K value for butane is approximately equal to L_M^S/G_M^0).

In Fig. 14-11, the composition of the gas with respect to components more volatile than butane will approach equilibrium with the liquid phase at the bottom of the tower. The gas compositions of the components less volatile (heavier) than butane will approach equilibrium with the oil entering the tower, and since $X_2 = 0$, the components heavier than butane will be completely absorbed.

Four theoretical trays have been stepped off for the key component (butane) on Fig. 14-11, and are seen to give a recovery of 75 percent of the butane. The operating lines for the other components have been drawn with the same slope and placed so as to give approximately the same number of theoretical trays. Figure 14-11 shows that equilibrium is easily achieved in fewer than four theoretical trays and that for the heavier components nearly complete recovery is obtained in four theoretical trays. The diagram also shows that absorption of the light components takes place in the upper part of the tower, and the final recovery of the heavier components takes place in the lower section of the tower.

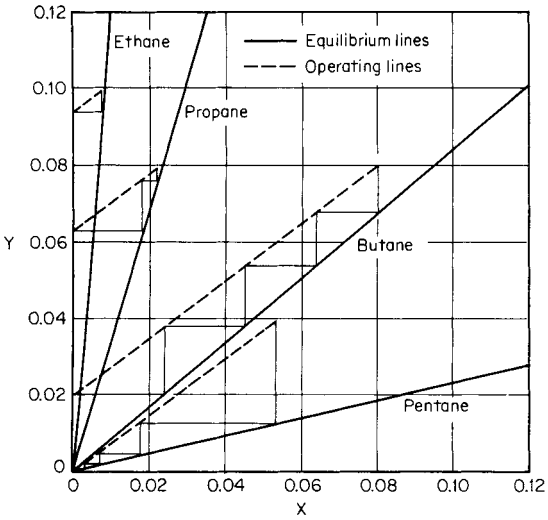

FIG. 14-11 Graphical design method for multicomponent systems; absorption of butane and heavier components in a solute-free lean oil.

Algebraic Design Method for Dilute Systems The design method described above can be performed algebraically by employing the following modified version of the Kremser formula:

$$\frac{Y_1 - Y_2}{Y_1 - mX_2} = \frac{(A^0)^{N+1} - A^0}{(A^0)^{N+1} - 1} \tag{14-55}$$

where for dilute gas absorption $A^0 = L_M^S/mG_M^0$ and $m \approx K = y^0/x$.

The left side of Eq. (14-55) represents the efficiency of absorption of any one component of the feed gas mixture. If the solvent is solute-free so that $X_2 = 0$, the left side is equal to the fractional absorption of the component from the rich feed gas. When the number of theoretical trays N and the liquid and gas feed rates L_M^S and G_M^0 have been fixed, the fractional absorption of each component may be computed directly, and the operating lines need not be placed by trial and error as in the graphical method described above.

According to Eq. (14-55), when A^0 is less than unity and N is large,

$$(Y_1 - Y_2)/(Y_1 - mX_2) = A^0 \tag{14-56}$$

Equation (14-56) may be used to estimate the fractional absorption of more volatile components when A^0 of the component is greater than A^0 of the key component by a factor of 3 or more.

When A^0 is much larger than unity and N is large, the right side of Eq. (14-55) becomes equal to unity. This signifies that the gas will leave the top of the tower in equilibrium with the incoming oil, and when $X_2 = 0$, it corresponds to complete absorption of the component in question. Thus, the least volatile components may be assumed to be at equilibrium with the lean oil at the top of the tower.

When $A^0 = 1$, the right side of Eq. (14-56) simplifies as follows:

$$(Y_1 - Y_2)/(Y_1 - mX_2) = N/(N + 1) \tag{14-57}$$

For systems in which the absorption factor A^0 for each component is not constant throughout the tower, an effective absorption factor for use in the equations just presented can be estimated by the Edmister formula

$$A_e^0 = \sqrt{A_1^0(A_2^0 + 1) + 0.25} - 0.5 \tag{14-58}$$

This procedure is a reasonable approximation only when no pinch points exist within the tower and when the absorption factors vary in a regular manner between the bottom and the top of the tower.

Example 8: Multicomponent Absorption, Concentrated Case A hydrocarbon feed gas is to be treated in an existing four-theoretical-tray absorber to remove butane and heavier components. The recovery specification for the key component, butane, is 75 percent. The composition of the exit gas from the absorber and the required liquid-to-gas ratio are to be estimated. The feed-gas composition and the equilibrium K values for each component at the temperature of the (solute-free) lean oil are presented in the following table:

Component	Mole %	K value
Methane	68.0	74.137
Ethane	10.0	12.000
Propane	8.0	3.429
Butane	8.0	0.833
Pentane	4.0	0.233
C_6 plus	2.0	0.065

For $N = 4$ and $Y_2/Y_1 = 0.25$, the value of A^0 for butane is found to be equal to 0.89 from Eq. (14-55) by using a trial-and-error method. The values of A^0 for the other components are then proportional to the ratios of their K values to that of butane. For example, $A^0 = 0.89(0.833/12.0) = 0.062$ for ethane. The values of A^0 for each of the other components and the exit-gas composition as computed from Eq. (14-55) are shown in the following table:

Component	A^0	Y_2, mol/mol feed	Exit gas, mole %
Methane	0.010	67.3	79.1
Ethane	0.062	9.4	11.1
Propane	0.216	6.3	7.4
Butane	0.890	2.0	2.4
Pentane	3.182	0.027	0.03
C_6 plus	11.406	0.0012	0.0014

The molar liquid-to-gas ratio required for this separation is computed as $L_M^s/G_M^0 = A^0 \times K = 0.89 \times 0.833 = 0.74$.

We note that this example is the analytical solution to the graphical design problem shown in Fig. 14-11, which therefore is the design diagram for this system.

The simplified design calculations presented in this section are intended to reveal the key features of gas absorption involving multicomponent systems. It is expected that rigorous computations, based upon the methods presented in Sec. 13, will be used in design practice. Nevertheless, it is valuable to study these simplified design methods and examples since they provide insight into the key elements of multicomponent absorption.

ABSORPTION WITH CHEMICAL REACTION

Introduction Many present-day commercial gas absorption processes involve systems in which chemical reactions take place in the liquid phase; an example of the absorption of CO_2 by MEA has been presented earlier in this section. These reactions greatly increase the capacity of the solvent and enhance the rate of absorption when compared to physical absorption systems. In addition, the selectivity of reacting solutes is greatly increased over that of nonreacting solutes. For example, MEA has a strong selectivity for CO_2 compared to chemically inert solutes such as CH_4, CO, or N_2. Note that the design procedures presented here are theoretically and practically related to biofiltration, which is discussed in Sec. 25 (Waste Management).

A necessary prerequisite to understanding the subject of absorption with chemical reaction is the development of a thorough understanding of the principles involved in physical absorption, as discussed earlier in this section and in Sec. 5. Excellent references on the subject of absorption with chemical reactions are the books by Dankwerts (*Gas-Liquid Reactions*, McGraw-Hill, New York, 1970) and Astarita et al. (*Gas Treating with Chemical Solvents*, Wiley, New York, 1983).

Recommended Overall Design Strategy When one is considering the design of a gas absorption system involving chemical reactions, the following procedure is recommended:

1. Consider the possibility that the physical design methods described earlier in this section may be applicable.
2. Determine whether commercial design overall $K_G a$ values are available for use in conjunction with the traditional design method, being careful to note whether the conditions under which the $K_G a$ data were obtained are essentially the same as for the new design. Contact the various tower-packing vendors for information as to whether $K_G a$ data are available for your system and conditions.
3. Consider the possibility of scaling up the design of a new system from experimental data obtained in a laboratory bench-scale or small pilot-plant unit.
4. Consider the possibility of developing for the new system a rigorous, theoretically based design procedure which will be valid over a wide range of design conditions. Note that commercial software is readily available today to develop a rigorous model in a relatively small amount of time.

These topics are further discussed in the subsections that follow.

Dominant Effects in Absorption with Chemical Reaction When the solute is absorbing into a solution containing a reagent that chemically reacts with it, diffusion and reaction effects become closely coupled. It is thus important for the design engineer to understand the key effects. Figure 14-12 shows the concentration profiles that occur when solute A undergoes an irreversible second-order reaction with component B, dissolved in the liquid, to give product C.

$$A + bB \rightarrow cC \tag{14-59}$$

The rate equation is

$$r_A = -k_2 C_A C_B \tag{14-60}$$

Figure 14-12 shows that the fast reaction takes place entirely in the liquid film. In such instances, the dominant mass-transfer mechanism is physical absorption, and physical design methods are applicable but the resistance to mass transfer in the liquid phase is lower due to the reaction. On the other extreme, a slow reaction occurs in the bulk of the liquid, and its rate has little dependence on the resistance to diffusion in either the gas or the liquid films. Here the mass-transfer mechanism is that of chemical reaction, and holdup in the bulk liquid is the determining factor.

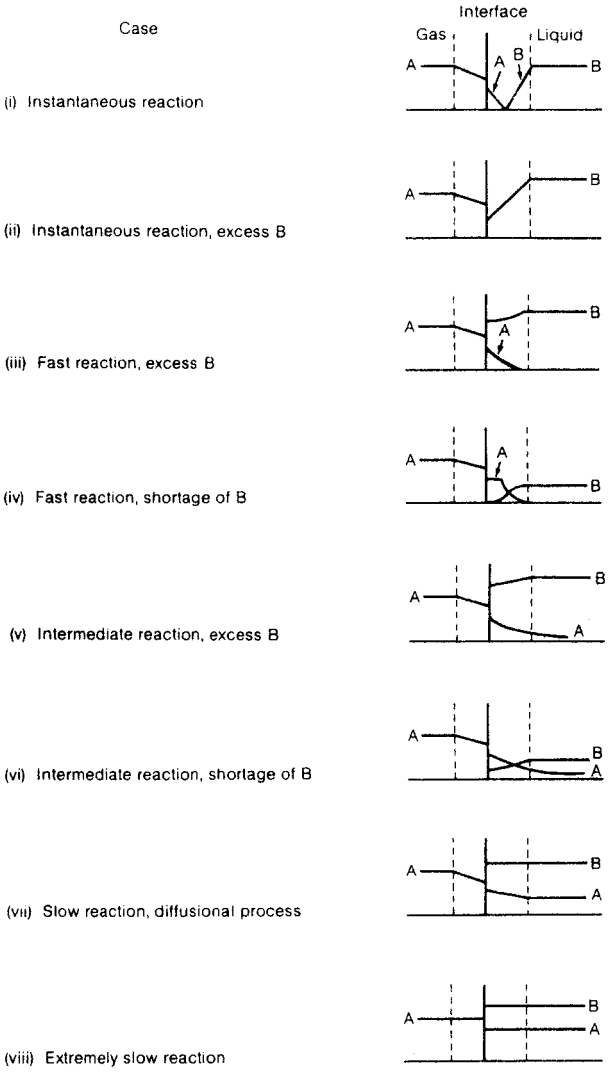

FIG. 14-12 Vapor- and liquid-phase concentration profiles near an interface for absorption with chemical reaction.

The Hatta number is a dimensionless group used to characterize the importance of the speed of reaction relative to the diffusion rate.

$$N_{\text{Ha}} = \frac{\sqrt{D_A k_2 C_{B0}}}{k_L^0} \tag{14-61}$$

As the Hatta number increases, the effective liquid-phase mass-transfer coefficient increases. Figure 14-13, which was first developed by Van Krevelen and Hoftyzer [*Rec. Trav. Chim.*, **67,** 563 (1948)] and later refined by Perry and Pigford and by Brian et al. [*AIChE J.*, **7,** 226 (1961)], shows how the enhancement (defined as the ratio of the effective liquid-phase mass-transfer coefficient to its physical equivalent $\phi = k_L/k_L^0$) increases with N_{Ha} for a second-order, irreversible reaction of the kind defined by Eqs. (14-60) and (14-61). The various curves in Fig. 14-13 were developed based upon penetration theory and

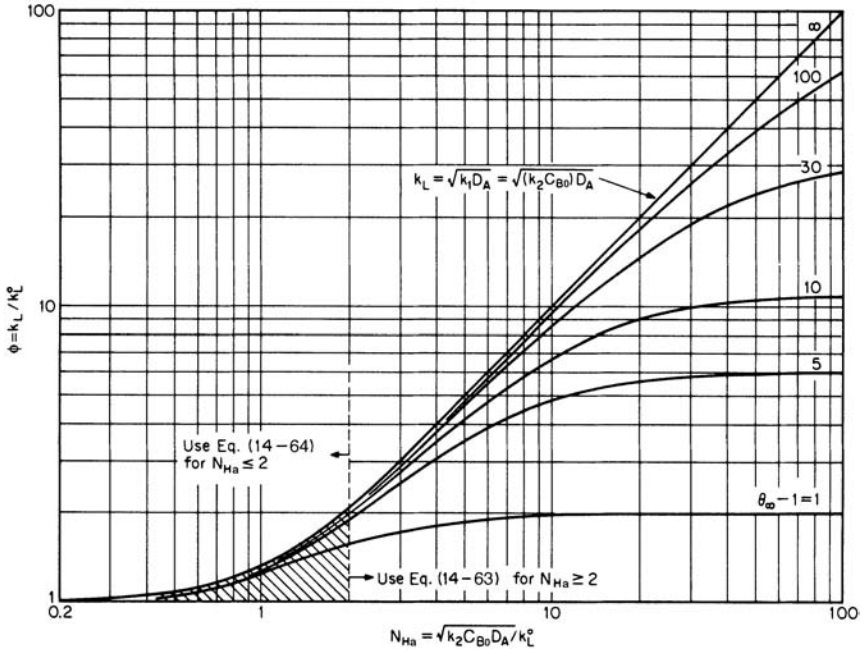

FIG. 14-13 Influence of irreversible chemical reactions on the liquid-phase mass-transfer coefficient k_L. [*Adapted from Van Krevelen and Hoftyzer,* Rec. Trav. Chim., ***67,*** *563 (1948).*]

depend on the parameter $\phi_\infty - 1$, which is related to the diffusion coefficients and reaction coefficients, as shown below.

$$\phi_\infty = \sqrt{\frac{D_A}{D_B}} + \sqrt{\frac{D_A}{D_B}} \left(\frac{C_B}{C_A b} \right) \qquad (14\text{-}62)$$

For design purposes, the entire set of curves in Fig. 14-13 may be represented by the following two equations:
For, $N_{Ha} \ge 2$:

$$k_L/k_L^0 = 1 + (\phi_\infty - 1)\{1 - \exp[-(N_{Ha} - 1)/(\phi_\infty - 1)]\} \qquad (14\text{-}63)$$

For, $N_{Ha} \le 2$:

$$k_L/k_L^0 = 1 + (\phi_\infty - 1)\{1 - \exp[-(\phi_\infty - 1)^{-1}]\} \exp[1 - 2/N_{Ha}] \qquad (14\text{-}64)$$

Equation (14-64) was originally reported by Porter [*Trans. Inst. Chem. Eng.,* **44,** T25 (1966)], and Eq. (14-64) was derived by Edwards and first reported in the 6th edition of this handbook.

The Van Krevelen-Hoftyzer (Fig. 14-13) relationship was tested by Nijsing et al. [*Chem. Eng. Sci.,* **10,** 88 (1959)] for the second-order system in which CO_2 reacts with either NaOH or KOH solutions. Nijsing's results are shown in Fig. 14-14 and can be seen to be in excellent

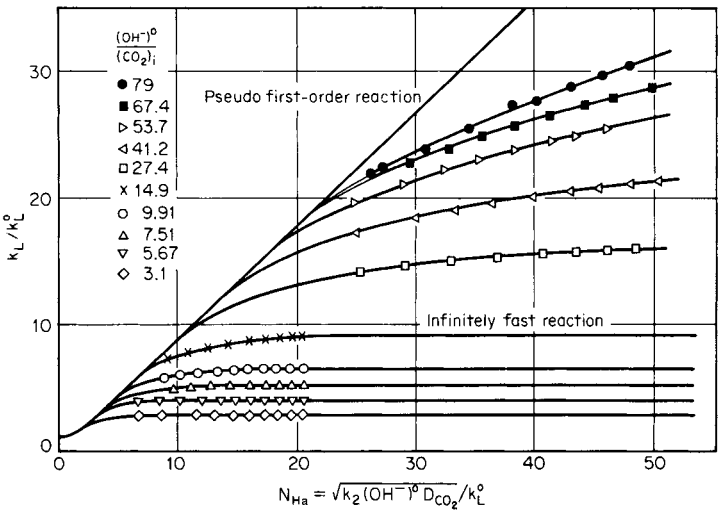

FIG. 14-14 Experimental values of k_L/k_L^0 for absorption of CO_2 into NaOH solutions at 20°C. [*Data of Nijsing et al.,* Chem. Eng. Sci., ***10,*** 88 (1959).]

agreement with the second-order-reaction theory. Indeed, these experimental data are well described by Eqs. (14-62) and (14-63) when values of $b = 2$ and $D_A/D_B = 0.64$ are employed in the equations.

Applicability of Physical Design Methods Physical design models such as the classical isothermal design method or the classical adiabatic design method may be applicable for systems in which chemical reactions are either extremely fast or extremely slow, or when chemical equilibrium is achieved between the gas and liquid phases.

If the chemical reaction is extremely fast and irreversible, the rate of absorption may in some cases be completely governed by gas-phase resistance. For practical design purposes, one may assume, e.g., that this gas-phase mass-transfer-limited condition will exist when the ratio y_i/y is less than 0.05 everywhere in the apparatus.

From the basic mass-transfer flux relationship for species A (Sec. 5)

$$N_A = k_G(y - y_i) = k_L(x_i - x) \tag{14-65}$$

one can readily show that this condition on y_i/y requires that the ratio x/x_i be negligibly small (i.e., a fast reaction) and that the ratio $mk_G/k_L = mk_G/k_L^0\phi$ be less than 0.05 everywhere in the apparatus. The ratio $mk_G/k_L^0\phi$ will be small if the equilibrium backpressure of the solute over the liquid is small (i.e., small m or high reactant solubility), or the reaction enhancement factor $\phi = k_L/k_L^0$ is very large, or both. The reaction enhancement factor ϕ will be large for all extremely fast pseudo-first-order reactions and will be large for extremely fast second-order irreversible reaction systems in which there is sufficiently large excess of liquid reagent.

Figure 14-12, case (ii), illustrates the gas-film and liquid-film concentration profiles one might find in an extremely fast (gas-phase mass-transfer-limited), second-order irreversible reaction system. The solid curve for reagent B represents the case in which there is a large excess of bulk liquid reagent B^0. Figure 14-12, case (iv), represents the case in which the bulk concentration B^0 is not sufficiently large to prevent the depletion of B near the liquid interface.

Whenever these conditions on the ratio y_i/y apply, the design can be based upon the physical rate coefficient k_G or upon the height of one gas-phase mass-transfer unit H_G. The gas-phase mass-transfer-limited condition is approximately valid for the following systems: absorption of NH_3 into water or acidic solutions, absorption of H_2O into concentrated sulfuric acid, absorption of SO_2 into alkali solutions, absorption of H_2S from a gas stream into a strong alkali solution, absorption of HCl into water or alkaline solutions, or absorption of Cl_2 into strong alkali solutions.

When the liquid-phase reactions are extremely slow, the gas-phase resistance can be neglected and one can assume that the rate of reaction has a predominant effect upon the rate of absorption. In this case the differential rate of transfer is given by the equation

$$dn_A = R_A f_H S\, dh = (k_L^0 a/\rho_L)(c_i - c)S\, dh \tag{14-66}$$

where n_A = rate of solute transfer, R_A = volumetric reaction rate (function of c and T), f_H = fractional liquid volume holdup in tower or apparatus, S = tower cross-sectional area, h = vertical distance, k_L^0 = liquid-phase mass-transfer coefficient for pure physical absorption, a = effective interfacial mass-transfer area per unit volume of tower or apparatus, ρ_L = average molar density of liquid phase, c_i = solute concentration in liquid at gas-liquid interface, and c = solute concentration in bulk liquid.

Although the right side of Eq. (14-66) remains valid even when chemical reactions are extremely slow, the mass-transfer driving force may become increasingly small, until finally $c \approx c_i$. For extremely slow first-order irreversible reactions, the following rate expression can be derived from Eq. (14-66):

$$R_A = k_1 c = k_1 c_i/(1 + k_1\rho_L f_H/k_L^0 a) \tag{14-67}$$

where k_1 = first-order reaction rate coefficient.

For dilute systems in countercurrent absorption towers in which the equilibrium curve is a straight line (i.e., $y_i = mx_i$), the differential relation of Eq. (14-66) is formulated as

$$dn_A = -G_M S\, dy = k_1 c f_H S\, dh \tag{14-68}$$

where G_M = molar gas-phase mass velocity and y = gas-phase solute mole fraction.

Substitution of Eq. (14-67) into Eq. (14-68) and integration lead to the following relation for an extremely slow first-order reaction in an absorption tower:

$$y_2 = y_1 \exp\left[-\frac{k_1\rho_L f_H h_T/(mG_m)}{1 + k_1\rho_L f_H/(k_L^0 a)}\right] \tag{14-69}$$

In Eq. (14-69) subscripts 1 and 2 refer to the bottom and top of the tower, respectively.

As discussed above, the Hatta number N_{Ha} usually is employed as the criterion for determining whether a reaction can be considered extremely slow. A reasonable criterion for slow reactions is

$$N_{Ha} = \sqrt{k_1 D_A}/k_L^0 \le 0.3 \tag{14-70}$$

where D_A = liquid-phase diffusion coefficient of the solute in the solvent. Figure 14-12, cases (vii) and (viii), illustrates the concentration profiles in the gas and liquid films for the case of an extremely slow chemical reaction.

Note that when the second term in the denominator of the exponential in Eq. (14-69) is very small, the liquid holdup in the tower can have a significant influence upon the rate of absorption if an extremely slow chemical reaction is involved.

When chemical equilibrium is achieved quickly throughout the liquid phase, the problem becomes one of properly defining the physical and chemical equilibria for the system. It is sometimes possible to design a tray-type absorber by assuming chemical equilibrium relationships in conjunction with a stage efficiency factor, as is done in distillation calculations. Rivas and Prausnitz [*AIChE J.*, **25,** 975 (1979)] have presented an excellent discussion and example of the correct procedures to be followed for systems involving chemical equilibria.

Traditional Design Method The traditional procedure for designing packed-tower gas absorption systems involving chemical reactions makes use of overall mass-transfer coefficients as defined by the equation

$$K_G a = n_A/(h_T S p_T \Delta y^\circ_{1\,m}) \tag{14-71}$$

where $K_G a$ = overall volumetric mass-transfer coefficient, n_A = rate of solute transfer from the gas to the liquid phase, h_T = total height of tower packing, S = tower cross-sectional area, p_T = total system pressure, and $\Delta y^\circ_{1\,m}$ is defined by the equation

$$\Delta y^\circ_{1\,m} = \frac{(y - y^\circ)_1 - (y - y^\circ)_2}{\ln\left[(y - y^\circ)_1/(y - y^\circ)_2\right]} \tag{14-72}$$

in which subscripts 1 and 2 refer to the bottom and top of the absorption tower respectively, y = mole-fraction solute in the gas phase, and y° = gas-phase solute mole fraction in equilibrium with bulk-liquid-phase solute concentration x. When the equilibrium line is straight, $y^\circ = mx$.

The traditional design method normally makes use of overall $K_G a$ values even when resistance to transfer lies predominantly in the liquid phase. For example, the CO_2-NaOH system which is most commonly used for comparing $K_G a$ values of various tower packings is a liquid-phase-controlled system. When the liquid phase is controlling, extrapolation to different concentration ranges or operating conditions is not recommended since changes in the reaction mechanism can cause k_L to vary unexpectedly and the overall $K_G a$ do not capture such effects.

Overall $K_G a$ data may be obtained from tower-packing vendors for many of the established commercial gas absorption processes. Such data often are based either upon tests in large-diameter test units or upon actual commercial operating data. Since application to untried operating conditions is not recommended, the preferred procedure for applying the traditional design method is equivalent to duplicating a previously successful commercial installation. When this is not possible, a commercial demonstration at the new operating conditions may be required, or else one could consider using some of the more rigorous methods described later.

While the traditional design method is reported here because it has been used extensively in the past, it should be used with extreme

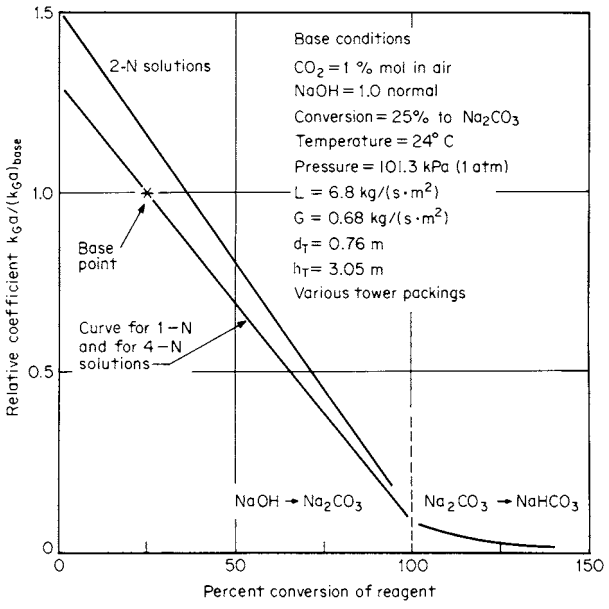

FIG. 14-15 Effects of reagent-concentration and reagent-conversion level upon the relative values of K_Ga in the CO_2-NaOH-H_2O system. [*Adapted from Eckert et al.,* Ind. Eng. Chem., ***59****(2), 41 (1967).*]

caution. In addition to the lack of an explicit liquid-phase resistance term, the method has other limitations. Equation (14-71) assumes that the system is dilute ($y_{BM} \approx 1$) and that the operating and equilibrium lines are straight, which are weak assumptions for reacting systems. Also, Eq. (14-65) is strictly valid only for the temperature and solute partial pressure at which the original test was done even though the total pressure p_T appears in the denominator.

In using Eq. (14-71), therefore, it should be understood that the numerical values of K_Ga will be a complex function of pressure, temperature, the type and size of packing employed, the liquid and gas mass flow rates, and the system composition (e.g., the degree of conversion of the liquid-phase reactant).

Figure 14-15 illustrates the influence of system composition and degree of reactant conversion upon the numerical values of K_Ga for the absorption of CO_2 into sodium hydroxide at constant conditions of temperature, pressure, and type of packing. An excellent experimental study of the influence of operating variables upon overall K_Ga values is that of Field et al. (*Pilot-Plant Studies of the Hot Carbonate Process for Removing Carbon Dioxide and Hydrogen Sulfide,* U.S. Bureau of Mines Bulletin 597, 1962).

Table 14-2 illustrates the observed variations in K_Ga values for different packing types and sizes for the CO_2-NaOH system at a 25 percent reactant conversion for two different liquid flow rates. The lower rate of 2.7 kg/(s·m²) or 2000 lb/(h·ft²) is equivalent to 4 U.S. gal/(min·ft²) and is typical of the liquid rates employed in fume scrubbers. The higher rate of 13.6 kg/(s·m²) or 10,000 lb/(h·ft²) is equivalent to 20 U.S. gal/(min·ft²) and is more typical of absorption towers such as used in CO_2 removal systems, for example. We also note that two gas velocities are represented in the table, corresponding to superficial velocities of 0.59 and 1.05 m/s (1.94 and 3.44 ft/s).

Table 14-3 presents a typical range of K_Ga values for chemically reacting systems. The first two entries in the table represent systems that can be designed by the use of purely physical design methods, because they are completely gas-phase mass-transfer-limited. To ensure a negligible liquid-phase resistance in these two tests, the HCl was absorbed into a solution maintained at less than 8 wt % HCl, and the NH_3 was absorbed into a water solution maintained below pH 7 by the addition of acid. The last two entries in Table 14-3 represent liquid-phase mass-transfer-limited systems.

Scaling Up from Laboratory Data Laboratory experimental techniques offer an efficient and cost-effective route to develop commercial absorption designs. For example, Ouwerkerk (*Hydrocarbon Process.*, April 1978, 89–94) revealed that both laboratory and small-scale pilot plant data were employed as the basis for the design of an 8.5-m (28-ft) diameter commercial Shell Claus off-gas treating (SCOT) tray-type absorber. Ouwerkerk claimed that the cost of developing comprehensive design procedures can be minimized, especially in the development of a new process, by the use of these modern techniques.

In a 1966 paper that is considered a classic, Dankwerts and Gillham [*Trans. Inst. Chem. Eng.*, 44, T42 (1966)] showed that data taken in a small stirred-cell laboratory apparatus could be used in the design of a packed-tower absorber when chemical reactions are involved. They showed that if the packed-tower mass-transfer coefficient in the absence of reaction (k_L^0) can be reproduced in the laboratory unit, then the rate of absorption in the laboratory apparatus will respond to chemical reactions in the same way as in the packed column, even though the means of agitating the liquid in the two systems may be quite different.

According to this method, it is not necessary to investigate the kinetics of the chemical reactions in detail; nor is it necessary to determine the solubilities or diffusivities of the various reactants in their unreacted forms. To use the method for scaling up, it is necessary to independently obtain data on the values of the interfacial area per unit volume a and the physical mass-transfer coefficient k_L^0 for the commercial packed tower. Once these data have been measured and tabulated, they can be used directly for scaling up the experimental laboratory data for any new chemically reacting system.

Dankwerts and Gillham did not investigate the influence of the gas-phase resistance in their study (for some processes, gas-phase resistance

TABLE 14-2 Typical Effects of Packing Type, Size, and Liquid Rate on K_Ga in a Chemically Reacting System, K_Ga, kmol/(h·m³)

	L = 2.7 kg/(s·m²)				L = 13.6 kg/(s·m²)			
Packing size, mm	25	38	50	75–90	25	38	50	75–90
Berl-saddle ceramic	30	24	21		45	38	32	
Raschig-ring ceramic	27	24	21		42	34	30	
Raschig-ring metal	29	24	19		45	35	27	
Pall-ring plastic	29	27	26*	16	45	42	38*	24
Pall-ring metal	37	32	27	21*	56	51	43	27*
Intalox-saddle ceramic	34	27	22	16*	56	43	34	26*
Super-Intalox ceramic	37*		26*		59*		40*	
Intalox-saddle plastic	40*		24*	16*	56*		37*	26*
Intalox-saddle metal	43*	35*	30*	24*	66*	58*	48*	37*
Hy-Pak metal	35	32*	27*	18*	54	50*	42*	27*

Data courtesy of the Norton Company.

Operating conditions: CO_2, 1 percent mole in air; NaOH, 4 percent weight (1 normal); 25 percent conversion to sodium carbonate; temperature, 24°C (75°F); pressure, 98.6 kPa (0.97 atm); gas rate = 0.68 kg/(s·m²) = 0.59 m/s = 500 lb/(h·ft²) = 1.92 ft/s except for values with asterisks, which were run at 1.22 kg/(s·m²) = 1.05 m/s = 900 lb/(h·ft²) = 3.46 ft/s superficial velocity; packed height, 3.05 m (10 ft); tower diameter, 0.76 m (2.5 ft). To convert table values to units of (lb·mol)/(h·ft³), multiply by 0.0624.

TABLE 14-3 Typical K_Ga Values for Various Chemically Reacting Systems, kmol/(h·m³)

Gas-phase reactant	Liquid-phase reactant	K_Ga	Special conditions
HCl	H_2O	353	Gas-phase limited
NH_3	H_2O	337	Gas-phase limited
Cl_2	NaOH	272	8% weight solution
SO_2	Na_2CO_3	224	11% weight solution
HF	H_2O	152	
Br_2	NaOH	131	5% weight solution
HCN	H_2O	114	
HCHO	H_2O	114	Physical absorption
HBr	H_2O	98	
H_2S	NaOH	96	4% weight solution
SO_2	H_2O	59	
CO_2	NaOH	38	4% weight solution
Cl_2	H_2O	8	Liquid-phase limited

Data courtesy of the Norton Company.

Operating conditions (see text): 38-mm ceramic Intalox saddles; solute gases, 0.5–1.0 percent mole; reagent conversions = 33 percent; pressure, 101 kPa (1 atm); temperature, 16–24°C; gas rate = 1.3 kg/(s·m²) = 1.1 m/s; liquid rates = 3.4 to 6.8 kg/(s·m²); packed height, 3.05 m; tower diameter, 0.76 m. Multiply table values by 0.0624 to convert to (lb·mol)/(h·ft³).

may be neglected). However, in 1975 Dankwerts and Alper [*Trans. Inst. Chem. Eng.*, 53, T42 (1975)] showed that by placing a stirrer in the gas space of the stirred-cell laboratory absorber, the gas-phase mass-transfer coefficient k_G in the laboratory unit could be made identical to that in a packed-tower absorber. When this was done, laboratory data for chemically reacting systems having a significant gas-side resistance could successfully be scaled up to predict the performance of a commercial packed-tower absorber.

If it is assumed that the values for k_G, k_L^0, and a have been measured for the commercial tower packing to be employed, the procedure for using the laboratory stirred-cell reactor is as follows:

1. The gas-phase and liquid-phase stirring rates are adjusted so as to produce the same values of k_G and k_L^0 as will exist in the commercial tower.
2. For the reaction system under consideration, experiments are made at a series of bulk-liquid and bulk-gas compositions representing the compositions to be expected at different levels in the commercial absorber (on the basis of material balance).
3. The ratios of $r_A(c_i,B^0)$ are measured at each pair of gas and liquid compositions.

For the dilute-gas systems, one form of the equation to be solved in conjunction with these experiments is

$$h_T = \frac{G_M}{a}\int_{y2}^{y1}\frac{dy}{r_A} \tag{14-73}$$

where h_T = height of commercial tower packing, G_M = molar gas-phase mass velocity, a = effective mass-transfer area per unit volume in the commercial tower, y = mole fraction solute in the gas phase, and r_A = experimentally determined rate of absorption per unit of exposed interfacial area.

By using the series of experimentally measured rates of absorption, Eq. (14-73) can be integrated numerically to determine the height of packing required in the commercial tower.

A number of different types of experimental laboratory units could be used to develop design data for chemically reacting systems. Charpentier [*ACS Symp. Ser.*, **72,** 223–261 (1978)] has summarized the state of the art with respect to methods of scaling up laboratory data and has tabulated typical values of the mass-transfer coefficients, interfacial areas, and contact times to be found in various commercial gas absorbers, as well as in currently available laboratory units.

The laboratory units that have been employed to date for these experiments were designed to operate at a total system pressure of about 101 kPa (1 atm) and at near-ambient temperatures. In practical situations, it may become necessary to design a laboratory absorption unit that can be operated either under vacuum or at elevated pressure and over a range of temperatures in order to apply the Dankwerts method.

It would be desirable to reinterpret existing data for commercial tower packings to extract the individual values of the interfacial area a and the mass-transfer coefficients k_G and $k^0{}_L$ to facilitate a more general usage of methods for scaling up from laboratory experiments. Some progress has already been made, as described later in this section. In the absence of such data, it is necessary to operate a pilot plant or a commercial absorber to obtain k_G, k_L^0, and a as described by Ouwerkerk (op. cit.).

Modern techniques use rigorous modeling computer-based methods to extract fundamental parameters from laboratory-scale measurements and then apply them to the design of commercial absorption towers. These techniques are covered next.

Rigorous Computer-Based Absorber Design While the techniques described earlier in this section are very useful to gain an understanding of the key effects in commercial absorbers, current design methods used in industrial practice for chemically reactive systems are increasingly often based upon computerized rigorous methods, which are commercially available from software vendors. The advantages of these rigorous methods are as follows: (1) Approximations do not have to be made for special cases (e.g., fast chemical reactions or mass-transfer resistance dominated by the gas or liquid phase), and all effects can be simultaneously modeled. (2) Fundamental quantities such as kinetic parameters and mass-transfer coefficients can be extracted from laboratory equipment and applied to commercial absorber towers. (3) Integrated models can be developed for an entire absorption process flowsheet (e.g., the absorber-stripper system with heat integration presented in Fig. 14-3), and consequently the entire system may be optimized.

Computer programs for chemically reacting systems are available from several vendors, notably the following:

Program	Vendor	Reference
AMSIM	Schlumberger Limited	Zhang and Ng, *Proc. Ann. Conv.—Gas Proc. Assoc.,* Denver, Colo.; 1996, p. 22.
ProTreat	Sulphur Experts	Weiland and Dingman, *Proc. Ann. Conv., Gas Proc. Assoc.,* Houston, Tex., 2001, p. 80.
TSWEET	Bryan Research and Engineering	Polasek, Donnelly, and Bullin, Proc. 71st GPA Annual Conv., 1992, p. 58.
RateSep	Aspen Technology	Chen et al., AIChE Annual Meeting, San Francisco, Nov. 12–17, 2006.

The specific approaches used to model the chemically reacting absorption system are slightly different among the different vendors. The general approach used and the benefits obtained are highlighted

by considering a specific example: removal of CO_2 from flue gases discharged by a power plant using aqueous monoethanolamine (MEA), as presented by Freguia and Rochelle [*AIChE J.*, **49,** 1676 (2003)].

The development and application of a rigorous model for a chemically reactive system typically involves four steps: (1) development of a thermodynamic model to describe the physical and chemical equilibrium; (2) adoption and use of a modeling framework to describe the mass transfer and chemical reactions; (3) parameterization of the mass-transfer and kinetic models based upon laboratory, pilot-plant, or commercial-plant data; and (4) use of the integrated model to optimize the process and perform equipment design.

Development of Thermodynamic Model for Physical and Chemical Equilibrium The first and perhaps most important step in the development of the thermodynamic model is the *speciation,* or representation of the set of chemical reactions. For CO_2 absorption in aqueous MEA solutions, the set of reactions is

$$CO_2 + MEA + H_2O \leftrightarrow MEACOO^- + H_3O^+ \quad (14\text{-}74a)$$

$$CO_2 + OH^- \leftrightarrow HCO_3^- \quad (14\text{-}74b)$$

$$HCO_3^- + H_2O \leftrightarrow CO_3^{2-} + H_3O^+ \quad (14\text{-}74c)$$

$$MEAH^+ + H_2O \leftrightarrow MEA + H_3O^+ \quad (14\text{-}74d)$$

$$2H_2O \leftrightarrow H_3O^+ + OH^- \quad (14\text{-}74e)$$

In addition, a model is needed that can describe the nonideality of a system containing molecular and ionic species. Freguia and Rochelle adopted the model developed by Chen et al. [*AIChE J.*, **25,** 820 (1979)] and later modified by Mock et al. [*AIChE J.*, **32,** 1655 (1986)] for mixed-electrolyte systems. The combination of the speciation set of reactions [Eqs. (14-74*a*) to (14-74*e*)] and the nonideality model is capable of representing the solubility data, such as presented in Figs. 14-1 and 14-2, to good accuracy. In addition, the model accurately and correctly represents the actual species present in the aqueous phase, which is important for faithful description of the chemical kinetics and species mass transfer across the interface. Finally, the thermodynamic model facilitates accurate modeling of the heat effects, such as those discussed in Example 6.

Rafal et al. (Chapter 7, "Models for Electrolyte Solutions," in *Models for Thermodynamic and Phase Equilibria Calculations*, S. I. Sandler, ed., Marcel Dekker, New York, 1994, p. 686) have provided a comprehensive discussion of speciation and thermodynamic models.

Adoption and Use of Modeling Framework The rate of diffusion and species generation by chemical reaction can be described by film theory, penetration theory, or a combination of the two. The most popular description is in terms of a two-film theory, which is diagrammed in Fig. 14-16 for absorption. Accordingly, there exists a stable interface separating the gas and the liquid. A certain distance from the interface, large fluid motions exist, and these distribute the material rapidly and equally so that no concentration gradients develop. Next to the interface, however, there are regions in which the fluid motion is slow; in these regions, termed *films*, material is transferred by diffusion alone. At the gas-liquid interface, material is transferred instantaneously, so that the gas and liquid are in physical equilibrium at the interface. The rate of diffusion in adsorption is therefore the rate of diffusion in the gas and liquid films adjacent to the interface. The model framework is completed by including terms for species generation (chemical equilibrium *and* chemical kinetics) in the gas and liquid film and bulk regions. Taylor, Krishna, and Kooijman (*Chem. Eng. Progress*, July 2003, p. 28) have provided an excellent discussion of rate-based models; these authors emphasize that the diffusion flux for multicomponent systems must be based upon the Maxwell-Stefan approach. The book by Taylor and Krishna (*Multicomponent Mass Transfer*, Wiley, New York, 1993) provides a detailed discussion of the Maxwell-Stefan approach. More details and discussion have been provided by the program vendors listed above.

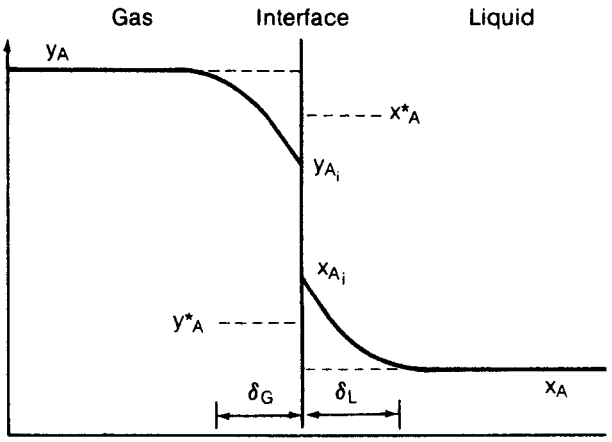

FIG. 14-16 Concentration profiles in the vapor and liquid phases near an interface.

Parameterization of Mass-Transfer and Kinetic Models The mass-transfer and chemical kinetic rates required in the rigorous model are typically obtained from the literature, but must be carefully evaluated; and fine-tuning through pilot-plant and commercial data is highly recommended.

Mass-transfer coefficient models for the vapor and liquid coefficients are of the general form

$$k^L_{ij} = a\rho_L f(D^m_{ij}, \mu_L, \rho_V, a, \text{internal characteristics}) \quad (14\text{-}75a)$$

$$k^V_{ij} = aP\, f(D^m_{ij}, \mu_V, \rho_V, a, \text{internal characteristics}) \quad (14\text{-}75b)$$

where a = effective interfacial area per unit volume, D^m_{ij} are the Stefan-Maxwell diffusion coefficients, P = pressure, ρ = molar density, and μ = viscosity. The functions in Eqs. (14-75*a*) and (14-75*b*) are correlations that depend on the column internals. Popular correlations in the literature are those by Onda at al. [*J. Chem.. Eng. Jap.*, **1,** 56 (1968)] for random packing, Bravo and Fair [*Ind. Eng. Chem. Proc. Des. Dev.*, **21,** 162 (1982)] for structured packing, Chan and Fair [*Ind. Eng. Chem. Proc. Des. Dev.*, **23,** 814 (1984)] for sieve trays, Scheffe and Weiland [*Ind. Eng. Chem. Res.*, **26,** 228 (1987)] for valve trays, and Hughmark [*AIChE J.*, **17,** 1295 (1971)] for bubble-cap trays.

It is highly recommended that the mass-transfer correlations be tested and improved by using laboratory, pilot-plant, or commercial data for the specific application. Commercial software generally provides the capability for correction factors to adjust generalized correlations to the particular application.

Kinetic models are usually developed by replacing a subset of the speciation reactions by kinetically reversible reactions. For example, Freguia and Rochelle replaced equilibrium reactions (14-74*a*) and (14-74*b*) with kinetically reversible reactions and retained the remaining three reactions as very fast and hence effectively at equilibrium. The kinetic constants were tuned using wetted-wall column data from Dang (M.S. thesis, University of Texas, Austin, 2001) and field data from a commercial plant.

Modern commercial software provides powerful capability to deploy literature correlations and to customize models for specific applications.

Deployment of Rigorous Model for Process Optimization and Equipment Design Techniques similar to those described above may be used to develop models for the stripper as well as other pieces of plant equipment, and thus an integrated model for the entire absorption system may be produced. The value of integrated models is that they can be used to understand the combined effects of many variables that determine process performance and to rationally optimize process performance. Freguia and Rochelle have shown that the reboiler duty (the dominant source of process operating costs) may be reduced by 10 percent if the absorber height is increased by 20 percent and by 4 percent if the absorber is intercooled with a duty equal to one-third of the reboiler duty. They also show that the power plant lost work is affected by varying stripper

pressure, but not significantly, so any convenient pressure can be chosen to operate the stripper.

In this section, we have used the example of CO_2 removal from flue gases using aqueous MEA to demonstrate the development and application of a rigorous model for a chemically reactive system. Modern software enables rigorous description of complex chemically reactive systems, but it is very important to carefully evaluate the models and to tune them using experimental data.

Use of Literature for Specific Systems A large body of experimental data obtained in bench-scale laboratory units and in small-diameter packed towers has been published since the early 1940s. One might wish to consider using such data for a particular chemically reacting system as the basis for scaling up to a commercial design. Extreme caution is recommended in interpreting such data for the purpose of developing commercial designs, as extrapolation of the data can lead to serious errors. Extrapolation to temperatures, pressures, or liquid-phase reagent conversions different from those that were employed by the original investigators definitely should be regarded with caution.

Bibliographies presented in the General References listed at the beginning of this section are an excellent source of information on specific chemically reacting systems. *Gas-Liquid Reactions* by Dankwerts (McGraw-Hill, New York, 1970) contains a tabulation of references to specific chemically reactive systems. *Gas Treating with Chemical Solvents* by Astarita et al. (Wiley, New York, 1983) deals with the absorption of acid gases and includes an extensive listing of patents. *Gas Purification* by Kohl and Nielsen (Gulf Publishing, Houston, 1997) provides a practical description of techniques and processes in widespread use and typically also sufficient design and operating data for specific applications.

In searching for data on a particular system, a computerized search of *Chemical Abstracts, Engineering Index,* and *National Technical Information Service* (NTIS) databases is recommended. In addition, modern search engines will rapidly uncover much potentially valuable information.

The experimental data for the system CO_2-NaOH-Na_2CO_3 are unusually comprehensive and well known as the result of the work of many experimenters. A serious study of the data and theory for this system therefore is recommended as the basis for developing a good understanding of the kind and quality of experimental information needed for design purposes.

EQUIPMENT FOR DISTILLATION AND GAS ABSORPTION: TRAY COLUMNS

Distillation and gas absorption are the prime and most common gas-liquid mass-transfer operations. Other operations that are often performed in similar equipment include stripping (often considered part of distillation), direct-contact heat transfer, flashing, washing, humidification, and dehumidification.

The most common types of contactors by far used for these are tray and packed towers. These are the focus of this subsection. Other contactors used from time to time and their applications are listed in Table 14-4.

In this subsection, the terms *gas* and *vapor* are used interchangeably. *Vapor* is more precise for distillation, where the gas phase is at equilibrium. Also, the terms *tower* and *column* are used interchangeably.

A crossflow tray (Fig. 14-17) consists of the *bubbling area* and the *downcomer*. Liquid descending the downcomer from the tray above enters the bubbling area. Here, the liquid contacts gas ascending through the tray perforations, forming froth or spray. An *outlet weir* on the downstream side of the bubbling area helps maintain liquid level on the tray. Froth overflowing the weir enters the outlet downcomer. Here, gas disengages from the liquid, and the liquid descends to the tray below. The bubbling area can be fitted with numerous types of tray hardware. The most common types by far are:

Sieve trays (Fig. 14-18*a*) are perforated plates. The velocity of upflowing gas keeps the liquid from descending through the perforations (weeping). At low gas velocities, liquid weeps through the perforations, bypassing part of the tray and reducing tray efficiency. Because of this, sieve trays have relatively poor turndown.

Fixed valve trays (Fig. 14-18*b*) have the perforations covered by a fixed cover, often a section of the tray floor pushed up. Their performance is similar to that of sieve trays.

Moving valve trays (Fig. 14-18*c*) have the perforations covered by movable disks (valves). Each valve rises as the gas velocity increases. The upper limit of the rise is controlled by restricting legs on the bottom of the valve (Fig. 14-18*c*) or by a cage structure around the valve. As the gas velocity falls, some valves close completely, preventing weeping. This gives the valve tray good turndown.

Table 14-5 is a general comparison of the three main tray types, assuming proper design, installation, and operation. Sieve and valve trays are comparable in capacity, efficiency, entrainment, and pressure drop. The turndown of moving valve trays is much better than that of sieve and fixed valve trays. Sieve trays are least expensive; valve trays cost only slightly more. Maintenance, fouling tendency, and effects of corrosion are least troublesome in fixed valve and sieve trays (provided the perforations or fixed valves are large enough) and most troublesome with moving valve trays.

Fixed valve and sieve trays prevail when fouling or corrosion is expected, or if turndown is unimportant. Valve trays prevail when high turndown is required. The energy saved, even during short turndown periods, usually justifies the small additional cost of the moving valve trays.

DEFINITIONS

Tray Area Definitions Some of these are illustrated in Fig. 14-17.

***Total tower cross-section area* A_T** The inside cross-sectional area of the empty tower (without trays or downcomers).

Net area* A_N *(also called free area) The total tower cross-sectional area A_T minus the area at the top of the downcomer A_{DT}. The

TABLE 14-4 Equipment for Liquid-Gas Systems

Equipment designation	Mode of flow	Gross mechanism	Continuous phase	Primary process applications
Tray column	Cross-flow, countercurrent	Integral	Liquid and/or gas	Distillation, absorption, stripping, DCHT, washing
Packed column	Countercurrent, cocurrent	Differential	Liquid and/or gas	Distillation, absorption, stripping, humidification, dehumidification, DCHT, washing
Wetted-wall (falling-film) column	Countercurrent, cocurrent	Differential	Liquid and/or gas	Distillation, absorption, stripping, evaporation
Spray chamber	Cocurrent, cross-flow, countercurrent	Differential	Gas	Absorption, stripping, humidification, dehumidification
Agitated vessel	Complete mixing	Integral	Liquid	Absorption
Line mixer	Cocurrent	Differential	Liquid or gas	Absorption, stripping

DCHT = direct contact heat transfer.

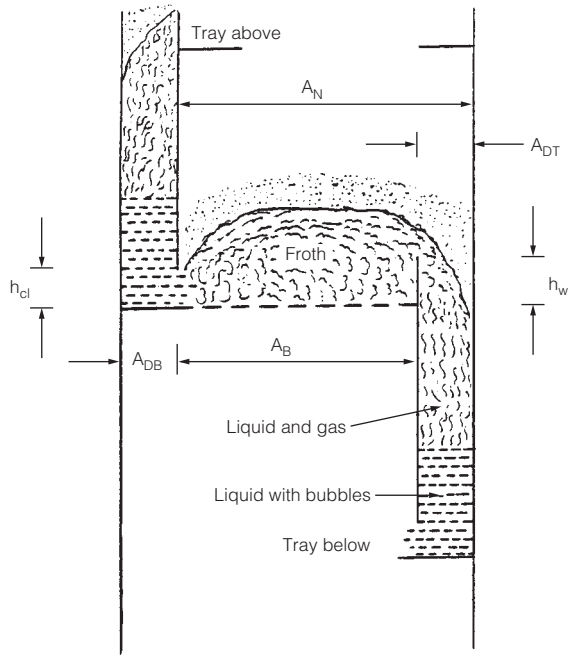

FIG. 14-17 Schematic of a tray operating in the froth regime. (*Based on H. Z. Kister,* Distillation Design, *copyright © 1992 by McGraw-Hill; reprinted by permission.*)

net area represents the smallest area available for vapor flow in the intertray spacing.

Bubbling area* A_B (also called *active area) The total tower cross-sectional area minus the sum of downcomer top area A_{DT}, downcomer seal area A_{DB}, and any other nonperforated areas on the tray. The bubbling area represents the area available for vapor flow just above the tray floor.

***Hole area* A_h** The total area of the perforations on the tray. The hole area is the smallest area available for vapor passage on a sieve tray.

***Slot area* A_S** The total (for all open valves) vertical curtain area through which vapor passes in a horizontal direction as it leaves the valves. It is a function of the narrowest opening of each valve and the number of valves that are open. The slot area is normally the smallest area available for vapor flow on a valve tray.

***Open slot area* A_{SO}** The slot area when all valves are open.

***Fractional hole area* A_f** The ratio of hole area to bubbling area (sieve trays) or slot area to bubbling area (valve trays).

Vapor and Liquid Load Definitions

F-*factor* F This is the square root of the kinetic energy of the gas, defined by Eq. (14-76). The velocity in Eq. (14-76) is usually (not always) based on the tower cross-sectional area A_T, the net area A_N, or the bubbling area A_B. The user should beware of any data for which the area basis is not clearly specified.

$$F = u\sqrt{\rho_G} \tag{14-76}$$

C-*factor* C The *C*-factor, defined in Eq. (14-77), is the best gas load term for comparing capacities of systems of different physical properties. It has the same units as velocity (m/s or ft/s) and is directly related to droplet entrainment. As with the *F*-factor, the user should beware of any data for which the area basis is not clearly specified.

$$C = u\sqrt{\frac{\rho_G}{\rho_L - \rho_G}} \tag{14-77}$$

Weir load For trays (as distinct from downcomers), liquid load is normally defined as

$$Q_L = \frac{\text{volume of liquid}}{\text{length of outlet weir}} = \frac{Q}{L_w} \tag{14-78}$$

This definition describes the flux of liquid horizontally across the tray. Units frequently used are $m^3/(h\cdot m)$, $m^3/(s\cdot m)$, and gpm/in.

Downcomer liquid load For downcomer design, the liquid load is usually defined as the liquid velocity at the downcomer entrance (m/s or ft/s):

$$Q_D = \frac{\text{volume of liquid}}{\text{downcomer entrance area}} = \frac{Q}{A_{DT}} \tag{14-79}$$

FLOW REGIMES ON TRAYS

Three main flow regimes exist on industrial distillation trays. These regimes may all occur on the same tray under different liquid and gas flow rates (Fig. 14-19). Excellent discussion of the fundamentals and modeling of these flow regimes was presented by Lockett (*Distillation Tray Fundamentals,* Cambridge University Press, Cambridge, 1986). An excellent overview of these as well as of less common flow regimes was given by Prince (*PACE,* June 1975, p. 31; July 1975, p. 18).

Froth regime (or mixed regime; Fig. 14-20a). This is the most common operating regime in distillation practice. Each perforation bubbles vigorously. The bubbles circulate rapidly through the liquid, are of nonuniform sizes and shapes, and travel at varying velocities. The froth surface is mobile and not level, and is generally covered by droplets. Bubbles are formed at the tray perforations and are swept away by the froth.

As gas load increases in the froth regime, jetting begins to replace bubbling in some holes. The fraction of holes that is jetting increases with gas velocity. When jetting becomes the dominant mechanism, the dispersion changes from froth to spray. Prado et al. [*Chemical Engineering Progr.* **83**(3), p. 32, (1987)] showed the transition from froth to spray takes place gradually as jetting replaces bubbling in 45 to 70 percent of the tray holes.

Emulsion regime (Fig. 14-20b). At high liquid loads and relatively low gas loads, the high-velocity liquid bends the swarms of gas bubbles leaving the orifices, and tears them off, so most of the gas becomes emulsified as small bubbles within the liquid. The mixture behaves as a uniform two-phase fluid, which obeys the Francis weir formula [see the subsection "Pressure Drop" and Eq. (14-109) *(Hofhuis and Zuiderweg, IChemE Symp. Ser.* **56,** p. 2.2/1 (1979); Zuiderweg, *Int. Chem. Eng.* **26**(1), 1 (1986)]. In industrial practice, the emulsion regime is the most common in high-pressure and high-liquid-rate operation.

Spray regime (or drop regime, Fig. 14-20c). At high gas velocities and low liquid loads, the liquid pool on the tray floor is shallow and easily atomized by the high-velocity gas. The dispersion becomes a turbulent cloud of liquid droplets of various sizes that reside at high elevations above the tray and follow free trajectories. Some droplets are entrained to the tray above, while others fall back into the liquid pools and become reatomized. In contrast to the liquid-continuous froth and emulsion regimes, the phases are reversed in the spray regime: here the gas is the continuous phase, while the liquid is the dispersed phase.

The spray regime frequently occurs where gas velocities are high and liquid loads are low (e.g., vacuum and rectifying sections at low liquid loads).

Three-layered structure. Van Sinderen, Wijn, and Zanting [*Trans. IChemE,* **81,** Part A, p. 94 (January 2003)] postulate a tray dispersion consisting of a bottom liquid-rich layer where jets/bubbles form; an intermediate liquid-continuous froth layer where bubbles erupt, generating drops; and a top gas-continuous layer of drops. The intermediate layer that dampens the bubbles and

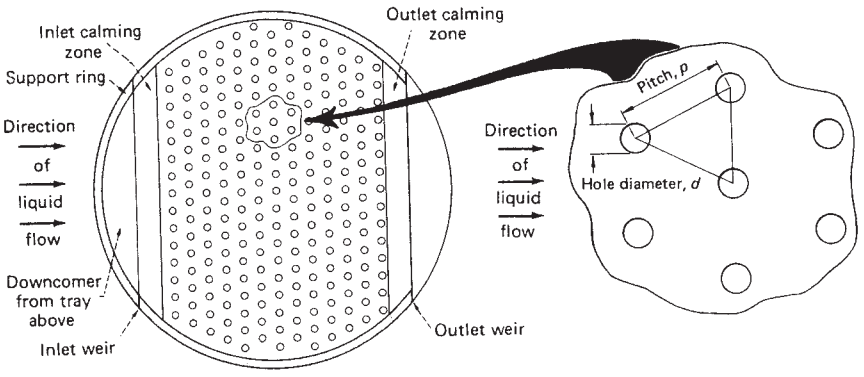

(a)

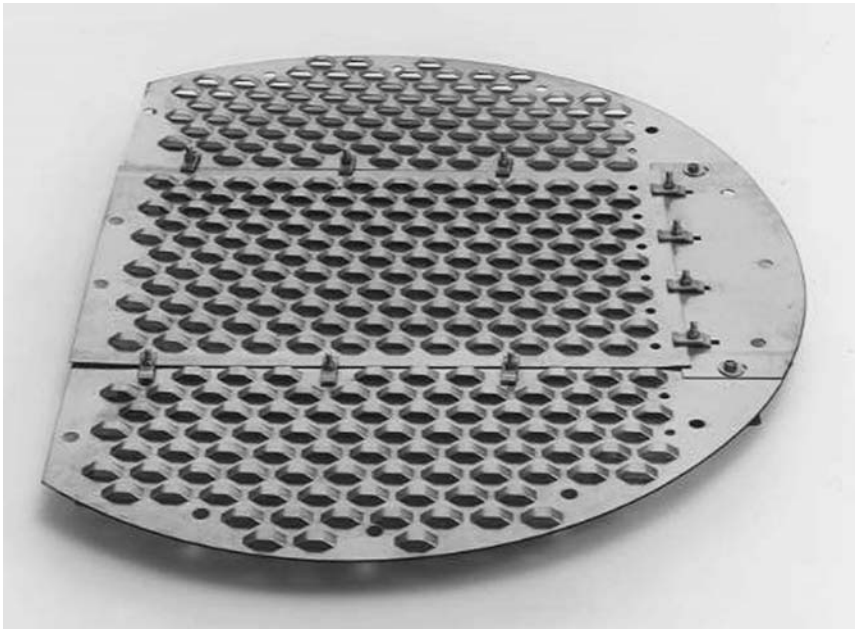

(b)

(c)

FIG. 14-18 Common tray types. (*a*) Sieve. (*b*) Fixed valve. (*c*) Moving valve with legs. [*Part a, from Henry Z. Kister,* Chem. Eng., *September 8, 1980; reprinted courtesy of* Chemical Engineering. *Part b, Courtesy of Sulzer Chemtech and Fractionation Research Inc. (FRI). Part c, courtesy of Koch-Glitsch LP.*]

TABLE 14-5 Comparison of the Common Tray Types

	Sieve trays	Fixed valve tray	Moving valve tray
Capacity	High	High	High to very high
Efficiency	High	High	High
Turndown	About 2:1. Not generally suitable for operation under variable loads	About 2.5:1. Not generally suitable for operation under variable loads	About 4:1 to 5:1. Some special designs achieve 8:1 or more
Entrainment	Moderate	Moderate	Moderate
Pressure drop	Moderate	Moderate	Slightly higher
Cost	Low	Low	About 20 percent higher
Maintenance	Low	Low	Moderate
Fouling tendency	Low to very low	Low to very low	Moderate
Effects of corrosion	Low	Very low	Moderate
Main applications	(1) Most columns when turndown is not critical (2) High fouling and corrosion potential	(1) Most columns when turndown is not critical (2) High fouling and corrosion potential	(1) Most columns (2) Services where turndown is important

jets disappears at low liquid rates, and the drop layer approaches the tray floor, similar to the classic spray regime.

PRIMARY TRAY CONSIDERATIONS

Number of Passes Tray liquid may be split into two or more flow passes to reduce tray liquid load Q_L (Fig. 14-21). Each pass carries $1/N_p$ fraction of the total liquid load (e.g., $\frac{1}{4}$ in four-pass trays). Liquid in each pass reverses direction on alternate trays. Two-pass trays have perfect symmetry with full remixing in the center downcomers. Four-pass trays are symmetric along the centerline, but the side and central passes are nonsymmetric. Also, the center and off-center downcomers only partially remix the liquid, allowing any maldistribution to propagate. Maldistribution can cause major loss of efficiency and capacity in four-pass trays. Three-pass trays are even more prone to maldistribution due to their complete nonsymmetry. Most designers avoid three-pass trays altogether, jumping from two to four passes. Good practices for liquid and vapor balancing and for avoiding maldistribution in multipass trays were described by Pilling [*Chemical Engineering Progr.*, p. 22 (June 2005)], Bolles [*AIChE J.*, **22**(1), p. 153 (1976)], and Kister (*Distillation Operation*, McGraw-Hill, New York, 1990).

Common design practice is to minimize the number of passes, resorting to a larger number only when the liquid load exceeds 100 to 140 $m^3/(h \cdot m)$ (11 to 15 gpm/in) of outlet weir length [*Davies and Gordon, Petro/Chem Eng.*, p. 228 (December 1961)]. Trays smaller than 1.5-m (5-ft) diameter seldom use more than a single pass; those with 1.5- to 3-m (5- to 10-ft) diameters seldom use more than two passes. Four-pass trays are common in high liquid services with towers larger than 5-m (16-ft) diameter.

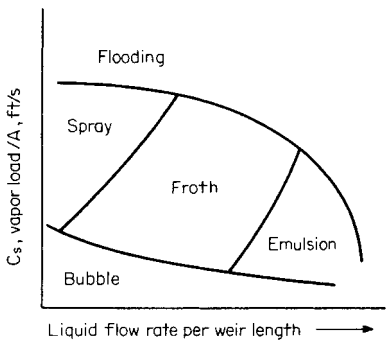

FIG. 14-19 The flow regime likely to exist on a distillation tray as a function of vapor and liquid loads. *(From H. Z. Kister,* Distillation Design, *copyright ©1992 by McGraw-Hill; reprinted by permission.)*

Tray Spacing Taller spacing between successive trays raises capacity, leading to a smaller tower diameter, but also raises tower height. There is an economic tradeoff between tower height and diameter. As long as the tradeoff exists, tray spacing has little effect on tower economies and is set to provide adequate access. In towers with larger than 1.5-m (5-ft) diameter, tray spacing is typically 600 mm (24 in), large enough to permit a worker to crawl between trays. In very large towers (>6-m or 20-ft diameter), tray spacings of 750 mm (30 in) are often used. In chemical towers (as distinct from petrochemical, refinery, and gas plants), 450 mm (18 in) has been a popular tray spacing. With towers smaller than 1.5 m (5 ft), tower walls are reachable from the manways, there is no need to crawl, and it becomes difficult to support thin and tall columns, so smaller tray spacing (typically 380 to 450 mm or 15 to 18 in) is favored. Towers taller than 50 m (160 ft) also favor smaller tray spacings (400 to 450 mm or 16 to 18 in). Finally, cryogenic towers enclosed in cold boxes favor very small spacings, as small as 150 to 200 mm (6 to 8 in), to minimize the size of the cold box.

More detailed considerations for setting tray spacing were discussed by Kister (*Distillation Operation*, McGraw-Hill, New York, 1990) and Mukherjee [*Chem. Eng.* p. 53 (September 2005)].

Outlet Weir The outlet weir should maintain a liquid level on the tray high enough to provide sufficient gas-liquid contact without causing excessive pressure drop, downcomer backup, or a capacity limitation. Weir heights are usually set at 40 to 80 mm (1.5 to 3 in). In this range, weir heights have little effect on distillation efficiency [Van Winkle, *Distillation*, McGraw-Hill, New York, 1967; Kreis and Raab, *IChemE Symp. Ser.* **56,** p. 3.2/63 (1979)]. In operations where long residence times are necessary (e.g., chemical reaction, absorption, stripping) taller weirs do improve efficiency, and weirs 80 to 100 mm (3 to 4 in) are more common (Lockett, *Distillation Tray Fundamentals*, Cambridge University Press, Cambridge, England, 1986).

Adjustable weirs (Fig. 14-22*a*) are used to provide additional flexibility. They are uncommon with conventional trays, but are used with some proprietary trays. Swept-back weirs (Fig. 14-22*b*) are used to extend the effective length of side weirs, either to help balance liquid flows to nonsymmetric tray passes or/and to reduce the tray liquid loads. Picket fence weirs (Fig. 14-22*c*) are used to shorten the effective length of a weir, either to help balance multipass trays' liquid flows (they are used in center and off-center weirs) or to raise tray liquid load and prevent drying in low-liquid-load services. To be effective, the pickets need to be tall, typically around 300 to 400 mm (12 to 16 in) above the top of the weir. An excellent discussion of weir picketing practices was provided by Summers and Sloley (*Hydroc. Proc.*, p. 67, January 2007).

Downcomers A downcomer is the drainpipe of the tray. It conducts liquid from one tray to the tray below. The fluid entering the downcomer is far from pure liquid; it is essentially the froth on the tray, typically 20 to 30 percent liquid by volume, with the balance being gas. Due to the density difference, most of this gas disengages in the downcomer and vents back to the tray from the downcomer entrance. Some gas bubbles usually remain in the liquid even at the bottom of the downcomer, ending on the tray below [Lockett and Gharani, *IChemE Symp. Ser.* **56,** p. 2.3/43 (1979)].

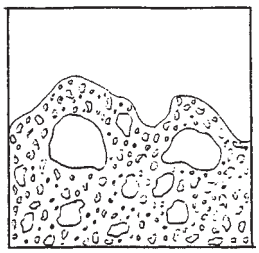

(a)

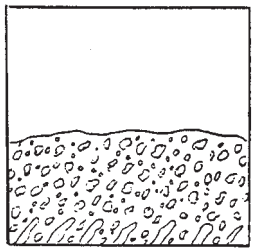

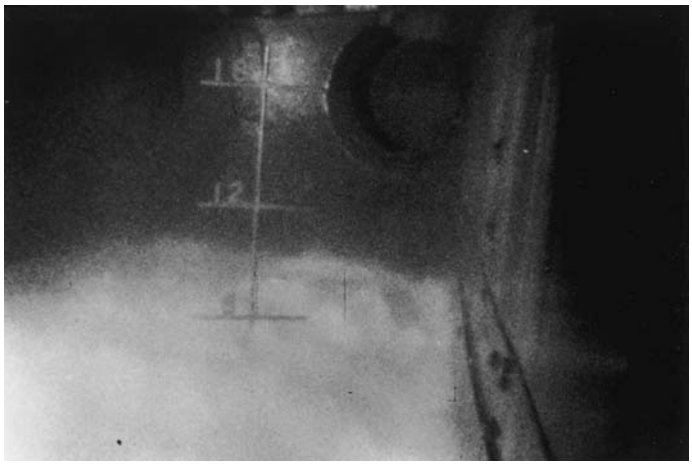

(b)

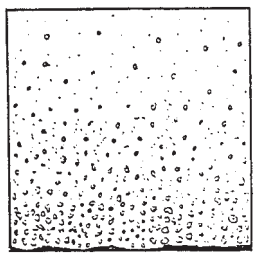

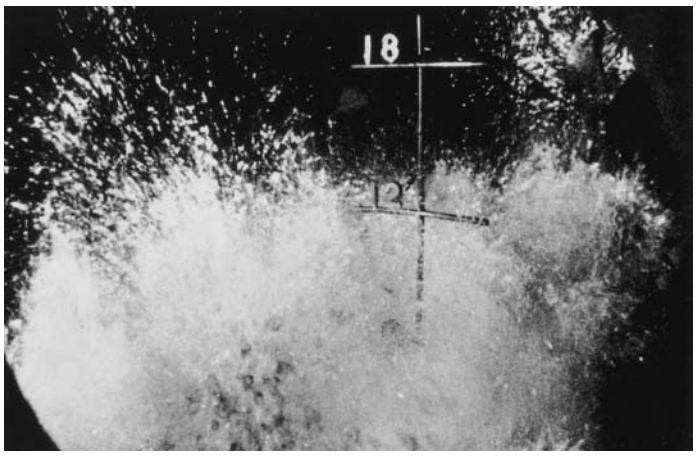

(c)

FIG. 14-20 Distillation flow regimes: schematics and photos. (*a*) Froth. (*b*) Emulsion. (*c*) Spray. [*Schematics from H. Z. Kister,* Distillation Design, *copyright © 1992 by McGraw-Hill, Inc.; reprinted by permission. Photographs courtesy of Fractionation Research Inc. (FRI).*]

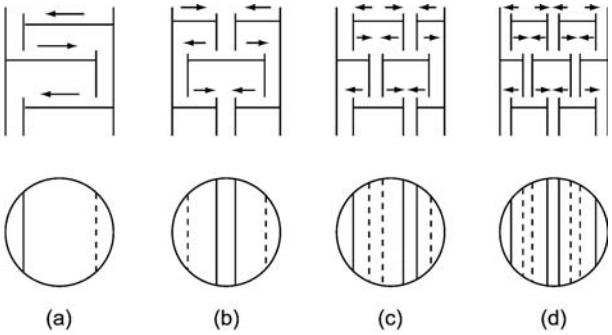

FIG. 14-21 Flow passes on trays. (*a*) Single-pass. (*b*) Two-pass. (*c*) Three-pass. (*d*) Four-pass.

The straight, segmental vertical downcomer (Fig. 14-23*a*) is the most common downcomer geometry. It is simple and inexpensive and gives good utilization of tower area for downflow. Circular downcomers (downpipes) (Fig. 14-23*b*), are cheaper, but poorly utilize tower area and are only suitable for very low liquid loads. Sloped downcomers (Fig. 14-23*c, d*) improve tower area utilization for downflow. They provide sufficient area and volume for gas-liquid disengagement at the top of the downcomer, gradually narrowing as the gas disengages, minimizing the loss of bubbling area at the foot of the downcomer. Sloped downcomers are invaluable when large downcomers are required such as at high liquid loads, high pressures, and foaming systems. Typical ratios of downcomer top to bottom areas are 1.5 to 2.

Antijump baffles (Fig. 14-24) are sometimes installed just above center and off-center downcomers of multipass trays to prevent liquid from one pass skipping across the downcomer onto the next pass. Such liquid jump adds to the liquid load on each pass, leading to premature flooding. These baffles are essential with proprietary trays that induce forward push (see below).

Clearance under the Downcomer Restricting the downcomer bottom opening prevents gas from the tray from rising up the downcomer and interfering with its liquid descent (*downcomer unsealing*). A common design practice makes the downcomer clearance 13 mm (0.5 in) lower than the outlet weir height (Fig. 14-25) to ensure submergence at all times [Davies and Gordon, *Petro/Chem Eng.*, p. 250 (November 1961)]. This practice is sound in the froth and emulsion regimes, where tray dispersions are liquid-continuous, but is ineffective in the spray regime where tray dispersions are gas-continuous and there is no submergence. Also, this practice can be unnecessarily restrictive at high liquid loads where high crests over the weirs sufficiently protect the downcomers from gas rise. Generally, downcomer clearances in the spray regime need to be smaller, while those in the emulsion regime can be larger, than those set by the above practice. Seal pans and inlet weirs are devices sometimes used to help with downcomer sealing while keeping downcomer clearances large. Details are in Kister's book (*Distillation Operation*, McGraw-Hill, New York, 1990).

Hole Sizes Small holes slightly enhance tray capacity when limited by entrainment flood. Reducing sieve hole diameters from 13 to 5 mm ($\frac{1}{2}$ to $\frac{3}{16}$ in) at a fixed hole area typically enhances capacity by 3 to 8 percent, more at low liquid loads. Small holes are effective for reducing entrainment and enhancing capacity in the spray regime ($Q_L < 20$ m^3/hm of weir). Hole diameter has only a small effect on pressure drop, tray efficiency, and turndown.

On the debit side, the plugging tendency increases exponentially as hole diameters diminish. Smaller holes are also more prone to corrosion. While 5-mm ($\frac{3}{16}$-in) holes easily plug even by scale and rust, 13-mm ($\frac{1}{2}$-in) holes are quite robust and are therefore very common. The small holes are only used in clean, noncorrosive services. Holes smaller than 5 mm are usually avoided because they require drilling (larger holes are punched), which is much more expensive. For highly fouling services, 19- to 25-mm ($\frac{3}{4}$- to 1-in) holes are preferred.

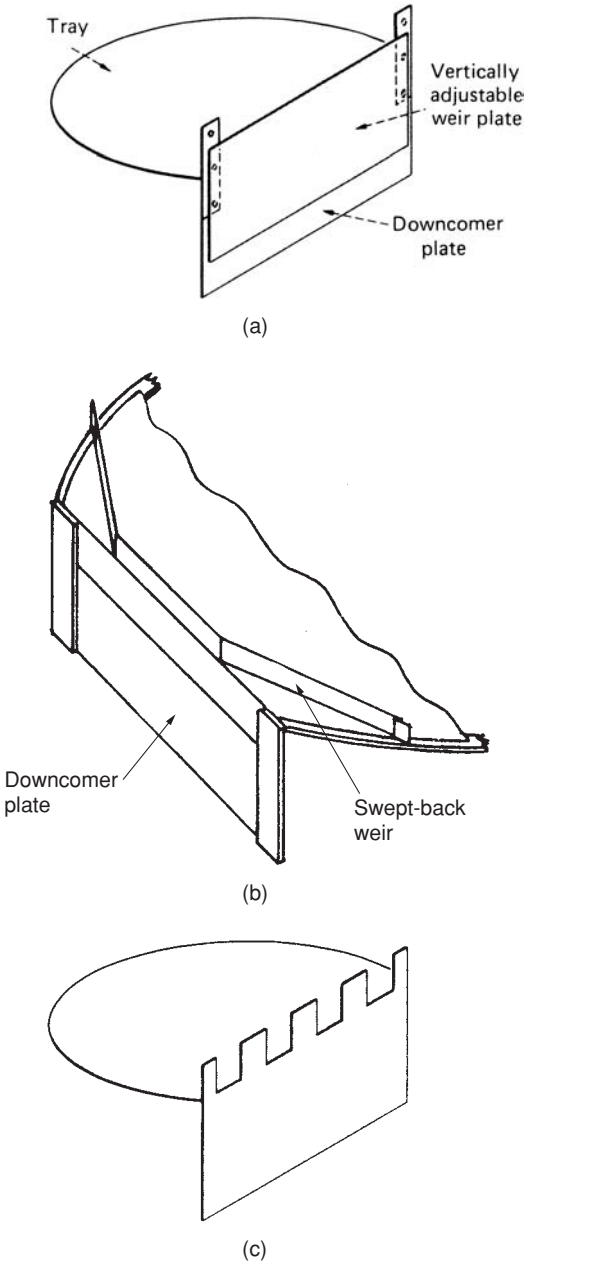

FIG. 14-22 Unique outlet weir types. (*a*) Adjustable. (*b*) Swept back. (*c*) Picket fence. *(Parts a, c, from H. Z. Kister,* Distillation Operation, *copyright © 1990 by McGraw-Hill; reprinted by permission. Part b, courtesy of Koch-Glitsch LP.)*

Similar considerations apply to fixed valves. Small fixed valves have a slight capacity advantage, but are far more prone to plugging than larger fixed valves.

For round moving valves, common orifice size is 39 mm (1^{17}⁄$_{32}$ in). The float opening is usually of the order of 8 to 10 mm (0.3 to 0.4 in).

In recent years there has been a trend toward minivalves, both fixed and moving. These are smaller and therefore give a slight capacity advantage while being more prone to plugging.

Fractional Hole Area Typical sieve and fixed valve tray hole areas are 8 to 12 percent of the bubbling areas. Smaller fractional hole

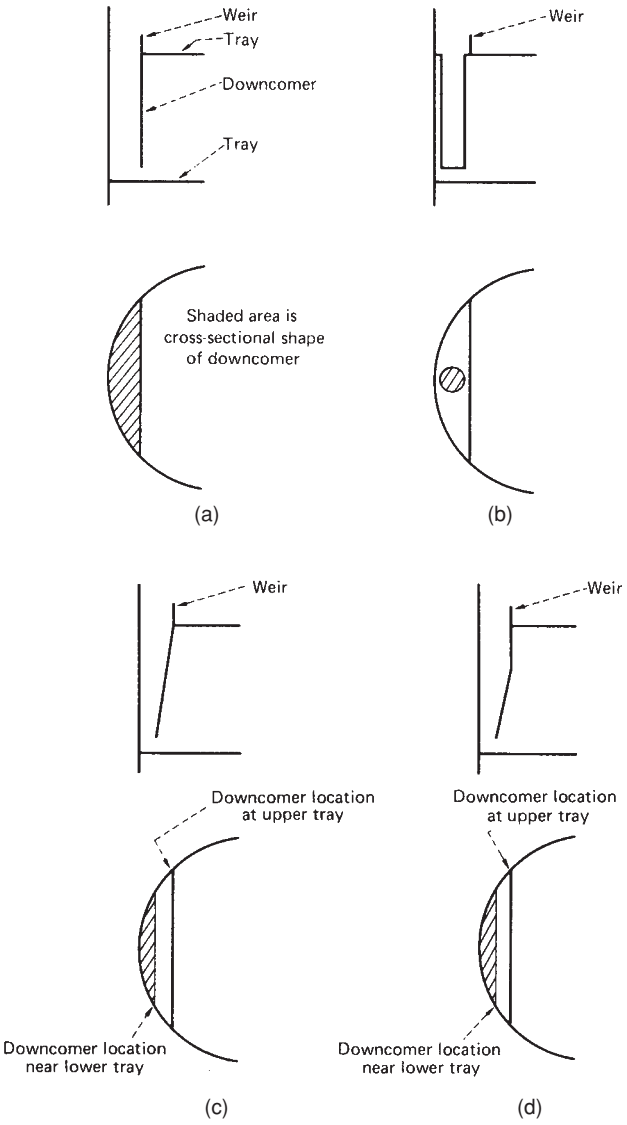

FIG. 14-23 Common downcomer types. (*a*) Segmental. (*b*) Circular. (*c, d*) Sloped. (*From Henry Z. Kister,* Chem. Eng., *December 29, 1980; reprinted courtesy of* Chemical Engineering.)

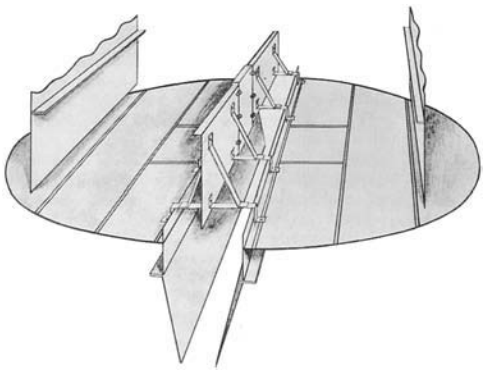

FIG. 14-24 Antijump baffle. *(Reprinted courtesy of Koch-Glitsch LP.)*

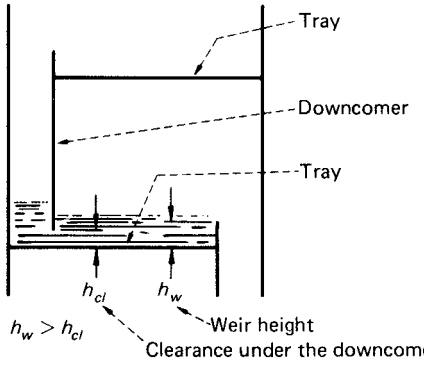

FIG. 14-25 A common design practice of ensuring a positive downcomer seal. (*From Henry Z. Kister,* Chem. Eng., *December 29, 1980; reprinted courtesy of* Chemical Engineering.)

areas bring about a capacity reduction when limited by entrainment or downcomer backup flood or by excessive pressure drop. At above 12 percent of the bubbling areas, the capacity gains from higher hole areas become marginal while weeping and, at high liquid loads also channeling, escalate.

Typical open-slot areas for moving valve trays are 14 to 15 percent of the bubbling area. Here the higher hole areas can be afforded due to the high turndown of the valves.

Moving valves can have a sharp or a smooth ("venturi") orifice. The venturi valves have one-half the dry pressure drop of the sharp-orifice valves, but are far more prone to weeping and channeling than the sharp-orifice valves. Sharp orifices are almost always preferred.

Multipass Balancing There are two balancing philosophies: equal bubbling areas and equal flow path lengths. Equal bubbling areas means that all active area panels on Fig. 14-21*d* are of the same area, and each panel has the same hole (or open-slot) area. In a four-pass tray, one-quarter of the gas flows through each panel. To equalize the *L/G* ratio on each panel, the liquid needs to be split equally to each panel. Since the center weirs are longer than the side weirs, more liquid tends to flow toward the center weir. To equalize, side weirs are often swept back (Fig. 14-22*b*) while center weirs often contain picket fences (Fig. 14-22*c*).

The alternative philosophy (equal flow path lengths) provides more bubbling and perforation areas in the central panels of Fig. 14-21*d* and less in the side panels. To equalize the *L/G* ratio, less liquid needs to flow toward the sides, which is readily achieved, as the center weirs are naturally longer than the side weirs. Usually there is no need for swept-back weirs, and only minimal picket-fencing is required at the center weir.

Equal flow path panels are easier to fabricate and are cheaper, while equal bubbling areas have a robustness and reliability advantage due to the ease of equally splitting the fluids. The author had good experience with both when well-designed. Pass balancing is discussed in detail by Pilling [*Chem. Eng. Prog.,* p. 22 (June 2005)] and by Jaguste and Kelkar [*Hydroc. Proc.,* p. 85 (March 2006)].

TRAY CAPACITY ENHANCEMENT

High-capacity trays evolved from conventional trays by including one or more capacity enhancement features such as those discussed below. These features enhance not only the capacity but usually also the complexity and cost. These features have varying impact on the efficiency, turndown, plugging resistance, pressure drop, and reliability of the trays.

Truncated Downcomers/Forward Push Trays Truncated downcomers/forward push trays include the Nye™ Tray, Maxfrac™ (Fig. 14-26*a*), Triton™, and MVGT™. In all these, the downcomer from the tray above terminates about 100 to 150 mm (4 to 6 in) above the tray floor. Liquid from the downcomer issues via holes or slots,

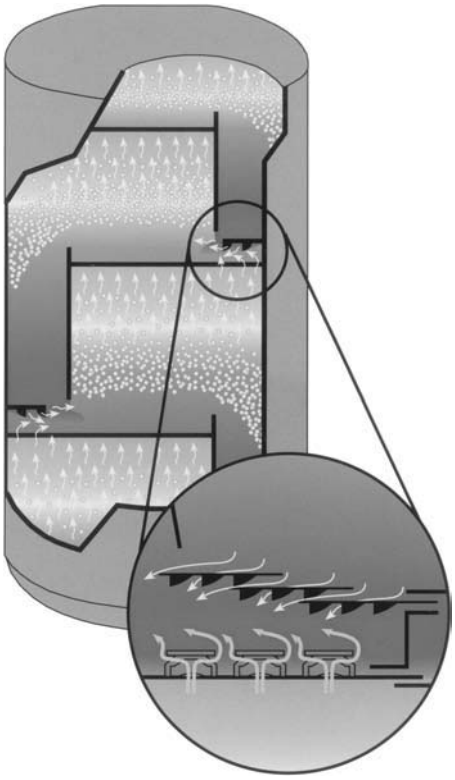

(a)

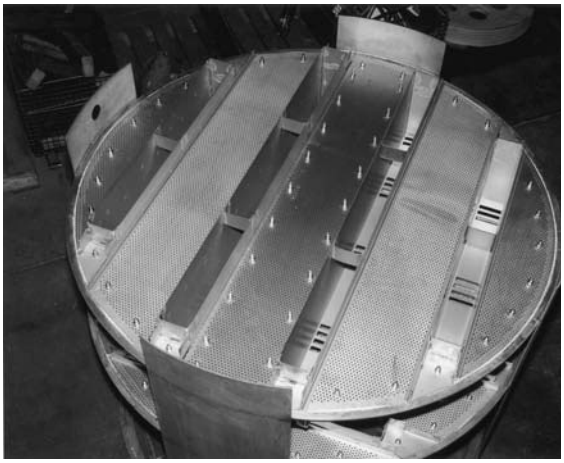

(c)

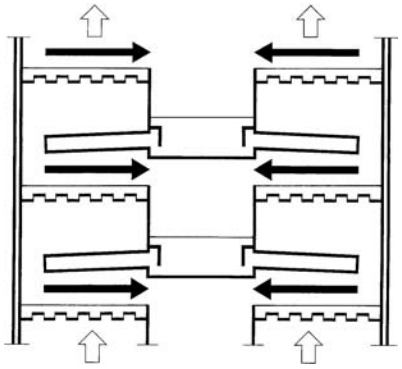

(d)

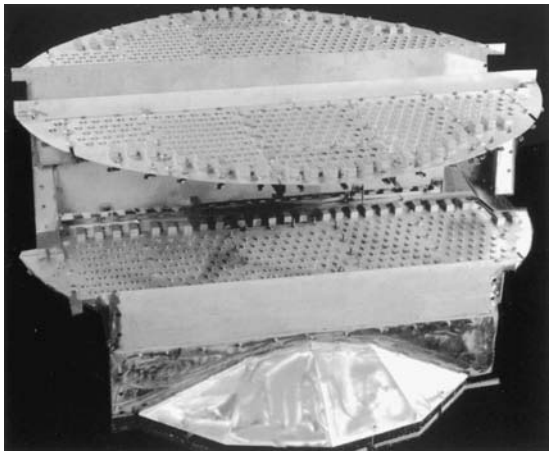

(b)

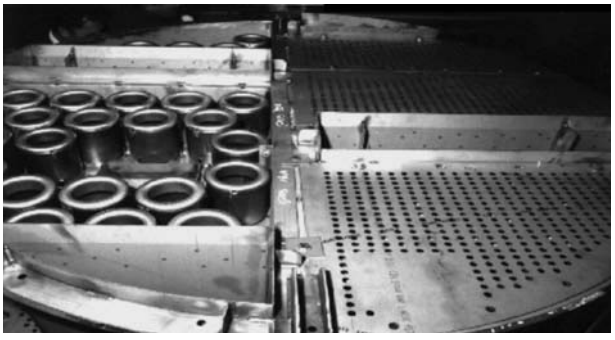

(e)

FIG. 14-26 Tray capacity enhancement. (*a*) Truncated downcomer/forward-push principle illustrated with a schematic of the Maxfrac™ tray. (*b*) High top-to-bottom area ratio illustrated with a two-pass Superfrac™ tray. Note the baffle in the front side downcomer that changes the side downcomer shape from segmental to multichordal. Also note the bubble promoters on the side of the upper tray and in the center of the lower tray, which give forward push to the tray liquid. (*c*) Top view of an MD™ tray with four downcomers. The decks are perforated. The holes in the downcomer lead the liquid to the active area of the tray below, which is rotated 90°. (*d*) Schematic of the Slit™ tray, type A, showing distribution pipes. Heavy arrows depict liquid movement; open arrows, gas movement. (*e*) The ConSep™ tray. The right-hand side shows sieve panels. On the left-hand side, these sieve panels were removed to permit viewing the contact cyclones that catch the liquid from the tray below. (*Parts a, b, courtesy of Koch-Glitsch LP; part c, courtesy of UOP LLC; part d, courtesy of Kühni AG; part e, courtesy of Sulzer Chemtech Ltd. and Shell Global Solutions International BV.*)

directed downward or in the direction of liquid flow. The tray floor under each downcomer is equipped with fixed valves or side perforations. Gas issuing in this region, typically 10 to 20 percent of the total tray gas, is deflected horizontally in the direction of liquid flow by the downcomer floor. This horizontal gas flow pushes liquid droplets toward the tower wall directly above the outlet downcomer. The tower wall catches this liquid, and directs it downward into the downcomer. This deentrains the gas space. In multipass trays, antijump baffles (Fig. 14-24), typically 300 mm or taller, are installed above center and off-center downcomers to catch the liquid and prevent its jumping from pass to pass. The rest of the tray features are similar to those of conventional trays. The tray floor may contain fixed valves, moving valves, or sieve holes.

Trays from this family are proprietary, and have been extensively used in the last two to three decades with great success. Compared to equivalent conventional trays, the truncated downcomer/forward push trays give about 8 to 12 percent more gas-handling capacity at much the same efficiency.

High Top-to-Bottom Downcomer Area and Forward Push Sloping downcomers from top to bottom raises the available tray bubbling area and, therefore, the gas-handling capacity (see "Downcomers"). As long as the ratio of top to bottom areas is not excessive, sloping does not lower downcomer capacity. Downcomer choke flood restricts the downcomer entrance, not exit, because there is much less gas at the downcomer bottom. However, a high top-to-bottom area ratio makes the downcomer bottom a very short chord, which makes distribution of liquid to the tray below difficult. To permit high top-to-bottom area ratios, some trays use a special structure (Fig. 14-26*b*) to change the downcomer shape from segmental to semiarc or multichordal. This high ratio of top to bottom areas, combined with forward push (above) imparted by bubblers and directional fixed or moving valves, and sometimes directional baffles, is used in trays including Superfrac™ III (Fig. 14-26*b*) and IV and V-Grid Plus™. When the downcomer inlet areas are large, these trays typically gain 15 to 20 percent capacity compared to equivalent conventional trays at much the same efficiency. Trays from this family are proprietary, and have been used successfully for about a decade.

Large Number of Truncated Downcomers These include the MD™ (Fig. 14-26*c*) and Hi-Fi™ trays. The large number of downcomers raises the total weir length, moving tray operation toward the peak capacity point of 20 to 30 m^3/hm (2 to 3 gpm/in) of outlet weir (see Fig. 14-29). The truncated downcomers extend about halfway to the tray below, discharging their liquid via holes or slots at the downcomer floor. The area directly under the downcomers is perforated or valved, and there is enough open height between the tray floor and the bottom of the downcomer for this perforated or valved area to be effective in enhancing the tray bubbling area.

Trays from this family are proprietary and have been successfully used for almost four decades. Their strength is in high-liquid-load services where reducing weir loads provides major capacity gains. Compared to conventional trays, they can gain as much as 20 to 30 percent capacity but at an efficiency loss. The efficiency loss is of the order of 10 to 20 percent due to the large reduction in flow path length (see "Efficiency"). When using these trays, the separation is maintained by either using more trays (typically at shorter spacing) or raising reflux and boilup. This lowers the net capacity gains to 10 to 20 percent above conventional trays. In some variations, forward push slots and antijump baffles are incorporated to enhance the capacity by another 10 percent.

Radial Trays These include the Slit™ tray and feature radial flow of liquid. In the efficiency-maximizing A variation (Fig. 14-26*d*), a multipipe distributor conducts liquid from each center downcomer to the periphery of the tray below, so liquid flow is from periphery to center on each tray. The capacity-maximizing B variation has central and peripheral (ring) downcomers on alternate trays, with liquid flow alternating from center-to-periphery to periphery-to-center on successive trays. The trays are arranged at small spacing (typically, 200 to 250 mm, or 8 to 10 in) and contain small fixed valves. Slit trays are used in chemical and pharmaceutical low-liquid-rate applications (<40 m^3/hm or 4 gpm/in of outlet weir), typically at pressures ranging from moderate vacuum to slight superatmospheric.

Centrifugal Force Deentrainment These trays use a contact step similar to that in conventional trays, followed by a separation step that disentrains the tray dispersion by using centrifugal force. Separation of entrained liquid before the next tray allows very high gas velocities, as high as 25 percent above the system limit (see "System Limit"), to be achieved. The capacity of these trays can be 40 percent above that of conventional trays. The efficiency of these trays can be 10 to 20 percent less than that of conventional trays due to their typical short flow paths (see "Efficiency").

These trays include the Ultrfrac™, the ConSep™ (Fig. 14-26*e*), and the Swirl Tube™ trays. This technology has been sporadically used in eastern Europe for quite some time. It is just beginning to make inroads into distillation in the rest of the world, and looks very promising.

OTHER TRAY TYPES

Bubble-Cap Trays (Fig. 14-27*a*) These are flat perforated plates with risers (chimneylike pipes) around the holes, and caps in the form of inverted cups over the risers. The caps are usually (but not always) equipped with slots through which some of the gas comes out, and may be round or rectangular. Liquid and froth are trapped on the tray to a depth at least equal to the riser or weir height, giving the bubble-cap tray a unique ability to operate at very low gas and liquid rates.

The bubble-cap tray was the workhorse of distillation before the 1960s. It was superseded by the much cheaper (as much as 10 times) sieve and valve trays. Compared to the bubble-cap trays, sieve and valve trays also offer slightly higher capacity and efficiency and lower entrainment and pressure drop, and are less prone to corrosion and fouling. Today, bubble-cap trays are only used in special applications where liquid or gas rates are very low. A large amount of information on bubble-cap trays is documented in several texts (e.g., Bolles in B. D. Smith, *Design of Equilibrium Stage Processes,* McGraw-Hill, 1963; Bolles, *Pet. Proc.*, February 1956, p. 65; March 1956, p. 82; April 1956, p. 72; May 1956, p. 109; Ludwig, *Applied Process Design for Chemical and Petrochemical Plants,* 2d ed., vol. 2, Gulf Publishing, Houston, 1979).

Dual-Flow Trays These are sieve trays with no downcomers (Fig. 14-27*b*). Liquid continuously weeps through the holes, hence their low efficiency. At peak loads they are typically 5 to 10 percent less efficient than sieve or valve trays, but as the gas rate is reduced, the efficiency gap rapidly widens, giving poor turndown. The absence of downcomers gives dual-flow trays more area, and therefore greater capacity, less entrainment, and less pressure drop, than conventional trays. Their pressure drop is further reduced by their large fractional hole area (typically 18 to 30 percent of the tower area). However, this low pressure drop also renders dual-flow trays prone to gas and liquid maldistribution.

In general, gas and liquid flows pulsate, with a particular perforation passing both gas and liquid intermittently, but seldom simultaneously. In large-diameter (>2.5-m, or 8-ft) dual-flow trays, the pulsations sometimes develop into sloshing, instability, and vibrations. The Ripple Tray™ is a proprietary variation in which the tray floor is corrugated to minimize this instability.

With large holes (16 to 25 mm), these trays are some of the most fouling-resistant and corrosion-resistant devices in the industry. This defines their main application: highly fouling services, slurries, and corrosive services. Dual-flow trays are also the least expensive and easiest to install and maintain.

A wealth of information for the design and rating of dual-flow trays, much of it originating from FRI data, was published by Garcia and Fair [*Ind. Eng. Chem. Res.* **41:**1632 (2002)].

Baffle Trays Baffle trays ("shed decks," "shower decks") (Fig. 14-28*a*) are solid half-circle plates, sloped slightly in the direction of outlet flow, with weirs at the end. Gas contacts the liquid as it showers from the plate. This contact is inefficient, typically giving 30 to 40 percent of the efficiency of conventional trays. This limits their application mainly to heat-transfer and scrubbing services. The capacity is high and pressure drop is low due to the high open area (typically 50 percent of the tower cross-sectional area). Since there is not much

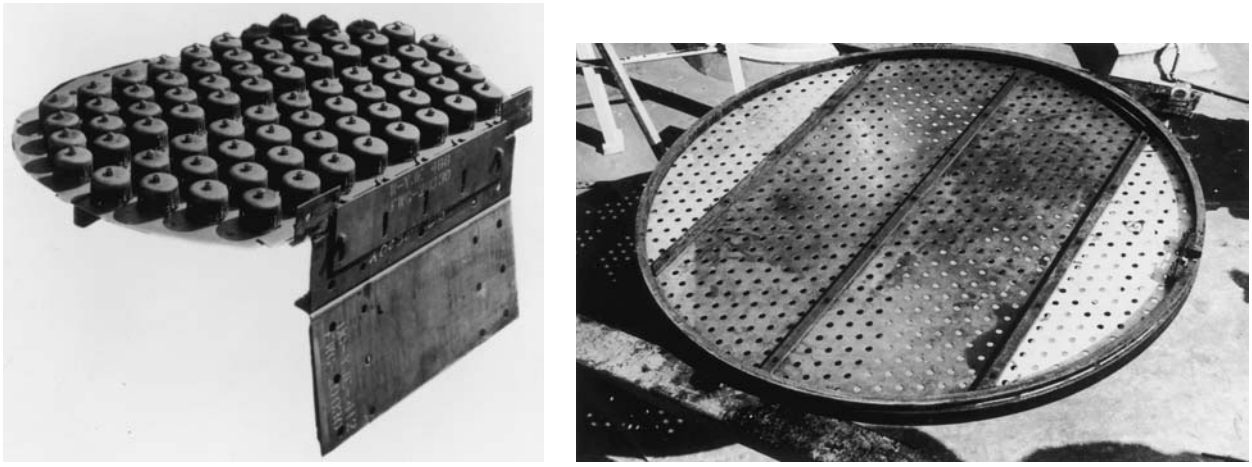

FIG. 14-27 Other trays. (*a*) Bubble-cap tray. (*b*) Dual-flow tray. [*Part a, courtesy of Koch-Glitsch LP; part b, courtesy of Fractionation Research Inc. (FRI).*]

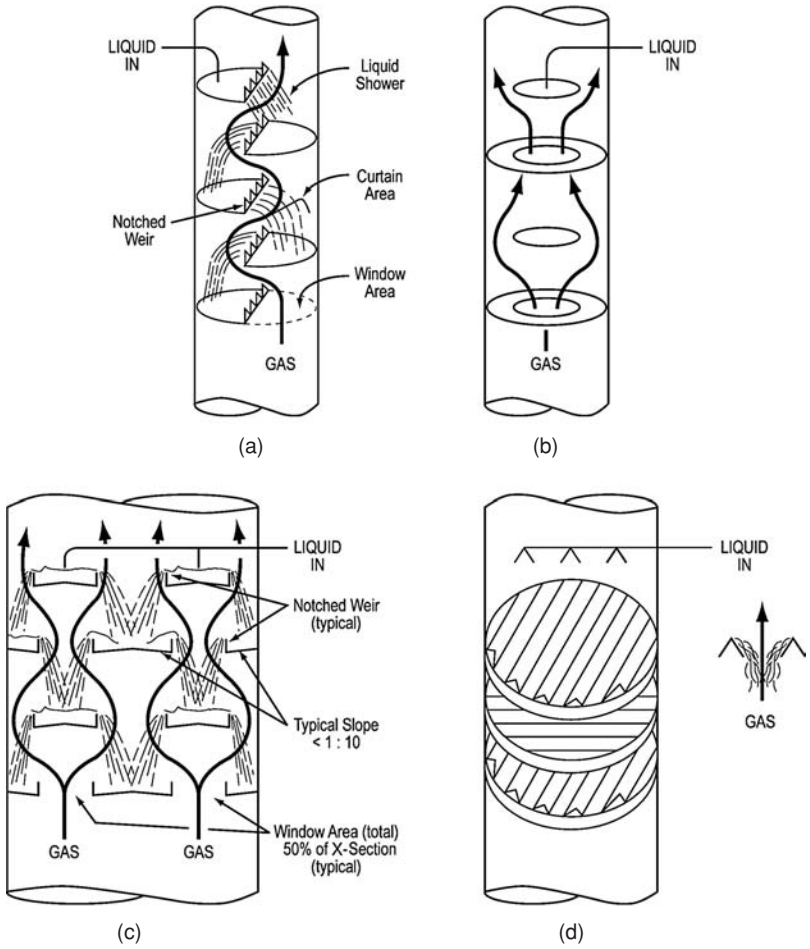

FIG. 14-28 Baffle tray variations. (*a*) Segmental. (*b*) Disk and doughnut. (*c*) Multipass. (*d*) Angle irons.

that can plug up, the baffle trays are perhaps the most fouling-resistant device in the industry, and their main application is in extremely fouling services. To be effective in these services, their liquid rate needs to exceed 20 m^3/hm (2 gpm/in) of outlet weir and dead spots formed due to poor support design (Kister, *Distillation Troubleshooting*, Wiley, 2006) eliminated.

There are several geometric variations. The disk and doughnut trays (Fig. 14-28*b*) replace the half-circle segmental plates by alternate plates shaped as disks and doughnuts, each occupying about 50 percent of the tower cross-sectional area. In large towers, multipass baffle trays (Fig. 14-28*c*) are common. Another variation uses angle irons, with one layer oriented at 90° to the one below (Fig. 14-28*d*). Multipass baffle trays, as well as angle irons, require good liquid (and to a lesser extent, also good gas) distribution, as has been demonstrated from field heat-transfer measurements [Kister and Schwartz, *Oil & Gas J.*, p. 50 (May 20, 2002)]. Excellent overviews of the fundamentals and design of baffle trays were given by Fair and Lemieux [Fair, *Hydro. Proc.*, p. 75 (May 1993); Lemieux, *Hydroc. Proc.*, p. 106 (September 1983)]. Mass-transfer efficiency data with baffle trays by Fractionation Research Inc. (FRI) have been released and presented together with their correlation (Fair, Paper presented at the AIChE Annual Meeting, San Francisco, November 2003).

FLOODING

Flooding is by far the most common upper capacity limit of a distillation tray. Column diameter is set to ensure the column can achieve the required throughput without flooding. Towers are usually designed to operate at 80 to 90 percent of the flood limit.

Flooding is an excessive accumulation of liquid inside a column. Flood symptoms include a rapid rise in pressure drop (the accumulating liquid increases the liquid head on the trays), liquid carryover from the column top, reduction in bottom flow rate (the accumulating liquid does not reach the tower bottom), and instability (accumulation is non-steady-state). This liquid accumulation is generally induced by one of the following mechanisms.

Entrainment (Jet) Flooding Froth or spray height rises with gas velocity. As the froth or spray approaches the tray above, some of the liquid is aspirated into the tray above as entrainment. Upon a further increase in gas flow rate, massive entrainment of the froth or spray begins, causing liquid accumulation and flood on the tray above.

Entrainment flooding can be subclassified into *spray entrainment flooding* (common) and *froth entrainment flooding* (uncommon). Froth entrainment flooding occurs when the froth envelope approaches the tray above, and is therefore only encountered with small tray spacings (<450 mm or 18 in) in the froth regime. At larger (and often even lower) tray spacing, the froth breaks into spray well before the froth envelope approaches the tray above.

The entrainment flooding prediction methods described here are based primarily on spray entrainment flooding. Considerations unique to froth entrainment flooding can be found elsewhere (Kister, *Distillation Design*, McGraw-Hill, New York, 1992).

Spray Entrainment Flooding Prediction Most entrainment flooding prediction methods derive from the original work of Souders and Brown [*Ind. Eng. Chem.* **26**(1), 98 (1934)]. Souders and Brown theoretically analyzed entrainment flooding in terms of droplet settling velocity. Flooding occurs when the upward vapor velocity is high enough to suspend a liquid droplet, giving

$$C_{SB} = u_{S,\text{flood}}\sqrt{\frac{\rho_G}{\rho_L - \rho_G}} \tag{14-80}$$

The Souders and Brown constant C_{SB} is the *C*-factor [Eq. (14-77)] at the entrainment flood point. Most modern entrainment flooding correlations retain the Souders and Brown equation (14-80) as the basis, but depart from the notion that C_{SB} is a constant. Instead, they express C_{SB} as a weak function of several variables, which differ from one correlation to another. Depending on the correlation, C_{SB} and $u_{S,\text{flood}}$ are based on either the net area A_N or on the bubbling area A_B.

The constant C_{SB} is roughly proportional to the tray spacing to a power of 0.5 to 0.6 (Kister, *Distillation Design*, McGraw-Hill, New York, 1992). Figure 14-29 demonstrates the effect of liquid rate and fractional hole area on C_{SB}. As liquid load increases, C_{SB} first increases, then peaks, and finally declines. Some interpret the peak as the transition from the froth to spray regime [Porter and Jenkins, *I. Chem. E. Symp. Ser.* **56,** Summary Paper, London (1979)]. C_{SB} increases slightly with fractional hole area at lower liquid rates, but there is little effect of fractional hole area on C_{SB} at high liquid rates. C_{SB} slightly increases as hole diameter is reduced.

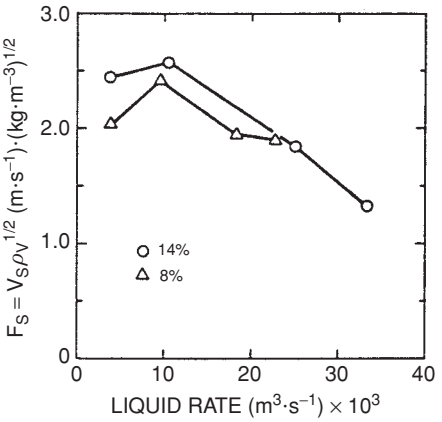

FIG. 14-29 Effect of liquid rate and fractional hole area on flood capacity. FRI sieve tray test data, cyclohexane/*n*-heptane, 165 kPa (24 psia), D_T = 1.2 m (4 ft), S = 610 mm (24 in), h_w = 51 mm (2 in), d_H = 12.7 mm (0.5 in), straight downcomers, A_D/A_T = 0.13. *(From T. Yanagi and M. Sakata,* Ind. Eng. Chem. Proc. Des. Dev. ***21,*** 712; copyright © 1982, *American Chemical Society, reprinted by permission.)*

For sieve trays, the entrainment flood point can be predicted by using the method by Kister and Haas [*Chem. Eng. Progr.*, **86**(9), 63 (1990)]. The method is said to reproduce a large database of measured flood points to within ± 15 percent. $C_{SB,\text{flood}}$ is based on the net area. The equation is

$$C_{SB,\text{flood}} = 0.0277(d_h^2\sigma/\rho_L)^{0.125}(\rho_G/\rho_L)^{0.1}(\text{TS}/h_{ct})^{0.5} \tag{14-81}$$

where d_h = hole diameter, mm
σ = surface tension, mN/m (dyn/cm)
ρ_G, ρ_L = vapor and liquid densities, kg/m^3
TS = tray spacing, mm
h_{ct} = clear liquid height at the froth-to-spray transition, mm; obtained from:

$$h_{ct} = h_{ct,\text{H}_2\text{O}}\,(996/\rho_L)^{0.5(1-n)} \tag{14-82}$$

$$h_{ct,\text{H}_2\text{O}} = \frac{0.497\,A_f^{-0.791}d_h^{0.833}}{1 + 0.013\,Q_L^{-0.59}A_f^{-1.79}} \tag{14-83}$$

$$n = 0.00091 d_h/A_f \tag{14-84}$$

In Eq. (14-83), Q_L = m^3 liquid downflow/(h·m weir length) and A_f = fractional hole area based on active ("bubbling") area; for instance, $A_f = A_h/A_a$.

The Kister and Haas method can also be applied to valve trays, but the additional approximations reduce its data prediction accuracy for valve trays to within ±20 percent. For valve trays, adaptations of Eqs. (14-81) to (14-84) are required:

$$d_h = \frac{4 \times (\text{area of opening of one fully open valve})}{\text{wetted perimeter of opening of one fully open valve}} \tag{14-85}$$

$$A_f = \frac{\text{no. valves} \times (\text{area of opening of one fully open valve})}{\text{active (bubbling) area}} \tag{14-86}$$

A correlation for valve tray entrainment flooding that has gained respect and popularity throughout the industry is the Glitsch "Equation 13" (Glitsch, Inc., *Ballast Tray Design Manual,* 6th ed., 1993;

available from Koch-Glitsch, Wichita, Kans.). This equation has been applied successfully for valve trays from different manufacturers, as well as for sieve trays with large fractional hole areas (12 to 15 percent). With tray spacings of 600 mm and higher, its flood prediction accuracy for valve trays has generally been within ±10 percent in the author's experience. The Glitsch correlation is

$$\frac{\%\ \text{flood}}{100} = \frac{C_B}{\text{CAF}} + 1.359\frac{Q\ \text{FPL}}{A_B\ \text{CAF}} \tag{14-87}$$

where

$$\text{CAF} = 0.3048\ \text{CAF}_0\ \text{SF} \tag{14-88}$$

C_B is the operating C-factor based on the bubbling area, m/s; Q is the liquid flow rate, m^3/s; A_B is the bubbling area, m^2; FPL is the flow path length, m, i.e., the horizontal distance between the inlet downcomer and the outlet weir. The flow path length becomes shorter as the number of passes increases. CAF_0 and CAF are the flood C-factors. CAF_0 is obtained from Fig. 14-30 in English units (ft/s). Equation (14-88) converts CAF_0 to the metric CAF (m/s), and corrects it by using a system factor SF. Values of SF are given in Table 14-9.

The Fair correlation [*Pet/Chem Eng.* **33**(10), 45 (September 1961)] for decades has been the standard of the industry for entrainment flood prediction. It uses a plot (Fig. 14-31) of surface-tension-corrected Souders and Brown flood factor C_{SB} against the dimensionless flow parameter shown in Fig. 14-31. The flow parameter represents a ratio of liquid to vapor kinetic energies:

$$F_{LG} = \frac{L}{G}\left(\frac{\rho_G}{\rho_L}\right)^{0.5} \tag{14-89}$$

Low values of F_{LG} indicate vacuum operation, high values indicate operation at higher pressures or at high liquid/vapor loadings. The liquid/gas ratio L/G is based on mass flow rates. For multipass trays, the ratio needs to be divided by the number of passes. The strength of the correlation is at the lower flow parameters. At higher flow parameters (high L/G ratios, high pressures, emulsion flow), Fig. 14-31 gives excessively conservative predictions, with the low values of C_{sbf} to the right likely to result from downcomer flow restrictions rather than excessive entrainment. The curves may be expressed in equation form as [Lygeros and Magoulas, *Hydrocarbon Proc.* **65**(12), 43 (1986)]:

$$C_{sbf} = 0.0105 + 8.127(10^{-4})(\text{TS}^{0.755})\exp[-1.463\ F_{LG}^{0.842}] \tag{14-90}$$

where TS = plate spacing, mm.

Figure 14-31 or Eq. (14-90) may be used for sieve, valve, or bubble-cap trays. The value of the capacity parameter (ordinate term in Fig. 14-31) may be used to calculate the maximum allowable vapor velocity through the net area of the plate:

$$U_{nf} = C_{sbf}\left(\frac{\sigma}{20}\right)^{0.2}\left(\frac{\rho_L - \rho_g}{\rho_g}\right)^{0.5} \tag{14-91}$$

where U_{nf} = gas velocity through net area at flood, m/s
C_{sbf} = capacity parameter corrected for surface tension, m/s

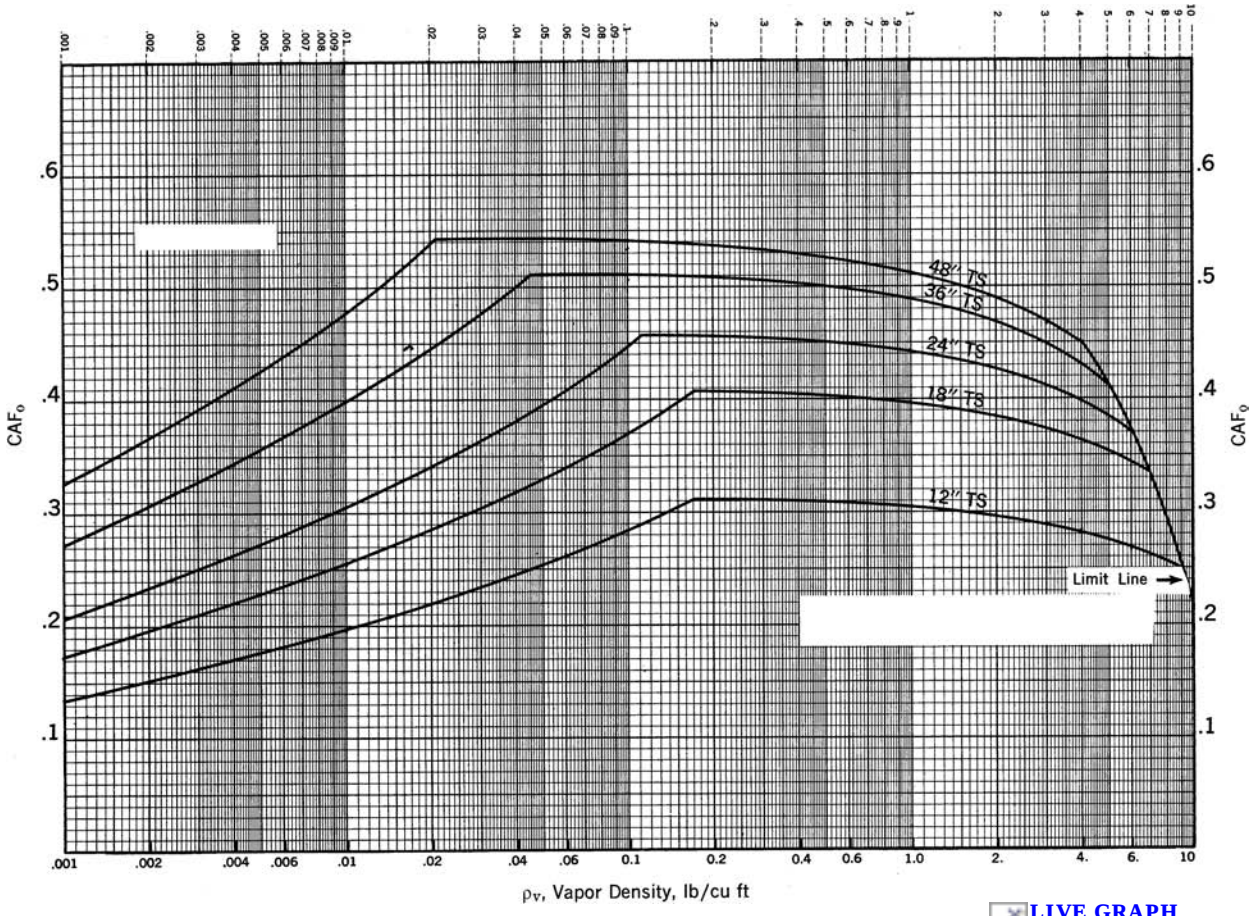

FIG. 14-30 Flood capacity of moving valve trays. *(Courtesy of Koch-Glitch LP.)*

LIVE GRAPH
Click here to view

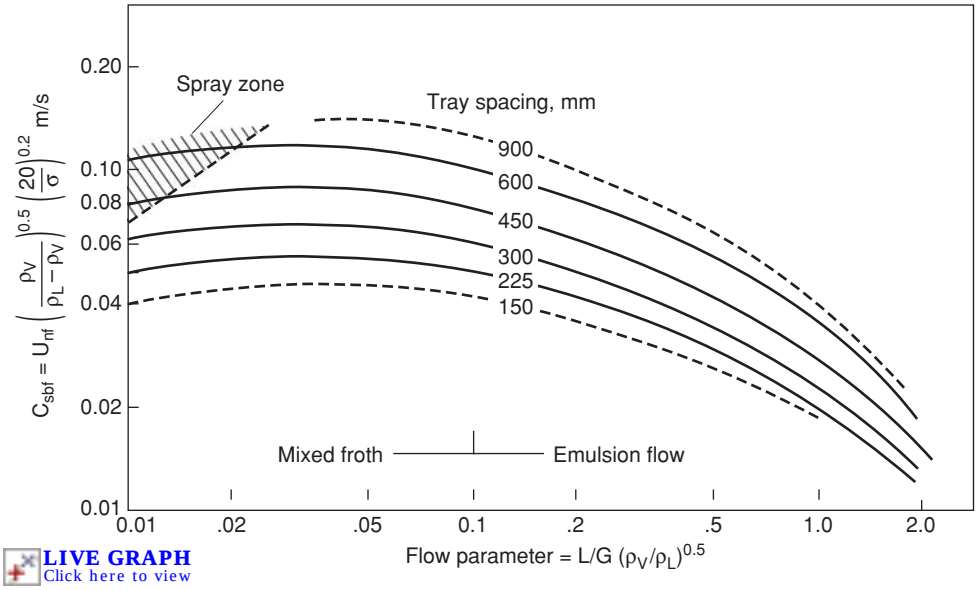

LIVE GRAPH
Click here to view

FIG. 14-31 Fair's entrainment flooding correlation for columns with crossflow trays (sieve, valve, bubble-cap). [*Fair, Pet/Chem Eng 33(10), 45 (September 1961).*]

σ = liquid surface tension, mN/m (dyn/cm)
ρ_L = liquid density, kg/m^3
ρ_G = gas density, kg/m^3

The application of the correlation is subject to the following restrictions:

1. System is low or nonfoaming.
2. Weir height is less than 15 percent of tray spacing.
3. Sieve-tray perforations are 13 mm (½ in) or less in diameter.
4. Ratio of slot (bubble cap), perforation (sieve), or full valve opening (valve plate) area A_h to active area A_a is 0.1 or greater. Otherwise the value of U_{nf} obtained from Fig. 14-31 should be corrected:

A_h/A_a	$U_{nf}/U_{nf,\text{Fig. 14-31}}$
0.10	1.00
0.08	0.90
0.06	0.80

where A_h = total slot, perforated, or open-valve area on tray.

Example 9: Flooding of a Distillation Tray An available sieve tray column of 2.5-m diameter is being considered for an ethylbenzene/styrene separation. An evaluation of loading at the top tray will be made. Key dimensions of the single-pass tray are:

Column cross section, m^2	4.91
Downcomer area, m^2	0.25
Net area, m^2	4.66
Active area, m^2	4.41
Hole area, m^2	0.617
Hole diameter, mm	4.76
Weir length, m	1.50
Weir height, mm	38
Tray spacing, mm	500

Conditions and properties at the top tray are:

Temperature, °C	78
Pressure, torr	100
Vapor flow, kg/h	25,500
Vapor density, kg/m^3	0.481
Liquid flow, kg/h	22,000
Liquid density, kg/m^3	841
Surface tension, mN/m	25

Solution. The method of Kister and Haas gives:

$$Q_L = \frac{22{,}000}{841 \times 1.50} = 17.44 \text{ m}^3\text{/h·m weir}$$

$$A_f = \frac{0.617}{4.41} = 0.14$$

By Eq. (14-83), $h_{ct,H_2O} = 7.98$ mm

Eq. (14-84): $n = 0.0309$

Eq. (14-82): $h_{ct} = 8.66$ mm

Finally, by Eq. (14-81),

$$C_{SB,\text{flood}} = 0.0277[(4.76^2)(25/841)]^{0.125} \times (0.481/841)^{0.1}(500/8.66)^{0.5}$$
$$= 0.0947 \text{ m/s}$$

Alternatively, applying the Fair correlation:

The flow parameter $F_{LG} = 0.021$ [Eq. (14-89)]. From Fig. 14-31, $C_{sbf} = 0.095$ m/s. Then, based on the net area,

$$C_{SB} = 0.095(25/20)^{0.2} = 0.0993 \text{ m/s}$$

about 5 percent higher than the answer obtained from Kister and Haas.

For the design condition, the C-factor based on the net area is

$$C = \frac{25{,}500}{3600(0.481)(4.66)}\sqrt{\frac{0.481}{841-0.481}} = 0.0756 \text{ m/s}$$

or about 80 percent of flood. The proposed column is entirely adequate for the service required.

System Limit (Ultimate Capacity) This limit is discussed later under "System Limit."

Downcomer Backup Flooding Aerated liquid backs up in the downcomer because of tray pressure drop, liquid height on the tray, and frictional losses in the downcomer apron (Fig. 14-32). All these increase with increasing liquid rate. Tray pressure drop also increases as the gas rate rises. When the backup of aerated liquid exceeds the tray spacing, liquid accumulates on the tray above, causing downcomer backup flooding.

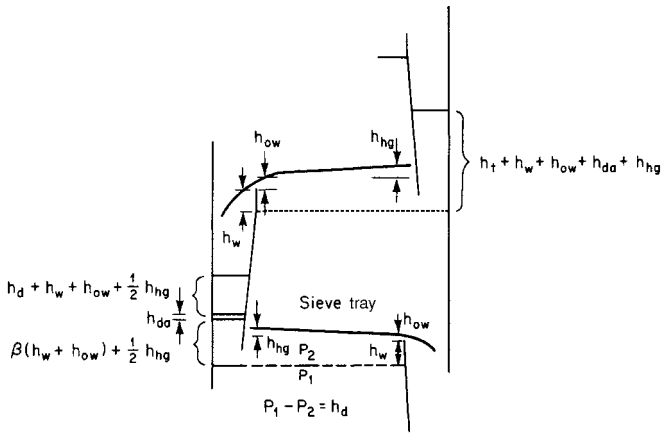

FIG. 14-32 Pressure-drop contributions for trays. h_d = pressure drop through cap or sieve, equivalent height of tray liquid; h_w = height of weir; h_{ow} = weir crest; h_{hg} = hydraulic gradient; h_{da} = loss under downcomer.

Downcomer backup is calculated from the pressure balance

$$h_{dc} = h_t + h_w + h_{ow} + h_{da} + h_{hg} \tag{14-92}$$

where h_{dc} = clear liquid height in downcomer, mm liquid
h_t = total pressure drop across the tray, mm liquid
h_w = height of weir at tray outlet, mm liquid
h_{ow} = height of crest over weir, mm liquid
h_{da} = head loss due to liquid flow under downcomer apron, mm liquid
h_{hg} = liquid gradient across tray, mm liquid

The heights of head losses in Eq. (14-92) should be in consistent units, e.g., millimeters or inches of liquid under operating conditions on the tray.

As noted, h_{dc} is calculated in terms of equivalent clear liquid. Actually, the liquid in the downcomer is aerated and actual backup is

$$h'_{dc} = \frac{h_{dc}}{\phi_{dc}} \tag{14-93}$$

where ϕ_{dc} is an average *relative* froth density (ratio of froth density to liquid density) in the downcomer. Design must not permit h'_{dc} to exceed the value of tray spacing plus weir height; otherwise, flooding can be precipitated.

The value of ϕ_{dc} depends upon the tendency for gas and liquid to disengage (froth to collapse) in the downcomer. For cases favoring rapid bubble rise (low gas density, low liquid viscosity, low system foamability) collapse is rapid, and fairly clear liquid fills the bottom of the downcomer (Fig. 14-17). For such cases, it is usual practice to employ a higher value of ϕ_{dc}. For cases favoring slow bubble rise (high gas density, high liquid viscosity, high system foamability), lower values of ϕ_{dc} should be used. As the critical point is approached in high-pressure distillations and absorptions, special precautions with downcomer sizing are mandatory. Table 14-6 lists values of ϕ_{dc} commonly used by the industry.

Downcomer Choke Flooding This is also called downcomer entrance flood or downcomer velocity flood. A downcomer must be sufficiently large to transport all the liquid downflow. Excessive friction losses in the downcomer entrance, and/or excessive flow rate of gas venting from the downcomer in counterflow, will impede liquid downflow, initiating liquid accumulation (termed downcomer choke flooding) on the tray above. The prime design parameter is the downcomer top area. Further down the downcomer, gas disengages from the liquid and the volumes of aerated liquid downflow and vented gas

TABLE 14-6 Criteria for Downcomer Aeration Factors

Foaming tendency	Bolles' criterion*		Glitsch's criterion†		Fair et al.'s criterion‡	
	Examples	ϕ_{dc}	Examples	ϕ_{dc}	Examples	ϕ_{dc}
Low	Low-molecular-weight hydrocarbons§ and alcohols	0.6	$\rho_G < 1.0$ lb/ft^3	0.6	Rapid bubble rise systems, such as low gas density, low liquid viscosity	0.5
Moderate	Distillation of medium-molecular-weight hydrocarbons	0.5	$1.0 < \rho_G < 3.0$ lb/ft^3	0.5		
High	Mineral oil absorbers	0.4	$\rho_G > 3.0$ lb/ft^3	0.4		
Very high	Amines, glycols	0.3			Slow bubble rise systems, such as high gas density, high liquid viscosity, foaming systems	0.2 – 0.3

*"Distillation Theory and Practice—an Intensive Course," University of New South Wales/University of Sydney, August 9–11, 1977.
† Glitsch, Inc., *Ballast Tray Design Manual,* 6th ed., 1993; available from Koch-Glitsch LP, Wichita, Kans.
‡ R. H. Perry and D. W. Green (eds.), *Perry's Chemical Engineers' Handbook*, 7th ed., McGraw-Hill, 1997.
§ The author believes that low-molecular-weight hydrocarbons refers to light hydrocarbons at near atmospheric pressure or under vacuum. The foam stability of light-hydrocarbon distillation at medium and high pressure is best inferred from the Glitsch criterion.
To convert from lb/ft^3, to kg/m^3, multiply by 16.0.
SOURCE: From H. Z. Kister, *Distillation Design,* copyright © 1992 by McGraw-Hill, Inc.; reprinted by permission.

upflow are greatly reduced. With sloped downcomers, the downcomer bottom area is normally set at 50 to 60 percent of the top downcomer area. This taper is small enough to keep the downcomer top area the prime choke variable.

There is no satisfactory published correlation for downcomer choke. The best that can be done in the absence of data or correlation is to apply the criteria for maximum velocity of clear liquid at the downcomer entrance. Kister *(Distillation Operation,* McGraw-Hill, New York, 1990) surveyed the multitude of published criteria for maximum downcomer velocity and incorporated them into a single set of guidelines (Table 14-7). The values for 30-in spacing were revised to reflect the author's recent experiences. The values given in Table 14-7 are not conservative. For a conservative design, multiply the values from Table 14-7 by a safety factor of 0.75. For very highly foaming systems, where antifoam application is undesirable, there are benefits for reducing downcomer design velocities down to 0.1 to 0.15 ft/s.

Another criterion sometimes used is to provide sufficient residence time in the downcomer to allow adequate disengagement of gas from the descending liquid, so that the liquid is relatively gas-free by the time it enters the tray below. Inadequate removal of gas from the liquid may choke the downcomer. Kister (loc. cit.) reviewed various published criteria for downcomer residence times and recommended those by Bolles (private communication, 1977) and Erbar and Maddox (Maddox, *Process Engineer's Absorption Pocket Handbook*, Gulf Publishing, Houston, 1985). Both sets of guidelines are similar and are summarized in Table 14-8. The residence times in Table 14-8 are *apparent residence times*, defined as the ratio of the total downcomer volume to the clear liquid flow in the downcomer.

As a segmental downcomer becomes smaller, its width decreases faster than its length, turning the downcomer into a long, narrow slot. This geometry increases the resistance to liquid downflow and to the upflow of disengaging gas. Small downcomers are also extremely sensitive to foaming, fouling, construction tolerances, and the introduction of debris. Generally, segmental downcomers smaller than 5 percent of the column cross-sectional area should be avoided. Additional discussion of small downcomers is available (Kister, *Distillation Operation,* McGraw-Hill, New York, 1990).

Derating ("System") Factors With certain systems, traditional flooding equations consistently give optimistic predictions. To allow for this discrepancy, an empirical derating or system factor (SF < 1.0) is applied. To obtain the actual or derated flood load, the flood gas load (entrainment flooding) or flood liquid load (downcomer choke) obtained from the traditional equations is multiplied by the derating factor. In the case of downcomer backup flood, the froth height from the traditional flood equation is divided by the derating factor.

Derating factors are vaguely related to the foaming tendency, but are also applied to nonfoaming systems where standard flooding equations consistently predict too high. Sometimes, derating factors are used solely as overdesign factors. Brierley *(Chem. Eng. Prog.,* July 1994, p. 68) states that some derating factors actually evolved from plant misoperation or from misinterpretation of plant data. Kister (loc. cit.) compiled the derating factors found in the literature into Table 14-9.

The application of derating factors is fraught with inconsistent practices and confusion. Caution is required. The following need to be carefully specified:

1. The flooding mechanism to which the derating factor applies (entrainment, downcomer backup, downcomer choke, or all these) must be specified.
2. Avoiding double derating. For instance, the values in Table 14-9 may apply with Eq. (14-81) because Eq. (14-81) does not take foaminess into account. However, they will double-derate a flood calculation that is made with a correlation or criteria that already take foaminess into account, such as the criteria for downcomer choke in Tables 14-7 and 14-8. Similarly, two different factors from Table 14-9 may apply to a single system; only one should be used.
3. Derating factors vary from source to source, and may depend on the correlation used as well as the system. For instance, some caustic wash applications have a track record of foaming more severely than other caustic wash applications (see note in Table 14-9). The derating factors in Table 14-9 are a useful guide, but are far from absolute.

ENTRAINMENT

Entrainment (Fig. 14-33) is liquid transported by the gas to the tray above. As the lower tray liquid is richer with the less-volatile components, entrainment counteracts the mass-transfer process, reducing tray efficiency. At times entrainment may transport nonvolatile impurities upward to contaminate the tower overhead product, or damage rotating machinery located in the path of the overhead gas.

Effect of Gas Velocity Entrainment increases with gas velocity to a high power. Generally, smaller powers, indicative of a relatively gradual change, are typical of low-pressure systems. Higher powers, which indicate a steep change, are typical of high-pressure systems.

Due to the steep change of entrainment with gas velocity at high pressure, the gas velocity at which entrainment becomes significant tends to coincide with the flood point. At low pressure, the rate of change of entrainment with gas velocity is much slower, and entrainment can be significant even if the tray is operating well below the flood point. For this reason, excessive entrainment is a common problem in low-pressure and vacuum systems, but is seldom troublesome with high-pressure systems. If encountered at high pressure, entrainment usually indicates flooding or abnormality.

Effect of Liquid Rate As the liquid rate is raised at constant gas rate, entrainment first diminishes, then passes through a minimum, and finally increases [Sakata and Yanagi, *I. Chem. E. Symp. Ser.* **56,** 3.2/21 (1979); Porter and Jenkins, *I. Chem. E. Symp. Ser.* **56,** Summary Paper, 1979; Friend, Lemieux, and Schreiner, *Chem. Eng.,* October 31, 1960, p. 101]. The entrainment minima coincide with the maxima in plots of entrainment flood *F*-factor against liquid load (Fig. 14-29). At the low liquid loads (spray regime), an increase in liquid load suppresses atomization, drop formation, and consequently entrainment. At higher liquid loads, an increase in liquid load reduces the effective tray spacing, thereby increasing entrainment. The entrainment minima have been interpreted by many workers as the tray dispersion change from predominantly spray to the froth regime [Porter and Jenkins, loc. cit.; Kister and Haas, *I. Chem. E. Symp. Ser.* **104,** p. A483 (1987)].

Effect of Other Variables Entrainment diminishes with higher tray spacing and increases with hole diameter [Kister and Haas, *I.*

TABLE 14-7 Maximum Downcomer Velocities

Foaming tendency	Example	Clear liquid velocity in downcomer, ft/s: 18-in spacing	24-in spacing	30-in spacing
Low	Low-pressure (<100 psia) light hydrocarbons, stabilizers, air-water simulators	0.4–0.5	0.5–0.6	0.5–0.6*
Medium	Oil systems, crude oil distillation, absorbers, midpressure (100–300 psia) hydrocarbons	0.3–0.4	0.4–0.5	0.4–0.5*
High	Amines, glycerine, glycols, high-pressure (>300 psia) light hydrocarbons	0.2–0.25	0.2–0.25	0.2–0.3

*Revised from previous versions.

To convert from ft/s to m/s, multiply by 0.3048; from in to mm, multiply by 25.4; from psia to bar, multiply by 0.0689.

SOURCE: From H. Z. Kister, *Distillation Operation,* copyright 1990 by McGraw-Hill, Inc.; reprinted by permission.

TABLE 14-8 Recommended Minimum Residence Time in the Downcomer

Foaming tendency	Example	Residence time, s
Low	Low-molecular-weight hydrocarbons,* alcohols	3
Medium	Medium-molecular-weight hydrocarbons	4
High	Mineral oil absorbers	5
Very high	Amines and glycols	7

*The author believes that low-molecular-weight hydrocarbons refers to light hydrocarbons at atmospheric conditions or under vacuum. The foaming tendency of light-hydrocarbon distillation at medium pressure [>7 bar (100 psia)] is medium; at high pressure [>21 bar (300 psia)], it is high.

SOURCE: W. L. Bolles (Monsanto Company), private communication, 1977.

Chem. E. Symp. Ser. **104,** p. A483 (1987); *Ind. Eng. Chem. Res.* **27,** p. 2331 (1988); Lemieux and Scotti, *Chem. Eng. Prog.* **65**(3), 52 (1969)]. The hole diameter effect is large in the spray regime but small in the froth regime. In the spray regime, entrainment also increases as the fractional hole area is lowered, but this variable has little effect in the froth regime [Yanagi and Sakata, *Ind. Eng. Chem. Proc. Des. Dev.* **21,** 712 (1982); and Kister and Haas, loc. cit.].

Entrainment Prediction For spray regime entrainment, the Kister and Haas correlation was shown to give good predictions to a wide commercial and pilot-scale data bank [*I. Chem. E. Symp. Ser.* **104,** A483 (1987)]. The correlation is

$$E_S = 4.742^{(10/\sigma)^{1.64}}\,\chi^{(10/\sigma)} \tag{14-94}$$

where

$$\chi = 872\left(\frac{u_B h_{Lt}}{\sqrt{d_H S}}\right)^4\left(\frac{\rho_G}{Q_L\rho_L}\right)\left(\frac{\rho_L-\rho_G}{\sigma}\right)^{0.25} \tag{14-95}$$

and

$$h_{Lt} = \frac{h_{ct}}{1+0.00262h_w} \tag{14-96}$$

The terms in Eqs. (14-94) through (14-96) are in the metric units described in the Nomenclature table at the beginning of this section.

The recommended range of application of the correlation is given in Table 14-10. The clear liquid height at the froth-to-spray transition h_{ct} is calculated using the corrected Jeronimo and Sawistowski [*Trans. Inst. Chem. Engnrs.* **51,** 265 (1973)] correlation as per Eqs. (14-82) to (14-84).

For decades, the Fair correlation [*Pet/Chem. Eng.,* **33**(10), 45 (September 1961)] has been used for entrainment prediction. In the spray regime the Kister and Haas correlation was shown to be more accurate [Koziol and Mackowiak, *Chem. Eng. Process.,* **27,** p. 145 (1990)]. In the froth regime, the Kister and Haas correlation does not apply, and Fair's correlation remains the standard of the industry. Fair's correlation (Fig. 14–34) predicts entrainment in terms of the flow parameter [Eq. (14-89)] and the ratio of gas velocity to entrainment flooding gas velocity. The ordinate values Ψ are fractions of gross liquid downflow, defined as follows:

$$\psi = \frac{e}{L_m + e} \tag{14-97}$$

where e = absolute entrainment of liquid, mol/time
L_m = liquid downflow rate without entrainment, mol/time

Figure 14-34 also accepts the validity of the Colburn equation [*Ind. Eng. Chem.,* **28,** 526 (1936)] for the effect of entrainment on efficiency:

$$\frac{E_a}{E_{mv}} = \frac{1}{1+E_{mv}[\psi/(1-\psi)]} \tag{14-98}$$

where E_{mv} = Murphree vapor efficiency [see Eq. (14-134)]
E_a = Murphree vapor efficiency, corrected for recycle of liquid entrainment

The Colburn equation is based on complete mixing on the tray. For incomplete mixing, e.g., liquid approaching plug flow on the tray, Rahman and Lockett [*I. Chem. E. Symp. Ser. No. 61,* 111 (1981)] and Lockett et al. [*Chem. Eng. Sci.,* **38,** 661 (1983)] have provided corrections.

TABLE 14-9 Derating ("System") Factors

System	Factor	Reference	Notes
Nonfoaming regular systems	1.0	1–4	
High pressure ($\rho_G > 1.8$ lb/ft^3)	$2.94/\rho_G^{0.32}$	2	Do not double-derate.
Low-foaming			
Depropanizers	0.9	4	
H_2S strippers	0.9	3, 4	
	0.85	2	
Fluorine systems (freon, BF_3)	0.9	1, 4	
Hot carbonate regenerators	0.9	2, 4	
Moderate-foaming			
Deethanizers			
Absorbing type, top section	0.85	1–4	
Absorbing type, bottom section	1.0	3	
	0.85	1, 2, 4	
Refrigerated type, top section	0.85	4	
	0.8	3	
Refrigerated type, bottom section	1.0	1, 3	
	0.85	4	
Demethanizers			
Absorbing type, top section	0.85	1–3	
Absorbing type, bottom section	1.0	3	
	0.85	1, 2	
Refrigerated type, top section	0.8	3	
Refrigerated type, bottom section	1.0	3	
Oil absorbers			
Above 0°F	0.85	1–4	Ref. 2 proposes these for "absorbers" rather than "oil absorbers."
Below 0°F	0.95	3	
	0.85	1, 4	
	0.8	2	
Crude towers	1.0	3	
	0.85	4	
Crude vacuum towers	1.0	3	
	0.85	2	
Furfural refining towers	0.85	2	
	0.8	4	
Sulfolane systems	1.0	3	
	0.85	4	
Amine regenerators	0.85	1–4	
Glycol regenerators	0.85	1, 4	
	0.8	3	
	0.65	2	
Hot carbonate absorbers	0.85	1, 4	
Caustic wash	0.65	2	The author suspects that this low factor refers only to some caustic wash applications but not to others.
Heavy-foaming			
Amine absorbers	0.8	2	
	0.75	3, 4	
	0.73	1	
Glycol contactors	0.73	1	Ref. 2 recommends 0.65 for glycol contactors in glycol synthesis gas service, 0.5 for others.
	0.65	3, 4	
	0.50	2	
Sour water strippers	0.5–0.7	3	
	0.6	2	
Oil reclaimer	0.7	2	
MEK units	0.6	1, 4	
Stable foam			
Caustic regenerators	0.6	2	
	0.3	1, 4	
Alcohol synthesis absorbers	0.35	2, 4	

References:

1. Glitsch, Inc., *Ballast Tray Design Manual,* Bulletin 4900, 6th ed., 1993. Available from Koch-Glitsch, Wichita, Kans.
2. Koch Engineering Co., Inc., *Design Manual—Flexitray,* Bulletin 960-1, Wichita, Kans., 1982.
3. Nutter Engineering, *Float Valve Design Manual,* 1976. Available from Sulzer ChemTech, Tulsa, Okla.
4. M. J. Lockett, *Distillation Tray Fundamentals,* Cambridge University Press, Cambridge, England, 1986.

To convert lb/ft^3 to kg/m^3, multiply by 16.0.

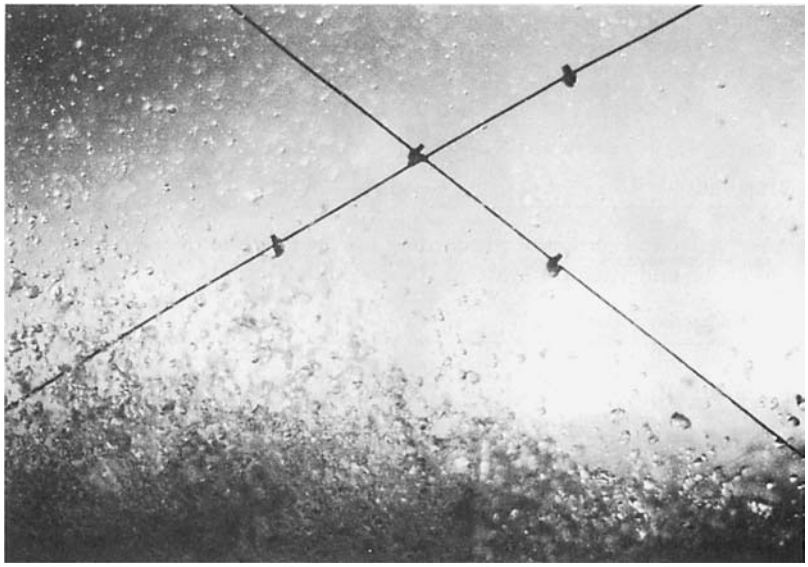

FIG. 14-33 Entrainment. [*Reprinted courtesy of Fractionation Research Inc. (FRI).*]

Fair (paper presented at the AIChE Annual Meeting, Chicago, Ill., November 1996) correlated data for efficiency reduction due to the rise of entrainment near entrainment flood, getting

$$\ln \psi = A + B\Phi + C\Phi^2 \qquad (14\text{-}99)$$

where Φ is the fractional approach to entrainment flood and A, B, and C are constants given by

	A	B	C
Highest likely efficiency loss	–3.1898	–4.7413	7.5312
Median (most likely) efficiency loss	–3.2108	–8.9049	11.6291
Lowest likely efficiency loss	4.0992	–29.9141	25.3343

Either the Kister and Haas or the Fair method can be used to evaluate Φ. The correlation has been tested with sieve trays in the flow parameter range of 0.024 to 0.087.

Example 10: Entrainment Effect on Tray Efficiency For the column in Example 9, estimate the efficiency loss should the operation be pushed from the design 80 percent of flood to 90 percent of flood. The midrange dry Murphree tray efficiency is 70 percent.

Solution The vapor and liquid densities and L/V ratio remain unchanged from Example 9, and so is the flow parameter (calculated 0.021 in Example 9). At 80 and 90 percent of flood, respectively, Fig. 14-34 gives $\psi = 0.15$ and 0.24. The respective efficiency reductions are calculated from Eq. (14-98),

TABLE 14-10 Recommended Range of Application for the Kister and Haas Spray Regime Entrainment Correlation

Flow regime	Spray only
Pressure	20–1200 kPa (3–180 psia)
Gas velocity	0.4–5 m/s (1.3–15 ft/s)
Liquid flow rate	3–40 $m^3/(m \cdot h)$ (0.5–4.5 gpm/in)
Gas density	0.5–30 kg/m^3 (0.03–2 lb/ft^3)
Liquid density	450–1500 kg/m^3 (30–90 lb/ft^3)
Surface tension	5–80 mN/m
Liquid viscosity	0.05–2 cP
Tray spacing	400–900 mm (15–36 in)
Hole diameter	3–15 mm (0.125–0.75 in)
Fractional hole area	0.07–0.16
Weir height	10–80 mm (0.5–3 in)

$$\frac{E_a}{E_{mv}} = \frac{1}{1 + 0.70[0.15/(1 - 0.15)]} = 0.89$$

$$\frac{E_a}{E_{mv}} = \frac{1}{1 + 0.70[0.24/(1 - 0.24)]} = 0.82$$

signifying an efficiency loss from 62 to 57 percent.

Alternatively, at 80 and 90 percent of entrainment flood, the median value of ψ from Eq. (14-99) is

$$\ln \psi = -3.2108 - 8.9049(0.80) + 11.6291(0.80^2)$$

giving $\psi = 0.056$ and from Eq. (14-98) $E_o/E_{mv} = 0.96$

$$\ln \psi = -3.2108 - 8.9049(0.90) + 11.6291(0.90^2)$$

giving $\psi = 0.164$ and from Eq. (14-98) $E_o/E_{mv} = 0.88$

signifying an efficiency reduction from 67 to 62 percent.

PRESSURE DROP

In vacuum distillation, excessive pressure drop causes excessive bottom temperatures which, in turn, increase degradation, polymerization, coking, and fouling, and also loads up the column, vacuum system, and reboiler. In the suction of a compressor, excessive pressure drop increases the compressor size and energy usage. Such services attempt to minimize tray pressure drop. Methods for estimating pressure drops are similar for most conventional trays. The total pressure drop across a tray is given by

$$h_t = h_d + h'_L \qquad (14\text{-}100)$$

where h_t = total pressure drop, mm liquid
h_d = pressure drop across the dispersion unit (dry hole for sieve trays; dry valve for valve trays), mm liquid
h'_L = pressure drop through aerated mass over and around the disperser, mm liquid

It is convenient and consistent to relate all of these pressure-drop terms to height of equivalent clear liquid (deaerated basis) on the tray, in either millimeters or inches of liquid.

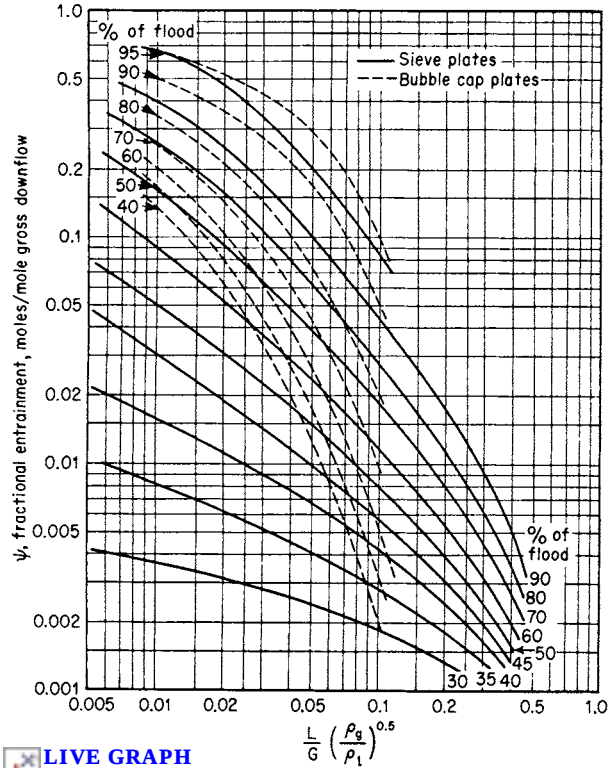

LIVE GRAPH
Click here to view

FIG. 14-34 Entrainment correlation. L/G = liquid-gas mass ratio; and ρ_l and ρ_g = liquid and gas densities. [*Fair,* Pet./Chem. Eng., ***33***(10), *45 (September 1961).*]

Pressure drop across the disperser is calculated by variations of the standard orifice equation:

$$h_d = K\left(\frac{\rho_G}{\rho_L}\right)U_h^2 \qquad (14\text{-}101)$$

where U_h = linear gas velocity through slots (valve trays) or perforations (sieve tray), m/s.

For sieve trays, $K = 50.8/C_v^2$. Values of C_v are taken from Fig. 14-35. Values from Fig. 14-35 may be calculated from

$$C_v = 0.74(A_h/A_a) + \exp[0.29(t_t/d_h) - 0.56] \qquad (14\text{-}102)$$

For Sulze's fixed valve trays, Summers and van Sinderen (*Distillation 2001: Topical Conference Proceedings,* AIChE Spring National Meeting, p. 444, Houston, April 22–26, 2001) provided the following equation for K:

$$K = 58 + 386A_f \quad \text{for MVG fixed valves} \qquad (14\text{-}103a)$$

$$K = 58 + 461A_f \quad \text{for SVG and LVG fixed valves} \qquad (14\text{-}103b)$$

Figure 14-36 illustrates the pressure drop of a typical moving valve tray as a function of gas velocity. At low velocities, all valves are closed. Gas rises through the crevices between the valves and the tray deck, with increasing pressure drop as the gas velocity rises. Once point *A*, the closed balance point (CBP), is reached, some valves begin to open. Upon further increase in gas velocity, more valves open until point *B*, the open balance point (OBP), is reached. Between points *A* and *B*, gas flow area increases with gas velocity, keeping pressure drop constant. Further increases in gas velocity increase pressure drop similar to that in a sieve tray.

The term K in Eq. (14-101) depends on valve slot area, orifice geometry, deck thickness, and the type, shape, and weight of the valves. These are best obtained from the manufacturer's literature,

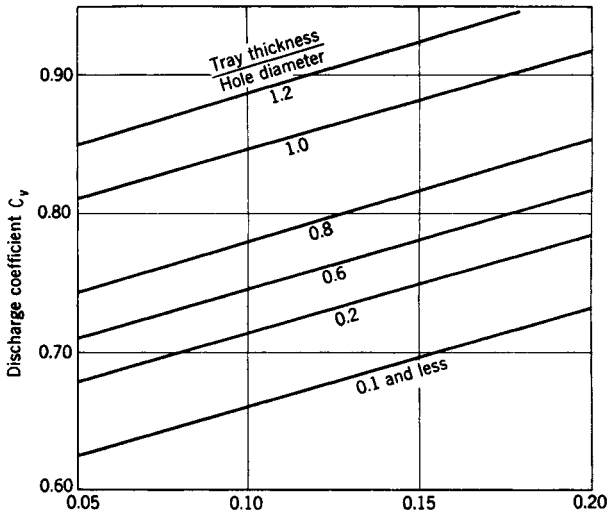

LIVE GRAPH
Click here to view

FIG. 14-35 Discharge coefficients for gas flow, sieve trays. [*Liebson, Kelley, and Bullington,* Pet. Refiner, ***36***(3), *288 (1957).*]

but can also be calculated from Bolles' [*Chem. Eng. Prog.* **72**(9), 43 (1976)], Lockett's *(Distillation Tray Fundamentals,* Cambridge University Press, Cambridge, England, 1986), and Klein's *(Chem. Eng.,* May 3, 1982, p. 81) methods.

For valve trays, Klein gives the following values for K (in $s^2 \cdot mm/m^2$) in Eq. (14-101), when based on the total hole area (not slot area):

	Sharp orifice	Venturi valve
All valves open (K_O)	$254.5(2.64/t_t)^{0.5}$	122
All valves closed (K_C)	1683	841

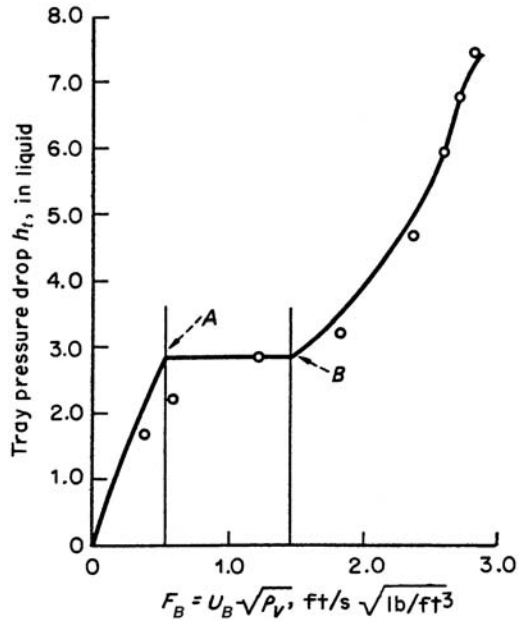

FIG. 14-36 Typical moving valve tray pressure-drop profile. *(From G. F. Klein,* Chem. Eng., *May 3, 1982, p. 81; reprinted courtesy of* Chemical Engineering.*)*

The velocity at which the valves start to open (point *A*) is given by

$$U_{h,\text{closed}} = 1.14[t_v(R_{vw}/K_C)(\rho_M/\rho_G)]^{0.5} \quad (14\text{-}104)$$

where $U_{h,\text{closed}}$ = hole area at point *A*, m/s; t_v = valve thickness, mm; R_{vw} = ratio of valve weight with legs to valve weight without legs, given in Table 14-11; K_C = orifice coefficient with all valves closed (see above), $s^2 \cdot mm/m^2$; ρ_M = valve metal density, kg/m^3 (about 8000 kg/m^3 for steel); ρ_G = gas density, kg/m^3.

The velocity at which all the valves are open $U_{h,\text{open}}$ can be calculated from

$$U_{h,\text{open}} = U_{h,\text{closed}}(K_C/K_O)^{0.5} \quad (14\text{-}105)$$

Pressure drop through the aerated liquid [h'_L, in Eq. (14-100)] is calculated by

$$h'_L = \beta h_{ds} \quad (14\text{-}106)$$

where β = aeration factor, dimensionless
h_{ds} = calculated height of clear liquid, mm (dynamic seal)

The aeration factor β has been determined from Fig. 14-37 for valve and sieve trays. For sieve trays, values of β in the figure may be calculated from

$$\beta = 0.0825 \ln \frac{Q}{L_w} - 0.269 \ln F_h + 1.679 \quad (14\text{-}107)$$

where L_w = weir length, m
F_h = *F*-factor for flow through holes, $F_h = U_h \rho_G^{0.5}$, m/s $(kg/m^3)^{0.5}$

For sieve and valve trays,

$$h_{ds} = h_w + h_{ow} + 0.5h_{hg} \quad (14\text{-}108)$$

where h_w = weir height, mm
h_{ow} = height of crest over weir, mm clear liquid
h_{hg} = hydraulic gradient across tray, mm clear liquid

The value of weir crest h_{ow} may be calculated from the Francis weir equation and its modifications for various weir types. For a segmental weir and for height in millimeters of clear liquid,

$$h_{ow} = 664\left(\frac{Q}{L_w}\right)^{2/3} \quad (14\text{-}109)$$

where Q = liquid flow, m^3/s
L_w = weir length, m

For serrated weirs,

$$h_{ow} = 851\left(\frac{Q'}{\tan \theta/2}\right)^{0.4} \quad (14\text{-}110)$$

where Q' = liquid flow, m^3/s per serration
θ = angle of serration, deg

For circular weirs,

$$h_{ow} = 44{,}300\left(\frac{Q}{d_w}\right)^{0.704} \quad (14\text{-}111)$$

where q = liquid flow, m^3/s
d_w = weir diameter, mm

For most sieve and valve trays, the hydraulic gradient is small and can be dropped from Eq. (14-108). Some calculation methods are available and are detailed in previous editions of this handbook. A rule of thumb by the author is 17 mm/m (0.2 in/ft) of flow path length. This rule only applies in the liquid-loaded froth and emulsion regimes (Q_L >50 m^3/hm or >5.5 gpm/in of outlet weir length). At lower liquid loads, the hydraulic gradient is less.

As noted, the weir crest h_{ow} is calculated on an equivalent clear-liquid basis. A more realistic approach is to recognize that in general a froth or spray flows over the outlet weir (settling can occur upstream of the weir if a large "calming zone" with no dispersers is used). Bennett et al. [*AIChE J.*, **29,** 434 (1983)] allowed for froth overflow in a comprehensive study of pressure drop across sieve trays; their correlation for residual pressure drop h'_L in Eq. (14-100) is presented in detail in the previous (seventh) edition of this handbook, including a worked example. Although more difficult to use, the method of Bennett et al. was recommended when determination of pressure drop is of critical importance.

Example 11: Pressure Drop, Sieve Tray For the conditions of Example 9, estimate the pressure drop for flow across one tray. The thickness of the tray metal is 2 mm. The superficial *F*-factor is 2.08 m/s$(kg/m^3)^{1/2}$.

Solution Equations (14-100), (14-106), and (14-107), where $h_t = h_d + \beta(h_w + h_{ow})$, are used. For $F_S = 2.08$, $F_B = 2.32$ and $F_H = 16.55$. From Example 9, L_w = 1.50 m and h_w = 38 mm. For a liquid rate of 22,000 kg/hr, $Q = 7.27(10^{-3})$ m^3/s, and $Q/L_w = 4.8(10^{-3})$. By Eq. (14-107) or Fig. 14-37, $\beta = 0.48$. From Eq. (14-102) or Fig. 14-35, $C_v = 0.75$. Then, by Eq. (14-101), h_d = 29.0 mm liquid. Using Eq. (14-109), h_{ow} = 18.9 mm. Finally, $h_t = h_d + \beta(h_w + h_{ow}) = 29.0 + 0.48(38 + 18.9) = 56.4$ mm liquid.

When straight or serrated segmental weirs are used in a column of circular cross section, a correction may be needed for the distorted pattern of flow at the ends of the weirs, depending on liquid flow rate. The correction factor F_w from Fig. 14-38 is used directly in Eq. (14-109). Even when circular downcomers are utilized, they are often fed by the overflow from a segmental weir.

Loss under Downcomer The head loss under the downcomer apron, as millimeters of liquid, may be estimated from

$$h_{da} = 165.2\left(\frac{Q}{A_{da}}\right)^2 \quad (14\text{-}112)$$

where Q = volumetric flow of liquid, m^3/s and A_{da} = most restrictive (minimum) area of flow under the downcomer apron, m^2. Equation (14-112) was derived from the orifice equation with an orifice coefficient of 0.6. Although the loss under the downcomer is small, the clearance is significant from the aspect of tray stability and liquid distribution.

The term A_{da} should be taken as the most restrictive area for liquid flow in the downcomer outlet. Usually, this is the area under the downcomer apron (i.e., the downcomer clearance times the length of the segmental downcomer), but not always. For instance, if an inlet weir is used and the area between the segmental downcomer and the inlet weir is smaller than the area under the downcomer apron, the smaller area should be used.

OTHER HYDRAULIC LIMITS

Weeping Weeping is liquid descending through the tray perforations, short-circuiting the contact zone, which lowers tray efficiency. At the tray floor, liquid static head that acts to push liquid down the perforations is counteracted by the gas pressure drop that acts to hold the liquid on the tray. When the static head overcomes the gas pressure drop, weeping occurs.

Some weeping usually takes place under all conditions due to sloshing and oscillation of the tray liquid. Generally, this weeping is too small to appreciably affect tray efficiency. The *weep point* is the gas velocity at which weeping first becomes noticeable. At this point, little efficiency is lost. As gas velocity is reduced below the weep point, the weep rate increases. When the weep rate becomes large enough to significantly reduce tray efficiency, the lower tray operating limit is reached.

The main factor that affects weeping is the fractional hole area. The larger it is, the smaller the gas pressure drop and the greater the weeping tendency. Larger liquid rates and taller outlet weirs increase

TABLE 14-11 R_{vw} Values for Eq. (14-104)

Valve type	Sharp	Venturi
Three-leg	1.23	1.29
Four-leg	1.34	1.45
Cages (no legs)	1.00	1.00

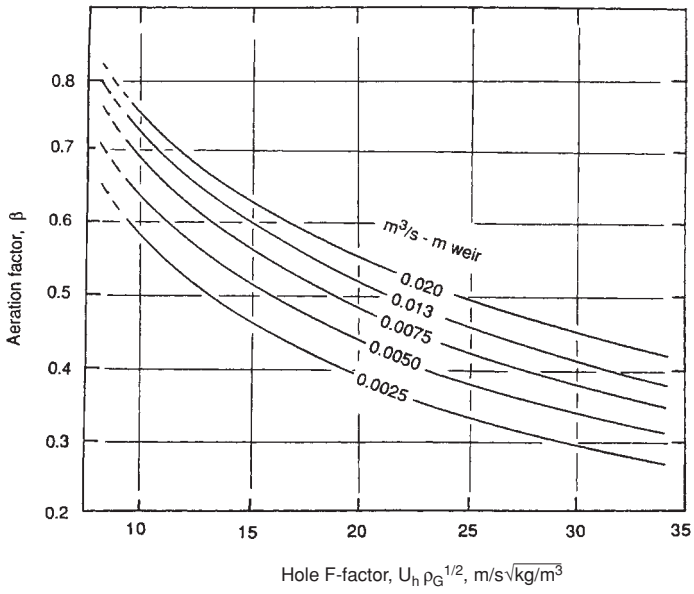

(a)

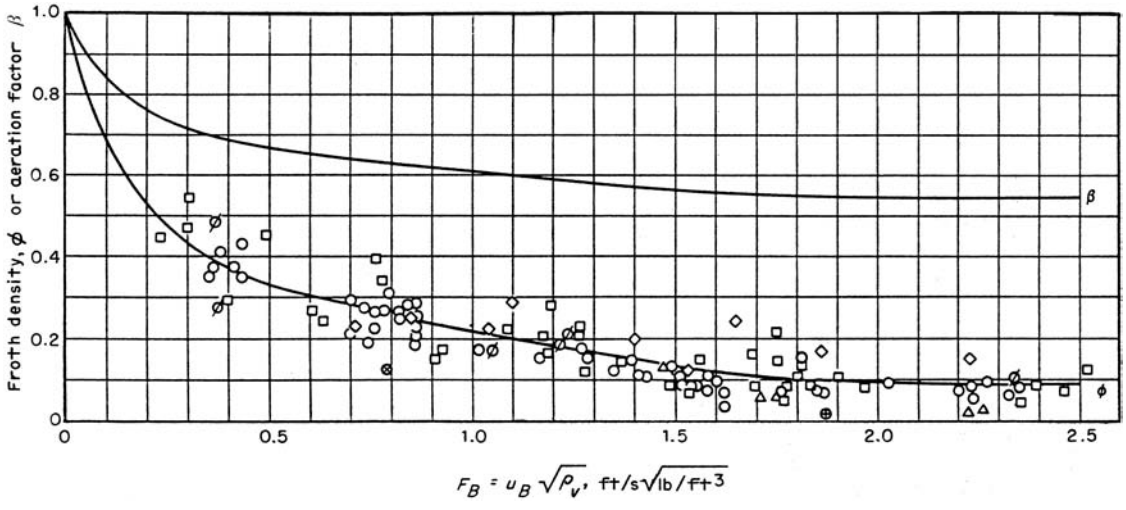

(b)

FIG. 14-37 Aeration factor for pressure drop calculation. (*a*) Sieve trays. [*Bolles and Fair,* Encyclopedia of Chemical Processing and Design, *vols. 16, 86. J. M. McKetta (ed.), Marcel Dekker, New York, 1982.*] (*b*) Valve trays. (*From G. F. Klein,* Chem. Eng., *May 3, 1982, p. 81; reprinted courtesy of* Chemical Engineering.)

liquid heads and therefore weeping. Hole diameter has a complex effect on weeping, detailed by Lockett and Banik [*Ind. Eng. Chem. Proc. Des. Dev.* **25,** 561 (1986)].

Tests by Lockett and Banik (loc. cit.) show that weeping is often nonuniform, with some hydraulic conditions favoring weeping from the tray inlet and others from the tray outlet. Weeping from the tray inlet is particularly detrimental to tray efficiency because the weeping liquid bypasses two trays.

Weep Rate Prediction Lockett and Banik (loc. cit.) and Hsieh and McNulty (*Chem. Eng. Progr.,* July 1993, p. 71) proposed correlations for predicting weep rates from sieve trays. Colwell and O'Bara (Paper presented at the AIChE Meeting, Houston, April 1989) recommended the Lockett and Banik correlation for low pressures (<1100 kPa or 165 psia), and the Hsieh and McNulty correlation for high pressures (>1100 kPa or 165 psia). They also corrected the Lockett and Banik correlation to improve its accuracy near the weep point.

The *Lockett and Banik correlation* (as corrected by Colwell and O'Bara) is

$$\frac{W}{A_h} = \frac{29.45}{\sqrt{\mathrm{Fr}_h}} - 44.18 \qquad \mathrm{Fr}_h < 0.2 \qquad (14\text{-}113a)$$

$$\frac{W}{A_h} = \frac{1.841}{\mathrm{Fr}_h^{1.533}} \qquad \mathrm{Fr}_h > 0.2 \qquad (14\text{-}113b)$$

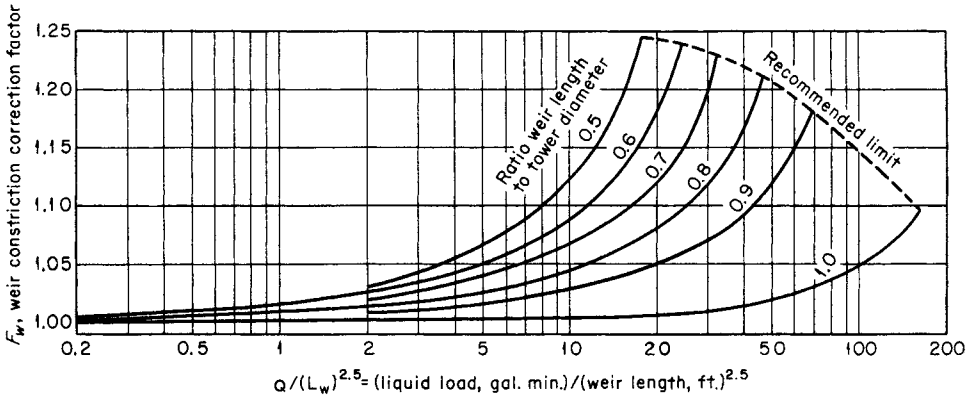

FIG. 14-38 Correction for effective weir length. To convert gallons per minute to cubic meters per second, multiply by 6.309×10^{-5}; to convert feet to meters, multiply by 0.3048. [*Bolles,* Pet. Refiner, **25,** *613 (1946).*]

where
$$\mathrm{Fr}_h = 0.373 \frac{u_h^2}{h_c} \frac{\rho_V}{\rho_L - \rho_V} \tag{14-114}$$

Equations (14-113) and (14-114) use English units: W is the weep rate, gpm; A_h is the hole area, ft^2; u_h is the hole velocity, ft/s; and h_c is the clear liquid height, in. Colwell's [*Ind. Eng. Chem. Proc. Des. Dev.* **20**(2), 298 (1981)] method below has been recommended for obtaining the clear liquid height h_c in Eq. (14-114).

$$h_c = \phi_f \left\{ 0.527 \left(\frac{Q_L(1 - f_w)}{C_d \phi_f} \right)^{2/3} + h_w \right\} \tag{14-115}$$

where ϕ_f is given by Eq. (14-119) and C_d is given by Eq. (14-116)

$$\left.\begin{aligned} C_d &= 0.61 + 0.08 \frac{h_{fow}}{h_w} \qquad \frac{h_{fow}}{h_w} < 8.135 \\ C_d &= 1.06 \left(1 + \frac{h_w}{h_{fow}} \right)^{1.5} \qquad \frac{h_{fow}}{h_w} > 8.135 \end{aligned}\right\} \tag{14-116}$$

$$h_{fow} = h_f - h_w \tag{14-117}$$

where h_f is given by Eq. (14-122). The froth density ϕ_f is calculated from

$$\eta = 12.6 \mathrm{Fr}^{0.4} \left(\frac{A_B}{A_h} \right)^{0.25} \tag{14-118}$$

$$\phi_f = \frac{1}{\eta + 1} \tag{14-119}$$

$$\mathrm{Fr} = 0.37 \frac{\rho_V u_B^2}{h_c(\rho_L - \rho_V)} \tag{14-120}$$

The term f_w in Eq. (14-115) is the ratio of weep rate from the tray to the total liquid flow entering the tray, calculated as follows:

$$f_w = W/\mathrm{GPM} \tag{14-121}$$

Some trial and error is required in this calculation because the clear liquid height h_c and the froth density ϕ_f depend on each other, and the weep fraction f_w depends on the clear liquid height h_c. Clear liquid height is related to froth height and froth density by

$$h_c = \phi_f h_f \tag{14-122}$$

The terms in Eqs. (14-115) to (14-122) are in the English units and are explained in the Nomenclature.

With large-diameter trays and low liquid loads, a small ratio of W/A_h corresponds to a large fractional weep. Under these conditions, the Lockett and Banik correlation is inaccurate. The correlation is unsuitable for trays with very small (<3-mm or $\frac{1}{8}$-in) holes. The correlation appears to fit most data points to an accuracy of ±15 to ±30 percent. The *Hsieh and McNulty correlation* (loc. cit.) is

$$\sqrt{J_G^*} + m\sqrt{J_L^*} = C_w \tag{14-123}$$

where
$$J_G^* = u_h \left[\frac{\rho_G}{gZ(\rho_L - \rho_G)} \right]^{0.5} \tag{14-124}$$

and
$$J_L^* = \frac{W}{448.83 A_h} \left[\frac{\rho_L}{gZ(\rho_L - \rho_G)} \right]^{0.5} \tag{14-125}$$

$$Z = h_c^{1.5}/(12 d_H^{0.5}) \tag{14-126}$$

The terms in Eqs. (14-123) to (14-126) are in English units and are explained in the Nomenclature. For sieve trays, $m = 1.94$ and $C_w = 0.79$. Note that the constants are a slight revision of those presented in the original paper (C. L. Hsieh, private communication, 1991). Clear liquid height is calculated from Colwell's correlation [Eqs. (14-115) to (14-122)]. The Hsieh and McNulty correlation applies to trays with 9 percent and larger fractional hole area. For trays with smaller hole area, Hsieh and McNulty expect the weeping rate to be smaller than predicted.

Weeping from Valve Trays An analysis of weeping from valve trays [Bolles, *Chem. Eng. Progs.* **72**(9), 43 (1976)] showed that in a well-designed valve tray, the weep point is below the gas load at which the valves open; and throughout the valve opening process, the operating point remains above the weep point. In contrast, if the tray contains too many valves, or the valves are too light, excessive valve opening occurs before the gas pressure drop is high enough to counter weeping. In this case, weeping could be troublesome.

Weep point correlations for valve trays were presented by Bolles (loc. cit.) and by Klein *(Chem. Eng.,* Sept. 17, 1984, p. 128). Hsieh and McNulty (loc. cit.) gave a complex extension of their weep rate correlation to valve trays.

Dumping As gas velocity is lowered below the weep point, the fraction of liquid weeping increases until all the liquid fed to the tray weeps through the holes and none reaches the downcomer. This is the *dump point*, or the *seal point*. The dump point is well below the range of acceptable operation of distillation trays. Below the dump point, tray efficiency is slashed, and mass transfer is extremely poor. Operation below the dump point can be accompanied by severe hydraulic instability due to unsealing of downcomers.

Extensive studies on dumping were reported by Prince and Chan [*Trans. Inst. Chem. Engr.* **43,** T49 (1965)]. The Chan and Prince

dump-point correlation was recommended and is presented in detail elsewhere (Kister, *Distillation Design,* McGraw-Hill, 1992). Alternatively, the dump point can be predicted by setting the weep rate equal to 100 percent of the liquid entering the tray in the appropriate weep correlation.

Turndown The turndown ratio is the ratio of the normal operating (or design) gas throughput to the minimum allowable gas throughout. The minimum allowable throughput is usually set by excessive weeping, while normal operating throughput is a safe margin away from the relevant flooding limit.

Sieve and fixed valve trays have a poor turndown ratio (about 2:1). Their turndown can be improved by blanking some rows of tray holes, which reduces the tendency to weep, but will also reduce the tray's maximum capacity. Turndown of *moving valve trays* is normally between about 4:1 to 5:1. Special valve designs can achieve even better turndown ratios, between 6:1 and 10:1, and even more. Turndown can also be enhanced by blanking strips (which require valve removal) or valve leg crimping. Sloley and Fleming (*Chem. Eng. Progr.,* March 1994, p. 39) stress that correct implementation of turndown enhancement is central to achieving a desired turndown. When poorly implemented, turndown may be restricted by poor vapor-liquid contact rather than by weeping.

Vapor Channeling All the correlations in this section assume an evenly distributed tray vapor. When the vapor preferentially channels through a tray region, premature entrainment flood and excessive entrainment take place due to a high vapor velocity in that region. At the same time, other regions become vapor-deficient and tend to weep, which lowers tray efficiency.

Work by Davies [*Pet. Ref.* **29**(8), p. 93, and **29**(9), p. 121 (1950)] based on bubble-cap tray studies suggests that the vapor pressure drop of the tray (the *dry pressure drop*) counteracts channeling. The higher the dry tray pressure drop, the greater the tendency for vapor to spread uniformly over the bubbling area. If the dry tray pressure drop is too small compared with the channeling potential, channeling prevails.

Perhaps the most common vapor channeling mechanism is *vapor crossflow channeling* (*VCFC,* Fig. 14-39). The hydraulic gradient on the tray induces preferential vapor rise at the outlet and middle of the tray, and a vapor-deficient region near the tray inlet. The resulting high vapor velocities near the tray outlet step up entrainment, while the low vapor velocities near the tray inlet induce weeping. Interaction between adjacent trays (Fig. 14-39) accelerates both the outlet entrainment and the inlet weeping. The net result is excessive entrainment and premature flooding at the tray middle and outlet, simultaneous with weeping from the tray inlet, accompanied by a loss of efficiency and turndown.

VCFC takes place when the following four conditions exist simultaneously [Kister, Larson, and Madsen, *Chem. Eng. Progr.,* p. 86 (Nov. 1992); Kister, *The Chemical Engineer*, **544,** p. 18 (June 10, 1993)]:

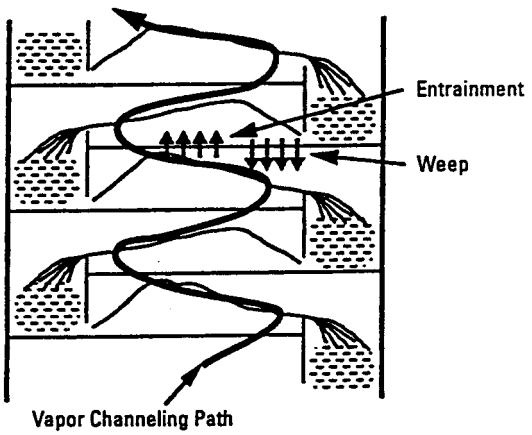

FIG. 14-39 Vapor crossflow channeling. Note entrainment near the tray middle and outlet, and weep near the tray inlet. *(Kister, H. Z., K. F. Larson, and P. Madsen,* Chem. Eng. Prog., *Nov. 1992, p. 86; reproduced with permission.)*

1. Absolute pressure < 500 kPa (70 psia).
2. High liquid rates [>50 $m^3/(m \cdot h)$ or 6 gpm/in of outlet weir].
3. High ratio (>2:1) of flow path length to tray spacing.
4. Low dry tray pressure drop. On sieve and fixed valve trays, this means high (>11 percent) fractional hole area. On moving valve trays, this means venturi valves (smooth orifices) or long-legged valves (>15 percent slot area). On all trays, the channeling tendency and severity escalate rapidly as the dry pressure drop diminishes (e.g., as fractional hole area increases).

Hartman (*Distillation 2001: Topical Conference Proceedings,* AIChE Spring National Meeting, p. 108, Houston, Tex. (April 22–26, 2001)] reports VCFC even with conventional valve trays (14 percent slot area) at very high ratio (3.6:1) of flow path length to tray spacing and tray truss obstruction.

VCFC is usually avoided by limiting fractional hole areas, avoiding venturi valves, and using forward-push devices. Resitarits and Pappademos [Paper presented at the AIChE Annual Meeting, Reno, Nev. (November 2001)] cited tray inlet inactivity as a contributor to VCFC, and advocate inlet forward-push devices to counter it.

TRANSITION BETWEEN FLOW REGIMES

Froth-Spray Froth-spray transition has been investigated for sieve trays using a variety of techniques. The gradual nature of this transition bred a multitude of criteria for defining it, and made its correlation difficult. Excellent overviews were given by Lockett (*Distillation Tray Fundamentals,* Cambridge University Press, Cambridge, England, 1986) and Prado, Johnson, and Fair [*Chem. Eng. Progr.* **83**(3), p. 32 (1987)]. Porter and Jenkins [*I. Chem. E. Symp. Ser.* **56,** Summary Paper (1979)] presented a simple correlation for the froth-to-spray transition.

$$F_{LG} \frac{N_p A_B}{L_w} = 0.0191 \tag{14-127}$$

The terms of this equation are in English units and are explained in the Nomenclature. This correlation is based on the premise that froth-to-spray transition occurs when the entrainment vs. liquid load relationship passes through a minimum (see "Entrainment"). Alternatively, it was argued that the minimum represents a transition from the froth regime to a partially developed spray region (Kister, Pinczewski, and Fell, Paper presented in the 90th National AIChE Meeting, Houston, April 1981). If this alternative argument is valid, then when the correlation predicts froth, it is highly unlikely that the column operates in the spray regime; but when it predicts spray, the column may still be operating in the froth regime. Recent entrainment studies by Ohe [*Distillation 2005: Topical Conference Proceedings,* AIChE Spring National Meeting, p. 283, Atlanta (April 10–13, 2005)] argue that the entrainment minima represent minimum liquid residence times on the tray, and are unrelated to the froth-spray transition.

A second correlation is by Pinczeweski and Fell [*Ind. Eng. Chem. Proc. Des. Dev.* **21,** p. 774 (1982)]

$$u_B \sqrt{\rho_G} = 2.25 \left(\frac{Q_L \sqrt{\rho_L}}{100} \right)^n \tag{14-128}$$

The terms of Eq. (14-128) are in English units and are explained in the Nomenclature. The exponent n is calculated from Eq. (14-84). Equation (14-128) is based on transition data obtained from orifice jetting measurements for the air-water system and on entrainment minimum data for some hydrocarbon systems.

A third recent correlation by Johnson and Fair (loc. cit.) is

$$U_a^* = C_1 \rho_G^{-0.50} \rho_L^{0.692} \sigma^{0.06} A_f^{0.25} \left(\frac{q}{L_w} \right)^{0.05} d_h^{-0.1} \tag{14-129}$$

where U_a^* = gas velocity through active area at inversion, m/s
ρ_G = gas density, kg/m^3
ρ_L = liquid density, kg/m^3
σ = surface tension, mN/m
A_f = hole/active area ratio

q/L_w = liquid flow, $m^3/(s \cdot m)$ weir
d_h = hole diameter, mm
C_1 = 0.0583 for 25.4-mm overflow weirs
= 0.0568 for 50.4-mm overflow weirs
= 0.0635 for 101.6-mm overflow weirs

Froth-Emulsion Froth-emulsion transition occurs [Hofhuis and Zuiderweg, *I. Chem. E. Symp. Ser.* **56,** p. 2, 2/1 (1979)] when the aerated mass begins to obey the Francis weir formula. Using this criterion, the latest version of this transition correlation is

$$F_{LG} \frac{N_p A_B}{L_w h_c} = 0.0208 \tag{14-130}$$

The terms of this equation are in English units and are explained in the Nomenclature; h_c is calculated from the Hofhuis and Zuiderweg (loc. cit.) equation.

$$h_c = 2.08 \left(F_{LG} \frac{N_p A_B}{L_w} p \right)^{0.25} h_w^{0.5} \tag{14-131}$$

An inspection of the experimental data correlated shows that this, too, is a gradual transition, which occurs over a range of values rather than at a sharp point.

Valve Trays The amount of work reported thus far on valve tray regime transition is small and entirely based on air-water tests. Correlations proposed to date require the knowledge of liquid holdup at transition, which is generally not available, and are therefore of limited application for commercial columns.

TRAY EFFICIENCY

Definitions

Overall Column Efficiency This is the ratio of the number of theoretical stages to the number of actual stages

$$E_{OC} = N_t / N_a \tag{14-132}$$

Since tray efficiencies vary from one section to another, it is best to apply Eq. (14-132) separately for the rectifying and stripping sections. In practice, efficiency data and prediction methods are often too crude to give a good breakdown between the efficiencies of different sections, and so Eq. (14-132) is applied over the entire column.

Point Efficiency This is defined by Eq. (14-133) (Fig. 14-40*a*):

$$E_{OG} = \left(\frac{y_n - y_{n-1}}{y_n^* - y_{n-1}} \right)_{\text{point}} \tag{14-133}$$

where y_n^* is the composition of vapor in equilibrium with the liquid at point n. The term y_n is actual vapor composition at that point. The point efficiency is the ratio of the change of composition at a point to the change that would occur on a theoretical stage. As the vapor composition at a given point cannot exceed the equilibrium composition, fractional point efficiencies are always lower than 1. If there is a composition gradient on the tray, point efficiency will vary between points on the tray.

Murphree Tray Efficiency [*Ind. Eng. Chem.* **17,** 747 (1925)] This is the same as point efficiency, except that it applies to the entire tray instead of to a single point (Fig. 14-40*b*):

$$E_{MV} = \left(\frac{y_n - y_{n-1}}{y_n^* - y_{n-1}} \right)_{\text{tray}} \tag{14-134}$$

If both liquid and vapor are perfectly mixed, liquid and vapor compositions on the tray are uniform, and the Murphree tray efficiency will coincide with the point efficiency at any point on the tray. In practice, a concentration gradient exists in the liquid, and x_n at the tray outlet is lower than x'_n on the tray (see Fig. 14-40*b*). This frequently lowers y_n^* relative to y_n, thus enhancing tray efficiency [Eq. (14-134)] compared with point efficiency. The value of y_n^* may even drop below y_n. In this case, E_{MV} exceeds 100 percent [Eq. (14-134)].

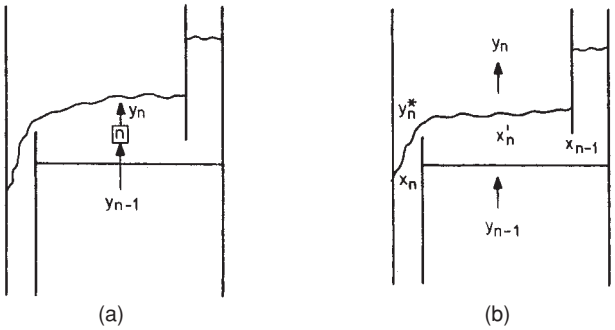

FIG. 14-40 Point and Murphree efficiencies. (*a*) Point. (*b*) Murphree. *(From H. Z. Kister,* Distillation Design, *copyright © 1992 by McGraw-Hill; reprinted by permission.)*

Overall column efficiency can be calculated from the Murphree tray efficiency by using the relationship developed by Lewis [*Ind. Eng. Chem.* **28,** 399 (1936)].

$$E_{OC} = \frac{\ln[1 + E_{MV}(\lambda - 1)]}{\ln \lambda} \tag{14-135}$$

where

$$\lambda = m \frac{G_M}{L_M} \tag{14-136}$$

Equation (14-135) is based on the assumption of constant molar overflow and a constant value of E_{MV} from tray to tray. It needs to be applied separately to each section of the column (rectifying and stripping) because G_M/L_M, and therefore λ, varies from section to section. Where molar overflow or Murphree efficiencies vary throughout a section of column, the section needs to be divided into subsections small enough to render the variations negligible.

The point and Murphree efficiency definitions above are expressed in terms of vapor concentrations. Analogous definitions can be made in terms of liquid concentrations. Further discussion is elsewhere (Lockett, *Distillation Tray Fundamentals,* Cambridge University, Press, Cambridge, England, 1986).

Fundamentals Figure 14-41 shows the sequence of steps for converting phase resistances to a tray efficiency. Gas and liquid film resistances are added to give the point efficiency. Had both vapor and liquid on the tray been perfectly mixed, the Murphree tray efficiency would have equaled the point efficiency. Since the phases are not perfectly mixed, a model of the vapor and liquid mixing patterns is needed for converting point efficiency to tray efficiency. Liquid mixture patterns are plug flow, backmixing, and stagnant zones, while vapor-mixing patterns are perfect mixing and plug flow.

Lewis (loc. cit.) was the first to derive quantitative relationships between the Murphree and the point efficiency. He derived three mixing cases, assuming plug flow of liquid in all. The Lewis cases give the maximum achievable tray efficiency. In practice, efficiency is lower due to liquid and vapor nonuniformities and liquid mixing.

Most tray efficiency models are based on Lewis case 1 with vapor perfectly mixed between trays. For case 1, Lewis derived the following relationship:

$$E_{MV,\text{dry}} = \frac{\exp(\lambda E_{OG}) - 1}{\lambda} \tag{14-137}$$

The "dry" Murphree efficiency calculated thus far takes into account the vapor and liquid resistances and the vapor-liquid contact patterns, but is uncorrected for the effects of entrainment and weeping. This correction converts the dry efficiency to a "wet" or actual Murphree tray efficiency. Colburn [Eq. (14-98), under "Entrainment"] incorporated the effect of entrainment on efficiency, assuming perfect mixing of liquid on the tray.

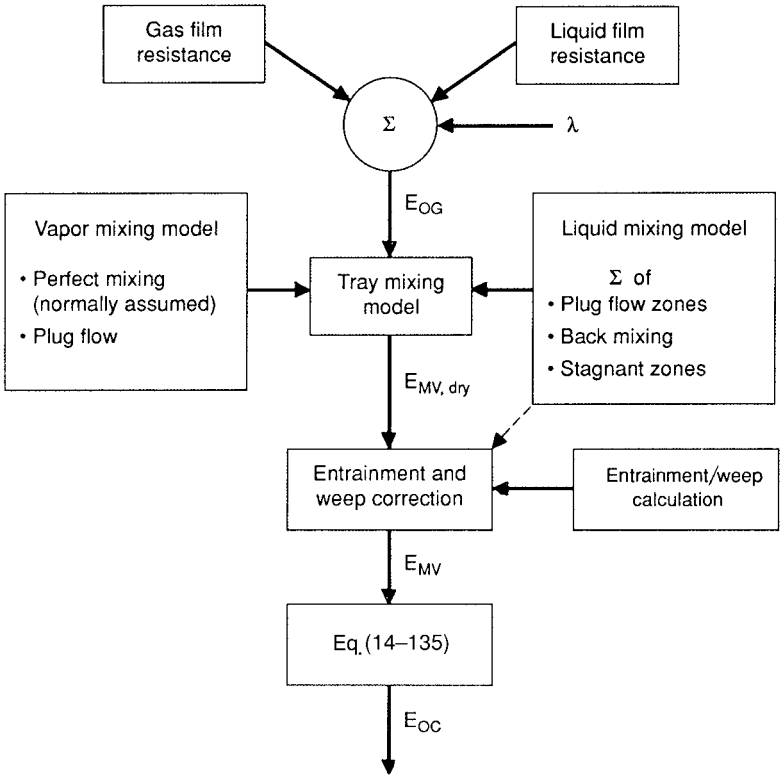

FIG. 14-41 Sequence of steps for theoretical prediction of tray efficiency. (*From H. Z. Kister,* Distillation Design, *copyright © 1992 by McGraw-Hill; reprinted by permission.*)

Factors Affecting Tray Efficiency Below is a summary based on the industry's experience. A detailed discussion of the fundamentals is found in Lockett's book *(Distillation Tray Fundamentals,* Cambridge University Press, Cambridge, England, 1986). A detailed discussion of the reported experience, and the basis of statements made in this section are in Kister's book *(Distillation Design,* McGraw-Hill, New York, 1992).

Errors in Vapor-Liquid Equilibrium (VLE) Errors in relative volatility are the most underrated factor affecting tray efficiency. Figure 14-42 shows the direct effect of the errors [Deibele and Brandt, *Chem. Ing. Tech.* **57**(5), p. 439 (1985); Roy P. and G. K. Hobson, *I. Chem. E. Symp. Ser.* **104,** p. A273 (1987)]. At very low relative volatilities ($\alpha < 1.2$), small errors in VLE have a huge impact on tray efficiency. For instance, at $\alpha = 1.1$, a –3 percent error gives a tray efficiency 40 to 50 percent higher than its true value (Fig. 14-42). Since VLE errors are seldom lower than ±2 to 3 percent, tray efficiencies of low-volatility systems become meaningless unless accompanied by VLE data. Likewise, comparing efficiencies derived for a low-volatility system by different sources is misleading unless one is using identical VLE.

Figure 14-42 shows that errors in relative volatility are a problem only at low relative volatilities; for $\alpha > 1.5$ to 2.0, VLE errors have negligible direct impact on tray efficiency.

Most efficiency data reported in the literature are obtained at total reflux, and there are no indirect VLE effects. For measurements at finite reflux ratios, the indirect effects below compound the direct effect of Fig. 14-42. Consider a case where $\alpha_{apparent} < \alpha_{true}$ and test data at a finite reflux are analyzed to calculate tray efficiency. Due to the volatility difference $R_{min,apparent} > R_{min,true}$. Since the test was conducted at a fixed reflux flow rate, $(R/R_{min})_{apparent} < (R/R_{min})_{true}$. A calculation based on the apparent R/R_{min} will give more theoretical stages than a calculation based on the true R/R_{min}. This means a higher apparent efficiency than the true value.

The indirect effects add to those of Fig. 14-42, widening the gap between true and apparent efficiency. The indirect effects exponentially escalate as minimum reflux is approached. Small errors in VLE or reflux ratio measurement (this includes column material balance as well as reflux rate) alter R/R_{min}. Near minimum reflux, even small R/R_{min} errors induce huge errors in the number of stages, and therefore in tray efficiency. Efficiency data obtained near minimum reflux are therefore meaningless and potentially misleading.

Liquid Flow Patterns on Large Trays The most popular theoretical models (below) postulate that liquid crosses the tray in plug flow with superimposed backmixing, and that the vapor is perfectly mixed. Increasing tray diameter promotes liquid plug flow and suppresses backmixing.

The presence of stagnant zones on large-diameter distillation trays is well established, but the associated efficiency loss is poorly understood; in some cases, significant efficiency losses, presumably due to stagnant zones, were reported [Weiler, Kirkpatrick, and Lockett, *Chem. Eng. Progr.* **77**(1), 63 (1981)], while in other cases, no efficiency difference was observed [Yanagi and Scott, *Chem. Eng. Progr.*, **69**(10), 75 (1973)]. Several techniques are available for eliminating stagnant regions (see Kister, *Distillation Design,* McGraw-Hill, New York, 1992, for some), but their effectiveness for improving tray efficiency is uncertain.

Weir Height Taller weirs raise the liquid level on the tray in the froth and emulsion regimes. This increases interfacial area and vapor contact time, which should theoretically enhance efficiency. In the spray regime, weir height affects neither liquid level nor efficiency. In distillation systems, the improvement of tray efficiency due to taller weirs is small, often marginal.

Length of Liquid Flow Path Longer liquid flow paths enhance the liquid-vapor contact time, the significance of liquid plug flow, and therefore raise efficiency. Typically, doubling the flow path length

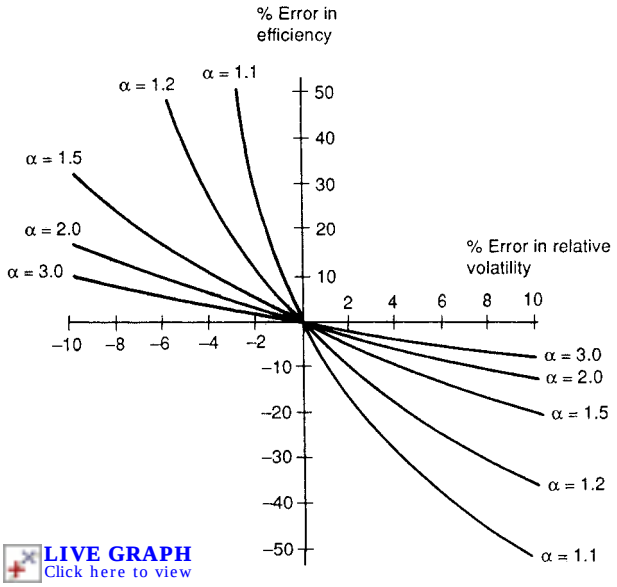

FIG. 14-42 Direct effect of errors in relative volatility on error in tray efficiency. *(From H. Z. Kister,* Distillation Design, *copyright © 1992 by McGraw-Hill; reprinted by permission.)*

(such as going from two-pass to one-pass trays at a constant tower diameter) raises tray efficiency by 5 to 15 percent.

Fractional Hole Area Efficiency increases with a reduction in fractional hole area. Yanagi and Sakata [*Ind. Eng. Chem. Proc. Des. Dev.* **21,** 712 (1982)] tests in commercial-scale towers show a 5 to 15 percent increase in tray efficiency when fractional hole area was lowered from 14 to 8 percent (Fig. 14-43).

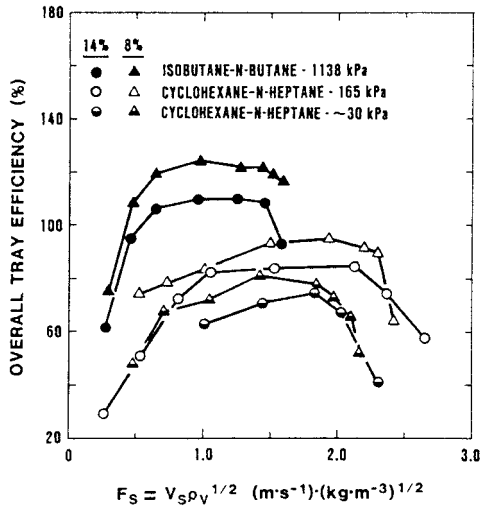

FIG. 14-43 Efficiency reduction when fractional hole area is increased, also showing little effect of vapor and liquid loads on efficiency in the normal operating range (between excessive weeping and excessive entrainment). Also shown is the small increase in efficiency with pressure. FRI data, total reflux, $D_T = 1.2$ m, $S = 610$ mm, $h_w = 50.8$ mm, $d_H = 12.7$ mm. *(Reprinted with permission from T. Yanagi and M. Sakata,* Ind. Eng. Chem. Proc. Des. Dev. ***21,*** *712; copyright © 1982, American Chemical Society.)*

Hole Diameter The jury is out on the effect of hole diameter on tray efficiency. There is, however, a consensus that the effect of hole diameter on efficiency is small, often negligible.

Vapor-Liquid Loads and Reflux Ratio Vapor and liquid loads, as well as the reflux ratio, have a small effect on tray efficiency (Fig. 14-43) as long as no capacity or hydraulic limits (flood, weep, channeling, etc.) are violated.

Viscosity, Relative Volatility Efficiency increases as liquid viscosity and relative volatility diminish. These effects are reflected in the O'Connell correlation (below).

Surface Tension There is uncertainty regarding the effect of surface tension on tray efficiency. Often, it is difficult to divorce the surface tension effects from those of other physical properties.

Pressure Tray efficiency slightly increases with pressure (Fig. 14-43), reflecting the rise of efficiency with a reduction in liquid viscosity and in relative volatility, which generally accompany a distillation pressure increase.

At pressures exceeding 10 to 20 bar (150 to 300 psia), and especially at high liquid rates, vapor entrainment into the downcomer liquid becomes important, and tray efficiency decreases with further increases in pressure [Zuiderweg, *Int. Chem. Eng.* **26**(1), 1 (1986)].

Maldistribution Maldistribution can cause major efficiency reduction in multipass trays (>two passes). Further discussion is given under "Number of Passes."

OBTAINING TRAY EFFICIENCY

Efficiency prediction methods are listed here in decreasing order of reliability.

Rigorous Testing Rigorous testing of a plant column is generally the most reliable method of obtaining tray efficiency. Test procedures can be found elsewhere (AIChE Equipment Testing Procedures Committee, *AIChE Equipment Testing Procedure—Tray Distillation Columns,* 2d ed., 1987; Kister, *Distillation Operation,* McGraw-Hill, New York, 1990).

Scale-up from an Existing Commercial Column As long as data are for the same system under similar process conditions, loadings, and operating regime, data obtained in one column directly extend to another. Fractional hole area and the number of tray passes will have a small but significant effect on efficiency, and any changes in these parameters need to be allowed for during scale-up. The empirical information in the section "Factors Affecting Tray Efficiency" can be used to estimate the magnitude of the changes on efficiency.

Scale-up from Existing Commercial Column to Different Process Conditions During scale-up, test data are analyzed by computer simulation. The number of theoretical stages is varied until the simulated product compositions and temperature profile match the test data. Tray efficiency is determined by the ratio of theoretical stages to actual trays. In this procedure, errors in VLE are offset by compensating errors in tray efficiency. For instance, if the relative volatility calculated by the simulation is too high, fewer stages will be needed to match the measured data, i.e., "apparent" tray efficiency will be lower. Scale-up will be good as long as the VLE and efficiency errors continue to offset each other equally. This requires that process conditions (feed composition, feed temperature, reflux ratio, etc.) remain unchanged during scale-up.

When process conditions change, the VLE and efficiency errors no longer offset each other equally. If the true relative volatility is higher than simulated, then the scale-up will be conservative. If the true relative volatility is lower than simulated, scale-up will be optimistic. A detailed discussion is found in Kister, *Distillation Design,* McGraw-Hill, New York, 1992.

Experience Factors These are tabulations of efficiencies previously measured for various systems. Tray efficiency is insensitive to tray geometry (above), so in the absence of hydraulic anomalies and issues with VLE data, efficiencies measured in one tower are extensible to others distilling the same system. A small allowance to variations in tray geometry as discussed above is in order. Caution is required with mixed aqueous-organic systems, where concentration may have a marked effect on physical properties, relative volatility, and efficiency. Table 14-12 shows typical tray efficiencies reported in the literature.

TABLE 14-12 Representative Tray Efficiencies

Tray	System	Column diameter, ft	Tray spacing, in	Pressure, psia	Efficiency, %	% hole (slot) area	Ref.
Sieve	Methanol-water	3.2	15.7	14.7	70–90	10.8	2
	Ethanol-water	2.5	14	14.7	75–85	10.4	1
	Methanol-water	3.2	15.7	14.7	90–100	4.8	2
	Ethylbenzene-styrene	2.6	19.7	1.9	70	12.3	5
	Benzene-toluene	1.5	15.7	14.7	60–75	8	10
	Methanol-*n* propanol-sec butanol	6.0	18	18	64*		6
	Mixed xylene + C_8-C_{10} paraffins and naphthenes	13.0	21	25	86*		4
	Cyclohexane-*n*-heptane	4.0	24	5	60–70	14	9
				24	80	14	9
		4.0	24	5	70–80	8	8
				24	90	8	8
	Isobutane-*n*-butane	4.0	24	165	110	14	9
		4.0	24	165	120	8	8
		4.0	24	300	110	8	8
		4.0	24	400	100	8	8
	n-Heptane-toluene	1.5	15.7	14.7	60–75	8	10
	Methanol-water	2.0	13.6	14.7	68–72	10	11
	Isopropanol-water	2.0	13.6	14.7	59–63		11
	Toluene-methylcyclohexane	2.0	13.6	14.7	70–82		11
	Toluene stripping from water	4	24	14.7	31–42	8	13
Valve	Methanol-water	3.2	15.7	14.7	70–80	14.7	2
	Ethanol-water	2.5	14	14.7	75–85		1
	Ethyl benzene-styrene	2.6	19.7	1.9	75–85		3
	Cyclohexane-*n*-heptane	4.0	24	24	70–96*		7
	Isobutane-*n*-butane	4.0	24	165	108–121*		7
	Cyclohexane-*n*-heptane	4.0	24	24	77–93†	14.7	12
				5	57–86†	14.7	12
	Isobutane-*n*-butane	4.0	24	165	110–123†	14.7	12
	C_3-C_4 splitter	5.6	24	212	65–67‡	12	14

References:

1. Kirschbaum, *Distillier-Rektifiziertechnik*, 4th ed., Springer-Verlag, Berlin and Heidelberg, 1969.
2. Kastanek and Standart, *Sep. Sci.* **2,** 439 (1967).
3. Billet and Raichle, *Chem. Ing. Tech.*, 38, 825 (1966); **40,** 377 (1968).
4. AIChE Research Committee, *Tray Efficiency in Distillation Columns*, final report, University of Delaware, Newark, 1958.
5. Billet R., *IChemE., Symp. Ser.* **32,** p. 4:42 (1969).
6. Mayfield et al., *Ind. Eng. Chem.*, **44,** 2238 (1952).
7. Fractionation Research, Inc. "Report of Tests of Nutter Type B Float Valve Tray," July 2, 1964 from Sulzer Chem Tech.
8. Sakata and Yanagi, *IChemE., Eng. Symp.* Ser., no. 56, 3.2/21 (1979).
9. Yanagi and Sakata, *Ind. Eng. Chem. Process Des. Dec.*, **21,** 712 (1982).
10. Zuiderweg and Van der Meer, *Chem. Tech.* (Leipzig), **24,** 10 (1972).
11. Korchinsky, *Trans. I. Chem. E.*, **72,** Part A, 472 (1994).
12. Gliltsch, Inc. "Glitsch Ballast Trays," Bulletin 159/160 (FRI Topical Report 15, 1958). Available from Koch-Glitsch LP, Wichita, Kans.
13. Kunesh et al., Paper presented at the AIChE Spring National Meeting, Atlanta, Ga., 1994.
14. Remesat, Chuang, and Svrcek, *Trans. I Chem. E.*, Vol. 83, Part A, p. 508, May 2005.

Notes:

*Rectangular Sulzer BDP valves.

†Glitsch V-1 round valves (Koch-Glitsch).

‡Two-pass trays, short path length.

To convert feet to meters, multiply by 0.3048; to convert inches to centimeters, multiply by 2.54; and to convert psia to kilopascals, multiply by 6.895.

Vital, Grossel and Olsen [*Hydroc. Proc.* **63,** 11, p. 147 (1984)] and Garcia and Fair [*Ind. Eng. Chem. Res.* **39,** p. 1809 (2000)] present an extensive tabulation of tray efficiency data collected from the published literature.

The *GPSA Engineering Data Book* (10th ed., Gas Processors Association, 1987) and Kaes (*Refinery Process Modeling—A Practical Guide to Steady State Modeling of Petroleum Processes Using Commercial Simulators*, Athens Printing Co., Athens, Ga., 2000) tabulate typical efficiencies in gas plant and refinery columns, respectively. Pilling (Paper presented at the 4th Topical Conference on Separations Science and Technology, November 1999, available from Sulzer Chemtech, Tulsa, Okla.) tabulated more typical efficiencies. Similar information is often available from simulation guide manuals. The quality and reliability of efficiencies from these sources vary and are generally lower than the reliability of actual measured data.

Scale-up from a Pilot- or Bench-Scale Column This is a very common scale-up. No reduction in efficiency on scale-up is expected as long as several precautions are observed. These precautions, generally relevant to pilot- or bench-scale columns, are spelled out with specific reference to the Oldershaw column.

Scale-up from Oldershaw Columns One laboratory-scale device that found wide application in efficiency investigations is the Oldershaw column [Fig. 14-44, Oldershaw, *Ind. Eng. Chem. Anal. Ed.* **13,** 265 (1941)]. This column is available from a number of laboratory supply houses and can be constructed from glass for atmospheric operation or from metal for higher pressures. Typical column diameters are 25 to 100 mm (1 to 4 in), with tray spacing the same as the column diameter.

Fair, Null, and Bolles [*Ind. Eng. Chem. Process Des. Dev.* **22,** 53 (1983)] found that efficiency measurements in Oldershaw columns closely approach the point efficiencies [Eq. (14-133)] measured in

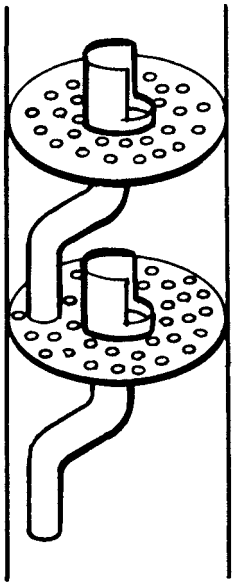

FIG. 14-44 An Oldershaw column. *(From H. Z. Kister,* Distillation Design, *copyright © 1992 by McGraw-Hill; reprinted by permission.)*

commercial sieve-tray columns (Fig. 14-45) providing (1) the systems being distilled are the same, (2) comparison is made at the same relative approach to the flood point, (3) operation is at total reflux, and (4) a standard Oldershaw device is used in the laboratory experimentation. Fair et al. compared several systems, utilizing as large-scale information the published efficiency studies of Fractionation Research, Inc. (FRI).

A mixing model can be used to convert the Oldershaw point efficiencies to overall column efficiencies. This enhances the commercial column efficiency estimates. A conservative approach suggested by Fair et al. is to apply the Oldershaw column efficiency as the estimate for the overall column efficiency of the commercial column, taking no credit for the greater plug-flow character upon scale-up. The author prefers this conservative approach, considering the poor reliability of mixing models.

Previous work with Oldershaw columns [Ellis, Barker, and Contractor, *Trans. Instn. Chem. Engnrs.* **38,** 21 (1960)], spells an additional note of caution. Cellular (i.e., wall-supported) foam may form in pilot or Oldershaw columns, but is rare in commercial columns. For a given system, higher Oldershaw column efficiencies were measured under cellular foam conditions than under froth conditions. For this reason, Gerster [*Chem. Eng. Progr.* **59**(3), 35 (1963)] warned that when cellular foam can form, scale-up from an Oldershaw column may be dangerous. The conclusions presented by Fair et al. do not extend to Oldershaw columns operating in the cellular foam regime. Cellular foam can be identified by lower pilot column capacity compared to a standard mixture that is visualized not to form cellular foam.

Heat losses are a major issue in pilot and Oldershaw columns and can lead to optimistic scale-up. Special precautions are needed to keep these at a minimum. Vacuum jackets with viewing ports are commonly used.

Uses of Oldershaw columns to less conventional systems and applications were described by Fair, Reeves, and Seibert [Topical Conference on Distillation, AIChE Spring Meeting, New Orleans, p. 27 (March 10–14, 2002)]. The applications described include scale-up in the absence of good VLE, steam stripping efficiencies, individual component efficiencies in multicomponent distillation, determining component behavior in azeotropic separation, and foam testing.

Empirical Efficiency Prediction Two empirical correlations which have been the standard of the industry for distillation tray efficiency prediction are the Drickamer and Bradford, in Fig. 14-46 [*Trans. Am. Inst. Chem. Eng.* **39,** 319 (1943)] and a modification of it by O'Connell [*Trans. Am. Inst. Chem. Eng.* **42,** 741 (1946)], in Fig. 14-47. The Drickamer-Bradford plot correlates efficiency as a function of liquid viscosity only, which makes it useful for petroleum cuts. O'Connell added the relative volatility to the x axis.

Lockett *(Distillation Tray Fundamentals,* Cambridge University Press, Cambridge, England, 1986) noted some theoretical sense in O'Connell's correlation. Higher viscosity usually implies lower diffusivity, and therefore greater liquid-phase resistance and lower efficiency. Higher relative volatility increases the significance of the liquid-phase resistance, thus reducing efficiency. Lockett expresses the O'Connell plot in equation form:

$$E_{OC} = 0.492(\mu_L \alpha)^{-0.245} \qquad (14\text{-}138)$$

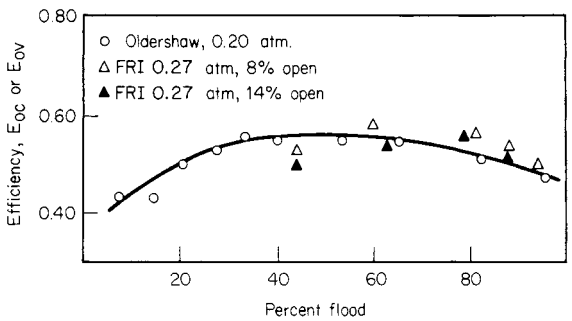

FIG. 14-45 Overall column efficiency of 25-mm Oldershaw column compared with point efficiency of 1.22-m-diameter-sieve sieve-plate column of Fractionation Research, Inc. System = cyclohexane-*n*-heptane. [*Fair, Null, and Bolles,* Ind. Eng. Chem. Process Des. Dev., **22,** 53 (1982).]

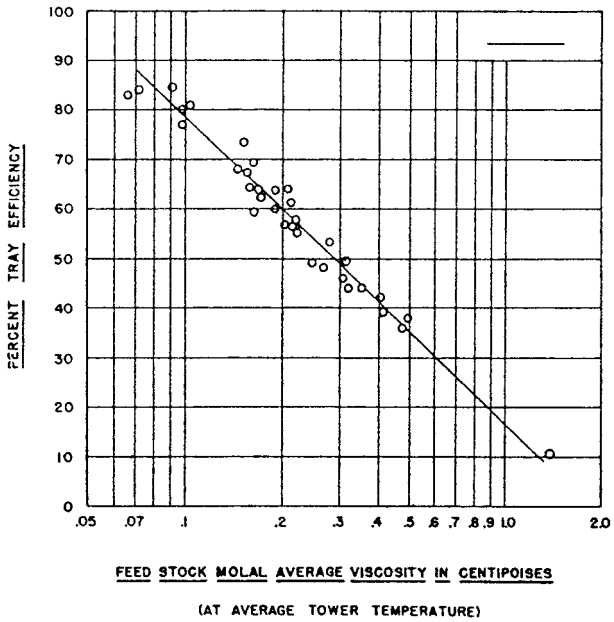

FIG. 14-46 The Drickamer and Bradford tray efficiency correlation for refinery towers. To convert centipoise to pascal-seconds, multiply by 0.0001. [*From Drickamer and Bradford,* Trans. Am. Inst. Chem. Eng. **39,** 319 *(1943). Reprinted courtesy of the AIChE.*]

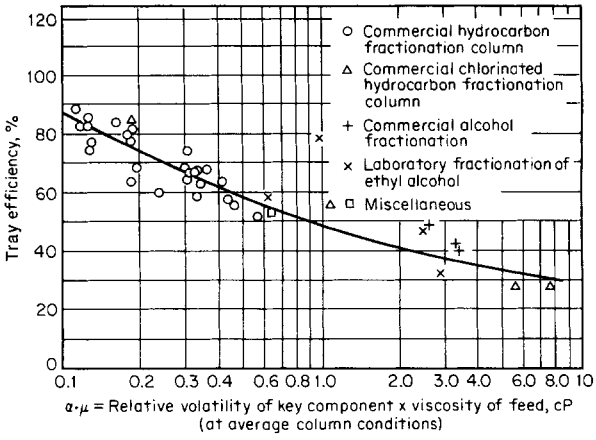

FIG. 14-47 O'Connell correlation for overall column efficiency E_{oc} for distillation. To convert centipoises to pascal-seconds, multiply by 10^{-3}. [*O'Connell,* Trans. Am. Inst. Chem. Eng., ***42,*** 741 (*1946*).]

(The viscosity is in cP and E_{OC} is fractional.) The volatility and viscosity are evaluated at the average arithmetic temperature between the column top and bottom temperatures. The relative volatility is between the key components.

The O'Connell correlation was based on data for bubble-cap trays. For sieve and valve trays, its predictions are likely to be slightly conservative.

Theoretical Efficiency Prediction Theoretical tray efficiency prediction is based on the two-film theory and the sequence of steps in Fig. 14-41. Almost all methods evolved from the AIChE model (AIChE Research Committee, *Bubble Tray Design Manual,* New York, 1958). This model was developed over 5 years in the late 1950s in three universities. Since then, several aspects of the AIChE model have been criticized, corrected, and modified. Reviews are given by Lockett (*Distillation Tray Fundamentals,* Cambridge University Press, Cambridge, England, 1986) and Chan and Fair [*Ind. Eng. Chem. Proc. Des. Dev.* **23,** 814 (1984)]. An improved version of the AIChE model, which alleviated several of its shortcomings and updated its hydraulic and mass-transfer relationships, was produced by Chan and Fair.

The Chan and Fair correlation generally gave good predictions when tested against a wide data bank, but its authors also observed some deviations. Its authors described it as "tentative until more data become available." The Chan and Fair correlation is considered the most reliable fundamental correlation for tray efficiency, but even this correlation has been unable to rectify several theoretical and practical limitations inherited from the AIChE correlation (see Kister, *Distillation Design,* McGraw-Hill, New York, 1992). Recently, Garcia and Fair (*Ind. Eng. Chem. Res.* **39,** 1818, 2000) proposed a more fundamental and accurate model that is also more complicated to apply.

The prime issue that appears to plague fundamental tray efficiency methods is their tendency to predict efficiencies of 80 to 100 percent for distillation columns larger than 1.2 m (4 ft) in diameter. In the real world, most columns run closer to 60 percent efficiency. Cai and Chen (Distillation 2003: Topical Conference Proceedings, AIChE Spring National Meeting, New Orleans, La., March 30–April 3, 2003) show that published eddy diffusivity models, which are based on small-column work, severely underestimate liquid backmixing and overestimate plug flow in commercial-scale columns, leading to optimistic efficiency predictions. Which other limitations (if any) in the theoretical methods contribute to the mismatch, and to what degree, is unknown. For this reason, the author would not recommend any currently published theoretical tray efficiency correlation for obtaining design efficiencies.

Example 12: Estimating Tray Efficiency For the column in Example 9, estimate the tray efficiency, given that at the relative volatility near the feed point is 1.3 and the viscosity is 0.25 cP.

Solution Table 14-12 presents measurements by Billet (loc. cit.) for ethylbenzene-styrene under similar pressure with sieve and valve trays. The column diameter and tray spacing in Billet's tests were close to those in Example 9. Since both have single-pass trays, the flow path lengths are similar. The fractional hole area (14 percent in Example 9) is close to that in Table 14-12 (12.3 percent for the tested sieve trays, 14 to 15 percent for standard valve trays). So the values in Table 14-12 should be directly applicable, that is, 70 to 85 percent. So a conservative estimate would be 70 percent. The actual efficiency should be about 5 to 10 percent higher.

Alternatively, using Eq. (14-138) or Fig. 14-47, $E_{OC} = 0.492(0.25 \times 1.3)^{-0.245} = 0.65$ or 65 percent. As stated, the O'Connell correlation tends to be slightly conservative. This confirms that the 70 percent above will be a good estimate.

EQUIPMENT FOR DISTILLATION AND GAS ABSORPTION: PACKED COLUMNS

Packings are generally divided into three classes:

1. *Random or dumped packings* (Figs. 14-48 and 14-49) are discrete pieces of packing, of a specific geometric shape, that are "dumped" or randomly packed into the column shell.
2. *Structured or systematically arranged packings* (Fig. 14-50) are crimped layers of corrugated sheets (usually) or wire mesh. Sections of these packings are stacked in the column.
3. *Grids*. These are also systematically arranged packings, but instead of wire mesh or corrugated sheets, these use an open-lattice structure.

Random and structured packings are common in commercial practice. The application of grids is limited primarily to heat-transfer and wash services and/or where a high fouling resistance is required. Grids are discussed in detail elsewhere (Kister, *Distillation Design,* McGraw-Hill, New York, 1992).

Figure 14-51 is an illustrative cutaway of a packed tower, depicting typical internals. This tower has a structured-packed top bed and a random-packed bottom bed. Each bed rests on a support grid or plate. The lower bed has a holddown grid at its top to restrict packing uplift. Liquid to each of the beds is supplied by a liquid distributor. An intermediate distributor, termed a *redistributor,* is used to introduce feed and/or to remix liquid at regular height intervals. The intermediate distributor in Fig. 14-51 is not self-collecting, so a chevron collector is used to collect the liquid from the bed above. An internal pipe passes this liquid to the distributor below. The collected liquid is mixed with the fresh feed (not shown) before entering the distributor. The reboiler return enters behind a baffle above the bottom sump.

As illustrated, the packing needs to be interrupted and a distributor added at each point where a feed enters or a product leaves. A simple distillation tower with a single feed will have a minimum of two beds, a rectifying bed and a stripping bed.

Packing Objectives The objective of any packing is to maximize efficiency for a given capacity, at an economic cost. To achieve these goals, packings are shaped to

1. *Maximize the specific surface area, i.e., the surface area per unit volume.* This maximizes vapor-liquid contact area, and, therefore, efficiency. A corollary is that efficiency generally increases as the random packing size is decreased or as the space between structured packing layers is decreased.
2. *Spread the surface area uniformly.* This improves vapor-liquid contact, and, therefore, efficiency. For instance, a Raschig ring (Fig. 14-48*a*) and a Pall® ring (Fig. 14-48*c*) of an identical size have identical surface areas per unit volume, but the Pall® ring has a superior spread of surface area and therefore gives much better efficiency.
3. *Maximize the void space per unit column volume.* This minimizes resistance to gas upflow, thereby enhancing packing capacity.

A corollary is that capacity increases with random packing size or with the space between structured packing layers. Comparing with the first objective, a tradeoff exists; the ideal size of packing is a compromise between maximizing efficiency and maximizing capacity.

4. *Minimize friction.* This favors an open shape that has good aerodynamic characteristics.

5. *Minimize cost.* Packing costs, as well as the requirements for packing supports and column foundations, generally rise with the weight per unit volume of packing. A corollary is that packings become cheaper as the size increases (random packing) and as the space between layers increases (structured packing).

Random Packings Historically, there were three generations of evolution in random packings. The first generation (1907 to the 1950s) produced two basic simple shapes—the Raschig ring and the Berl saddle (Fig. 14-48*a, b*) that became the ancestors of modern random packings. These packings have been superseded by more modern packing and are seldom used in modern distillation practice.

The second generation (late 1950s to the early 1970s) produced two popular geometries—the Pall® ring, which evolved from the Raschig ring, and the Intalox® saddle (Fig. 14-48*c–f*), which evolved from the Berl saddle.

BASF developed the Pall® ring by cutting windows in the Raschig ring and bending the window tongues inward. This opened up the ring, lowering the aerodynamic resistance and dramatically enhancing capacity. The bent tongues improved area distribution around the particle, giving also better efficiency. These improvements made the first generation Raschig rings obsolete for distillation.

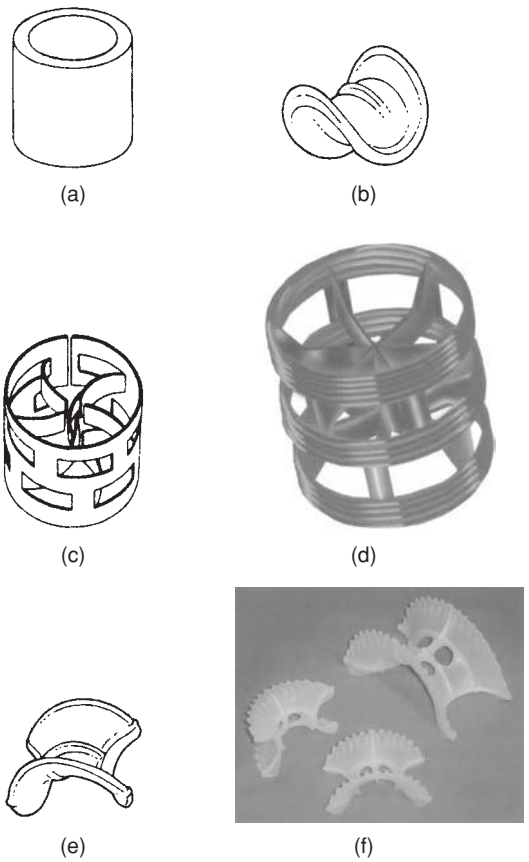

FIG. 14-48 Common first- and second-generation random packings. (*a*) Raschig ring (metal, plastic, ceramic). (*b*) Berl saddle (ceramic). (*c*) Pall ring (metal). (*d*) Pall ring (plastic). (*e*) Intalox saddle (ceramic). (*f*) Super Intalox saddle (plastic). *(Parts d, f, courtesy of Koch-Glitsch LP.)*

Berl saddles (ceramics) are still used due to their good breakage resistance.

The second-generation packings are still popular and extensively used in modern distillation practice. The third generation (the mid-1970s until present) has produced a multitude of popular geometries, most of which evolved from the Pall® ring and Intalox® saddle. Some are shown in Fig. 14-49. A more comprehensive description of the various packings is given elsewhere (Kister, *Distillation Design,* McGraw-Hill, New York, 1992).

The third generation of packing was a significant, yet not large, improvement over the second generation, so second-generation packings are still commonly used.

Structured Packings Structured packings have been around since as early as the 1940s. First-generation structured packings, such as Panapak, never became popular, and are seldom used nowadays.

The second generation of structured packings began in the late 1950s with high-efficiency wire-mesh packings such as Goodloe®, Hyperfil®, and the Sulzer® (wire-mesh) packings. By the early 1970s, these packings had made substantial inroads into vacuum distillation, where their low pressure drop per theoretical stage is a major advantage. In these services, they are extensively used today. Their high cost, high sensitivity to solids, and low capacity hindered their application outside vacuum distillation.

The corrugated-sheet packing, first introduced by Sulzer in the late 1970s, started a third generation of structured packings. With a high capacity, lower cost, and lower sensitivity to solids, while still retaining a high efficiency, these corrugated-sheet packings became competitive with conventional internals, especially for revamps. The 1980s saw an accelerated rise in popularity of structured packings, to the point of their becoming one of the most popular column internals in use today.

Corrugated structured packings are fabricated from thin, corrugated (crimped) metal sheets, arranged parallel to one another. The corrugated sheets are assembled into an element (Figs. 14-50*a, c* and 14-51). The sheets in each element are arranged at a fixed angle to the vertical. Table 14-14 contains geometric data for several corrugated packings.

Geometry (Fig. 14-52) The crimp size defines the opening between adjacent corrugated layers. Smaller *B, h,* and *S* yield narrower openings, more sheets (and, therefore, greater surface area) per unit volume, and more efficient packing, but higher resistance to gas upflow, lower capacity, and enhanced sensitivity to plugging and fouling.

The corrugations spread gas and liquid flow through a single element in a series of parallel planes. To spread the gas and liquid uniformly in all radial planes, adjacent elements are rotated so that sheets of one element are at a fixed angle to the layer below (Fig. 14-51). For good spread, element height *s* is relatively short (typically 200 to 300 mm, 8 to 12 in) and the angle of rotation is around 90°.

The surfaces of a few structured packings (especially those used in highly fouling environments) are smooth. Most structured packings have a roughened or enhanced surface that assists the lateral spread of liquid, promotes film turbulence, and enhances the area available for mass transfer. Texturing commonly employed is embossing and grooving (Fig. 14-50*a, b*).

The surfaces of most (but not all) structured packings contain holes that serve as communication channels between the upper and lower surfaces of each sheet. If the holes are too small, or nonexistent, both sides of a sheet will be wet only at low liquid rates. At high liquid rates, *sheeting* or *blanking* will cause liquid to run down the top surface with little liquid wetting the bottom surface [Chen and Chuang, *Hydroc. Proc.* **68**(2), 37 (1989)], which may lower efficiency. Usually, but not always, the holes are circular (Fig. 14-50*a, b*), about 4 mm in diameter. Olujic et al. (Distillation 2003: Topical Conference Proceedings, p. 523, AIChE, 2003, Spring National Meeting, New Orleans, La.) showed that the hole diameter has a complex effect, strongly dependent on packing size, on both capacity and efficiency.

Inclination Angle In each element, corrugated sheets are most commonly inclined at about 45° to the vertical (typically indicated by the letter Y following the packing size). This angle is large enough for good drainage of liquid, avoiding stagnant pockets and regions of liquid accumulation, and small enough to prevent gas from bypassing the metal surfaces. In some packings, the inclination angle to the vertical is steepened to 30° (typically indicated by the letter X following the

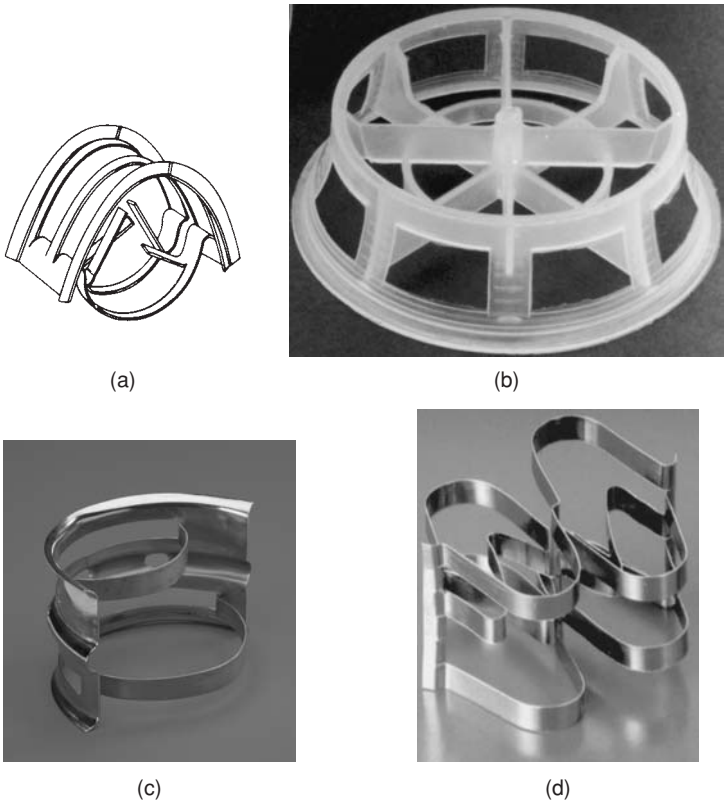

FIG. 14-49 Common third-generation random packings. (*a*) Intalox metal tower packing (IMTP). (*b*) Cascade mini-ring (CMR) (plastic). (*c*) Nutter ring (metal). (*d*) Raschig Super-Ring (metal). *(Parts a, b, courtesy of Koch-Glitsch LP; part c, courtesy of Sulzer Chemtech; part d, courtesy of Rashig AG.)*

packing size). This improves drainage, and therefore capacity, but at the expense of reduced gas-liquid contact, and therefore efficiency.

A recent development followed the realization that liquid drainage was restricted at the element-to-element transition rather than inside elements (Lockett and Billingham, *IChemE Symp. Ser.* **152,** London, 2006). This means that the liquid accumulation leading to flood initiates at the transition region. A fourth generation of structured packing started, in which the main body of each element has layers inclined at 45°, but the ends of each element are almost vertical to permit drainage at this end region (Fig. 14-50*d*; but keep in mind that successive elements are rotated 90° rather than continuous, as shown in Fig. 14-50*d*). These S-shaped or high-capacity packings offer greater capacity compared to equivalent 45° inclined packings with efficiency the same with some (Pilling and Haas, Topical Conference Proceedings, p. 132, AIChE Spring Meeting, New Orleans, March 10–14, 2002; McNulty and Sommerfeldt in "Distillation: Horizons for the New Millennium," Topical Conference Proceedings, p. 89, AIChE Spring Meeting, Houston, Tex., March 1999) and lower with others [Olujic et al., *Chem. Eng. and Proc.*, **42,** p. 55 (2003)].

PACKED-COLUMN FLOOD AND PRESSURE DROP

Pressure drop of a gas flowing upward through a packing countercurrently to liquid flow is characterized graphically in Fig. 14-53. At very low liquid rates, the effective open cross section of the packing is not appreciably different from that of dry packing, and pressure drop is due to flow through a series of variable openings in the bed. Thus, pressure drop is proportional approximately to the square of the gas velocity, as indicated in the region *AB*. At higher liquid rates, the effective open cross section is smaller because of the presence of liquid (region A′B′). The pressure drop is higher, but still proportional to the square of the gas velocity.

At higher gas rates, a portion of the energy of the gas stream is used to support an increasing quantity of liquid in the column. For all liquid rates, a zone is reached where pressure drop is proportional to a gas flow rate to a power distinctly higher than 2; this zone is called the *loading zone*. The increase in pressure drop is due to the liquid accumulation in the packing voids (region *BC* or *B′C′*)

As the liquid holdup increases, the effective orifice diameter may become so small that the liquid surface becomes continuous across the cross section of the column. Column instability occurs concomitantly with a rising continuous-phase liquid body in the column. Pressure drop shoots up with only a slight change in gas rate (condition *C* or *C′*). The phenomenon is called *flooding* and is analogous to entrainment flooding in a tray column.

Alternatively, a phase inversion occurs, and gas bubbles through the liquid. The column is not unstable and can be brought back to gas-phase continuous operation by merely reducing the gas rate. A stable operating condition beyond flooding (region *CD* or *C′D′*) may form with the liquid as the continuous phase and the gas as the dispersed phase [Lerner and Grove, *Ind. Eng. Chem.* **43,** 216 (1951); Teller, *Chem. Eng.* **61**(9), 168 (1954); Leung et al., *Ind. Eng. Chem. Fund.* **14** (1), 63 (1975); Buchanan, *Ind. Eng. Chem. Fund.* **15** (1), 87 (1976)].

For total-reflux distillation in packed columns, regions of loading and flooding are identified by their effects on mass-transfer efficiency, as shown in Fig. 14-54. Gas and liquid rate increase together, and a

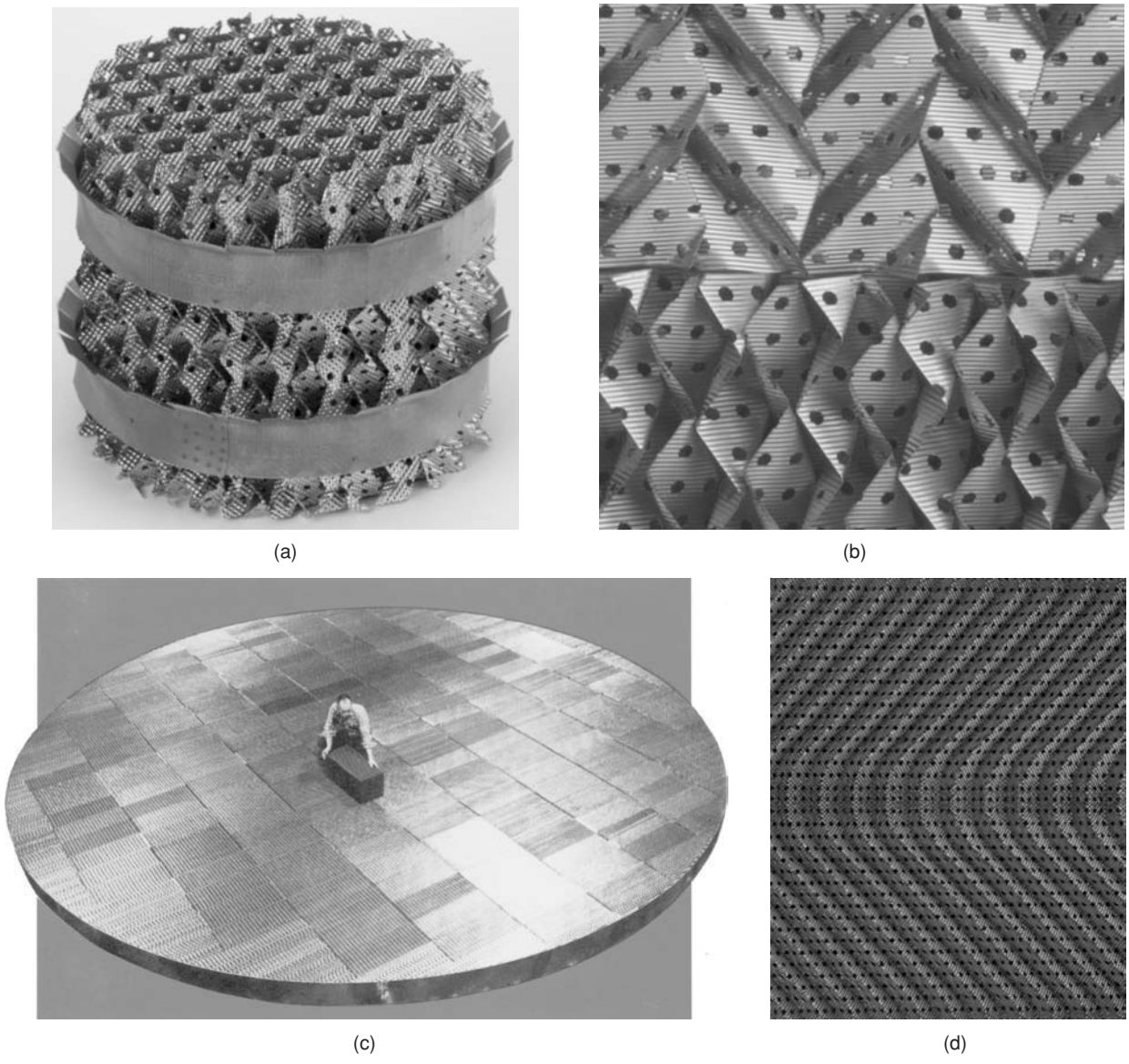

FIG. 14-50 Common structured packings. (*a*) A small element of Mellapak™ showing embossed surface, holes, and corrugated-sheet arrangement. (*b*) A closeup of the surface of Flexipac™ showing grooved surface and holes. (*c*) Fitting structured packing elements to a large-diameter tower. (*d*) Mellapak Plus™, a fourth-generation structured packing, showing a 45° inclination angle in the element and near-vertical inclination at the element-to-element transition. Note that in the tower, the successive layers will be oriented 90° to each other as in part *b*. (*Parts a, d, courtesy of Sulzer Chemtech; parts b, c, courtesy of Koch-Glitsch LP.*)

point is reached at which liquid accumulates rapidly (point *B*) and effective surface for mass transfer decreases rapidly.

Flood-Point Definition In 1966, Silvey and Keller [*Chem. Eng. Progr.* **62**(1), 68 (1966)] listed 10 different flood point definitions that have been used by different literature sources. A later survey (Kister and Gill, *Proceedings of Chemeca 92,* p. 185-2, Canberra, Australia, 1992) listed twice that many. As Silvey and Keller pointed out, the existence of so many definitions puts into question what constitutes flooding in a packed tower, and at what gas rate it occurs. Symptoms used to identify flood in these definitions include appearance of liquid on top of the bed, excessive entrainment, a sharp rise in pressure drop, a sharp rise in liquid holdup, and a sharp drop in efficiency. The survey of Kister and Gill suggests that most flood point definitions describe the point of flooding initiation (*incipient flooding*; point *C* or *C′* on Figs. 14-53 and 14-54). The different incipient flooding definitions gave surprisingly little scatter of flood point data (for a given packing under similar operating conditions). It follows that any definition describing flooding initiation should be satisfactory.

The author believes that due to the variations in the predominant symptom with the system and the packing, the use of multiple symptoms is most appropriate. The author prefers the following definition

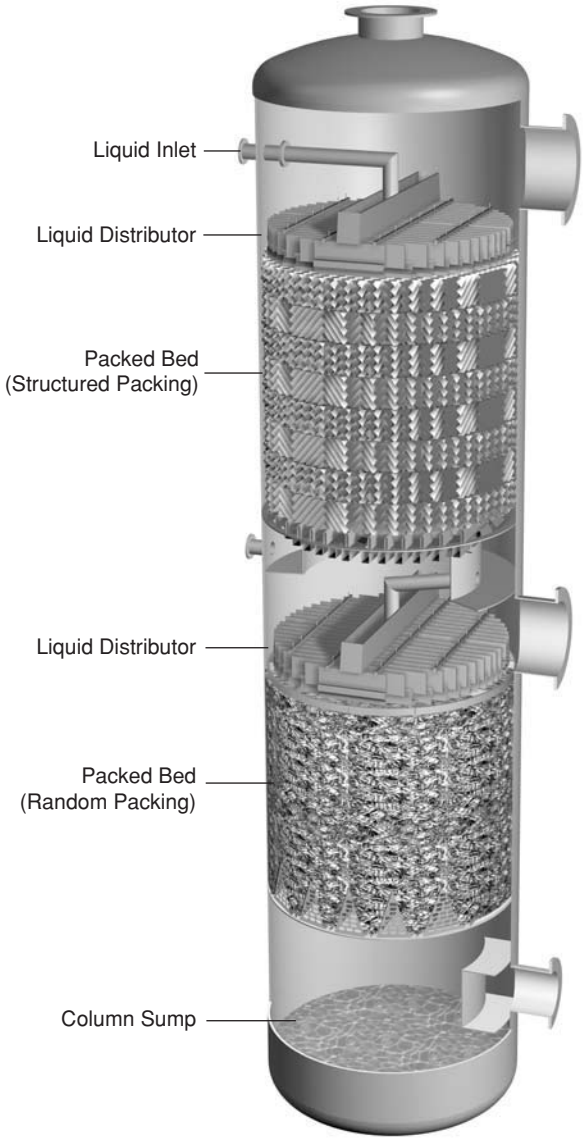

FIG. 14-51 Illustrative cutaway of a packed tower, depicting an upper bed of structured packing and a lower bed of random packing. *(Courtesy of Sulzer Chemtech.)*

by Fair and Bravo [*Chem. Eng. Symp. Ser.* **104,** A183 (1987)]: "A region of rapidly increasing pressure drop with simultaneous loss of mass transfer efficiency. Heavy entrainment is also recognized as a symptom of this region." An almost identical definition was presented earlier by Billet (*Distillation Engineering,* Chem. Publishing Co., New York, 1979).

The maximum operational capacity or throughput (often also referred to as maximum efficient capacity) is defined (Strigle, *Packed Tower Design and Applications,* 2d ed., Gulf Publishing, Houston, Tex., 1994) as the "Maximum vapor rate that provides normal efficiency of a packing" (i.e., point B in Fig. 14-54). The MOC is clear-cut in Fig. 14-54. On the other hand, locating the MOC in other cases is difficult and leaves a lot of room for subjectivity.

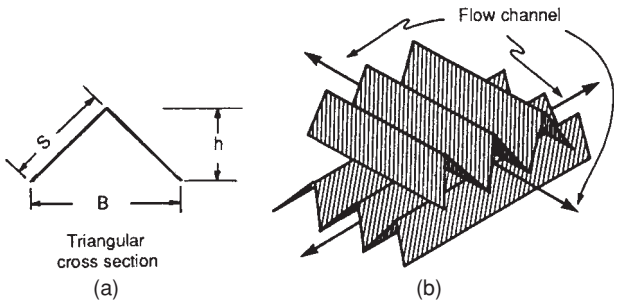

FIG. 14-52 Crimp geometry in structured packings. (*a*) Flow channel cross section. (*b*) Flow channel arrangement. *(From J. R. Fair and J. L. Bravo,* Chem. Eng. Progr., *Jan. 1990, p. 19; reproduced courtesy of the American Institute of Chemical Engineers.)*

In most cases, [Kister and Gill, *Chem. Eng. Progr.* **87**(2), 32 (1991)], the velocity at which MOC is reached is related to the flood point velocity by

$$u_{S,\mathrm{MOC}} = 0.95\, u_{S,\mathrm{Fl}} \tag{14-139}$$

Flood and Pressure Drop Prediction The first generalized correlation of packed-column flood points was developed by Sherwood, Shipley, and Holloway [*Ind. Eng. Chem.*, **30,** 768 (1938)] on the basis of laboratory measurements primarily on the air-water system with random packing. Later work with air and liquids other than water led to modifications of the Sherwood correlation, first by Leva [*Chem. Eng. Progr. Symp. Ser.,* **50**(1), 51 (1954)], who also introduced the pressure drop curves, and later in a series of papers by Eckert. The generalized flooding–pressure drop chart by Eckert [*Chem. Eng. Progr.* **66**(3), 39 (1970)], included in previous editions of this handbook, was modified and simplified by Strigle (*Packed Tower Design and Applications,* 2d ed., Gulf Publishing, Houston, Tex., 1994) (Fig. 14-55). It is often called the generalized pressure drop correlation (GPDC). The ordinate is a capacity parameter [Eq. (14-140)] related to the Souders-Brown coefficient used for tray columns.

$$\mathrm{CP} = C_S F_p^{0.5} \nu^{0.05} = U_S \left(\frac{\rho_G}{\rho_L - \rho_G} \right)^{0.50} F_p^{0.5} \nu^{0.05} \tag{14-140}$$

where U_S = superficial gas velocity, ft/s
ρ_G, ρ_L = gas and liquid densities, lb/ft^3 or kg/m^3

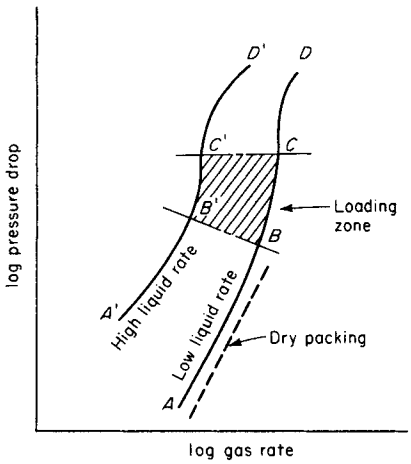

FIG. 14-53 Pressure-drop characteristics of packed columns.